Studies on the phylodynamics and pathogenicity of swine and avian influenza viruses

(豚及び鳥インフルエンザウイルスの遺伝的動態と病原性に関する研究)

Junki Mine

TABLE OF CONTENTS

Contents i

Abbreviations iii

Notes iv

Preface 1

Chapter I

Genetic characterization of influenza A viruses in Japanese swine in 2015 to 2019

Introduction 5

Materials and Methods 6

Results 9

Discussion 27

Summary 30

Chapter II

Genetic and antigenic dynamics of influenza A viruses of swine on pig farms in Thailand

Introduction 32

Materials and Methods 33

Results 39

Discussion 65

Summary 68

Chapter III

Genetics and pathogenicity of H5N6 highly pathogenic avian influenza viruses isolated from wild birds and a chicken in Japan during winter 2017-2018

Introduction 70

Materials and Methods 71

Results 74

Discussion **90**

Summary **92**

Chapter IV

Phylogeographic evidence for the inter- and intracontinental dissemination of avian influenza viruses via migration flyways

Introduction **94**

Materials and Methods **96**

Results **98**

Discussion **110**

Summary **114**

Conclusion **115**

Acknowledgements **117**

References **118**

Summary in Japanese（和文要旨） **135**

Abbreviations

BaTS	**bayesian tip-association significance testing**
BEAST	**bayesian evolutionary analysis by sampling tree**
BEAUti	**bayesian evolutionary analysis utility**
EID_{50}	**fifty percent egg infectious dose**
GISAID	**global initiative on sharing avian influenza data**
HA	**hemagglutinin**
HI	**hemagglutination-inhibition**
HPAIV	**highly pathogenic avian influenza virus**
HPDV	**highest posterior density value**
IAV-S	**influenza A virus of swine**
MCC	**maximum clade credibility**
MDCK	**Madin–Darby canine kidney cells**
ML	**maximum likelihood**
MP	**matrix protein**
NA	**neuraminidase**
NCBI	**National Center for Biotechnology Information**
NP	**nucleoprotein**
NS	**nonstructural protein**
PA	**acidic polymerase**
PB	**basic polymerase**
SpreaD	**spatial phylogenetic reconstruction of evolutionary dynamics using data-driven documents**

Notes

Contents of the present thesis were published in the following articles.

1. **Mine J, Uchida Y, Takemae N, Saito T.** Genetic characterization of influenza A viruses in Japanese swine in 2015 to 2019. J Virol 94, 2020.

2. **Mine J, Abe H, Parchariyanon S, Boonpornprasert P, Ubonyaem N, Nuansrichay B, Takemae N, Tanikawa T, Tsunekuni R, Uchida Y, Saito T.** Genetic and antigenic dynamics of influenza A viruses of swine on pig farms in Thailand. Arch Virol 164, 457-472, 2019.

3. **Mine J, Uchida Y, Nakayama M, Tanikawa T, Tsunekuni R, Sharshov K, Takemae N, Sobolev I, Shestpalov A, Saito T.** Genetics and pathogenicity of H5N6 highly pathogenic avian influenza viruses isolated from wild birds and a chicken in Japan during winter 2017-2018. Virology 533, 1-11, 2019.

4. **Mine J, Uchida Y, Sharshov K, Sobolev I, Shestopalov A, Saito T.** Phylogeographic evidence for the inter- and intracontinental dissemination of avian influenza viruses via migration flyways. PLoS One 14, e0218506, 2019.

Preface

Influenza is a major respiratory disease caused by influenza virus of the *Orthomyxoviridae* family. Influenza viruses are divided into types from A to D based on their genetic and antigenic characters, and influenza A virus (IAV) has a potential to infect various animals including humans, pigs, and birds and causes problems as zoonoses (1, 2). IAV is a negative-strand RNA virus that have 8-segments genes, with such characters they sometimes exchange their genes in a co-infected cell known as reassortment. IAVs are classified into H1 to H18 and N1 to N11 according to the genetic and antigenic characters of the surface proteins; hemagglutinin (HA) and neuraminidase (NA) (3-7). Waterfowl such as ducks—which are natural hosts of IAVs—retain these viruses (except for H17, H18, N10, N11 IAVs). Among the various subtypes, only the H5 and H7 subtypes of avian influenza virus (AIV) cause highly pathogenic avian influenza (HPAI) in nature. Once HPAI outbreak occurs, socio-economic damage is enormous through the movement and export restrictions in addition to the epidemic prevention measures such as stamping out. IAVs occasionally reassort with other IAVs, resulting in the emergence of IAVs that can infect to other hosts (1). Actually, the IAV that caused the pandemic in 2009 was a virus that had genes derived from humans, pigs, and birds (8). IAV of swine (IAV-S) causes economic loss to pig farms by themselves and/or by co-infection with other respiratory pathogens (9). Thus, surveillance activities on IAV-S have been accelerated not only for moderating the economic loss to the pig farming but also for monitoring newly-generated IAVs-S with a potential of next pandemic. In the present thesis, various genetic approaches based on genetic, time, and location information were performed to elucidate the character and origin of the IAVs-S in Japan and Thailand, where status of IAVs-S were still unknown, and AIVs that could be intruded and cause economic loss to Japan. The present thesis consists of four chapters; in Chapter I, surveillance activities on IAV-S were performed in Japan and isolated IAVs-S were genetically analyzed to elucidate the current status of IAV-S in Japan. In Chapter II, surveillance activities on IAV-S were performed in Thailand. Isolated IAVs-S were genetically and antigenically analyzed to characterize them and reveal the dynamics of IAVs-S in farm levels. In Chapter III, genetic origins of H5N6 highly pathogenic avian influenza viruses (HPAIVs) that were intruded to Japan in winter 2017-2018 were estimated through the phylogenetic analyses. Additionally, the pathogenicity and transmissibility of those HPAIVs were also investigated. In Chapter IV, N6 NA genes that include those of H5N6 HPAIVs described in the previous chapter were phylogeographically analyzed to elucidate the mechanism of the dissemination of

AIVs all over the world.

IAV-S is a major respiratory pathogen and causes broadly prevalent disease in pigs worldwide. IAV-S typically causes low mortality rates and mild symptoms, such as fever, loss of appetite, dullness (10), but co-infection with IAV-S and other pathogens, such as porcine reproductive and respiratory syndrome virus, increases the mortality rate and decreases average daily weight gain (9). Thus, IAV-S, alone and in combination with other pathogens, causes tremendous economic loss for pig farmers worldwide (11, 12). Additionally, pigs are susceptible to both human and avian influenza viruses as they express the receptors to both influenza viruses on their tracheal epithelial cells (13). With such characters, pigs serve as a reservoir and a "mixing vessel" in which reassortment events of influenza viruses occur to generate novel gene constellations with pandemic potential (8). Therefore, surveillance activities on IAV-S have been accelerated not only for moderating the economic loss to the pig farming all over the world but also for monitoring emerging IAVs-S with the potential to be the next pandemic. Worldwide circulation of IAV-S changed dramatically after the pandemic caused by A(H1N1)2009 [A(H1N1)pdm09] viruses. Before 2009, three subtypes of IAV-S—H1N1, H1N2, and H3N2—predominated in swine throughout the world (14). Classical swine H1N1 IAVs-S were first isolated in North America in 1930 and have been infecting pigs endemically there since the 1970s, currently circulating among pig population worldwide, whereas avian-like H1N1 IAVs-S have stably persisted in Europe since 1979 (14, 15). In Asia, avian-like H1N1 IAVs-S were first isolated in China in 1993 (14, 16, 17), and reassortant IAVs-S containing genes derived from avian-like H1N1 IAVs-S have been reported in Thailand (18-21), South Korea (22), and Vietnam (23). A/Hong Kong/1968 - like H3N2 viruses have been isolated from pigs in Asia and Europe, indicating the worldwide circulation of human-like H3N2 IAVs-S, while some cases of the isolation of avian-like H3N2 IAVs-S were reported in Asia in 1970s (24–28). In 1998, a triple-reassortant H3N2 virus emerged in North America through reassortment among a human seasonal virus, a classical swine IAV-S, and an avian influenza virus, which was followed by the emergence of H1N1 and H1N2 triple-reassortant IAVs-S and their circulation in North America. (29). Subsequently, in April 2009, an IAV containing a combination of segments from both the above-described triple-reassortant virus and Eurasian avian-like swine lineages spread rapidly to cause a worldwide pandemic in humans (30, 31). After the 2009 pandemic, A(H1N1)pdm09 viruses were introduced into swine populations and reassorted with endemic IAVs-S, further increasing genetic diversity among IAVs-S all over the world (32–43).

HPAIVs of the Goose/Guangdong (Gs/Gd) lineage arose from H5N1

HPAIVs that caused the first outbreaks among domestic geese in Guangdong province, China, in 1996 (44) and have now been circulating for more than 20 years. In Japan, outbreaks due to H5N1 HPAIVs of the Gs/Gd lineage were first reported in 2004 (45). In 2007, there were outbreaks of H5N1 HPAIVs related to the 2005 Qinghai strain belonging to the clade 2.2 (46); these were followed by the reintroduction of other H5N1 HPAIVs in clade 2.3.2 during winter 2010–2011. These massive outbreaks yielded 64 recorded cases in wild birds and 24 outbreaks in poultry farms throughout 21 prefectures in Japan (47, 48). In April 2014, H5N8 HPAIVs belonging to clade 2.3.4.4 that emerged through reassortment of above-mentioned H5N1 HPAIVs with other AIVs caused an outbreak at a chicken farm. During winter 2014-2015, reintroduction of clade 2.3.4.4 but phylogenetically distinct H5N8 HPAIVs from the isolate in April caused outbreaks in 5 other poultry farms and 13 cases in wild birds (49, 50). Among the evolution of clade 2.3.4.4 HPAIVs in Asia, they have been classified to Group A, B, C, and D (51-53). During winter 2016–2017, H5N6 HPAIVs of clade 2.3.4.4.C accounted for 218 cases in wild birds and 12 outbreaks in poultry farms (54-56).

Chapter I

Genetic characterization of influenza A viruses in Japanese swine in 2015 to 2019

Introduction

The pig farming in Japan has risen to intensive production recently; fewer but larger size pig farms are distributed around Japan, raising total of about 9 million pigs and producing about 900,000 tons of pig meat in Japan in 2019 (57). To evade the introduction of pathogens from foreign country, imported live pigs are quarantined for 15 days at an animal quarantine station. Classical swine H1N1 IAVs-S are thought to have been introduced into the swine population in Japan during the late 1970s (58, 59). Cases of the isolation of human-like H3N2 Influenza A viruses of swine (IAVs-S) from pigs were sporadic and few during 1970–2013 (40, 60, 61). After the introduction of a classical swine H1N1 IAV-S, it was replaced by the reassortant H1N2 IAVs-S that carried the HA gene of the classical swine lineage and NA gene of the human-like H3N2 virus. After 1980s, the H1N2 IAVs-S have circulated predominantly among Japanese swine and an H1N1 IAV-S possessing both H1 HA and N1 NA genes from the classical swine lineage has been rarely isolated (62-64). After the pandemic in 2009, A(H1N1)pdm09 viruses were introduced into pig populations in Japan, and genetic reassortment occurred between A(H1N1)pdm09 viruses and endemic H1N1, H1N2, and H3N2 IAVs-S that had circulated previously (40, 61). However, information regarding IAVs-S in Japan remains sparse and localized to limited areas. Furthermore, the dynamics of IAVs-S at the farm level in Japan are unclear.

To understand the status of IAVs-S among pig populations in Japan, from 2015 through 2019, nasal swab samples were collected from pigs on farms in 21 prefectures in Japan for virus isolation and phylogenetic analyses. Simultaneously, several pig farms were monitored for at least 3 years to examine how IAVs-S circulated within these populations. The findings from this study will improve our understanding of IAVs-S currently circulating in Japan and how they evolve at the farm level.

Materials and Methods

Sample collection

Through active surveillance efforts during 2015 through 2019, 7,133 nasal swabs were collected from pigs in various age groups at farms in Japan. During the same period, nasal swab samples and lung tissue samples collected from pigs suspected to have swine influenza were transferred from prefectural animal hygiene centers to the National Institute of Animal Health, Japan, for diagnosis. Through active and passive surveillance, samples were collected from 21 of all 47 prefectures. Nasal swabs collected through active surveillance were put promptly into transport media; Minimum Essential Media (Sigma-Aldrich, St. Louis, MO, USA) containing penicillin (1,000 units/ml) (Thermo Fisher Scientific, Waltham, MA, USA), streptomycin (1,000 μg/ml) (Thermo Fisher Scientific), amphotericin B (25 μg/ml) (Thermo Fisher Scientific), HEPES (Sigma-Aldrich), and 0.5% bovine serum albumin (Sigma-Aldrich) and were kept on ice packs until transport to the National Institute of Animal Health, Japan. Then, the swabs were removed and the medium aliquoted and stored at –80 °C until virus isolation. From each sample, 200 μl was used for RNA extraction and virus detection.

Virus detection and virus isolation

RNA was extracted from swab samples by using RNeasy Mini Kits (Qiagen, Hilden, Germany), as described previously (39, 65). The extracted RNA was reverse-transcribed to cDNA by using Superscript III (Thermo Fisher Scientific) and universal primers for IAV (66). This cDNA was the template for real-time PCR analysis by using SYBR Premix Ex Taq (Takara Bio, Shiga, Japan) with primers specific for the matrix protein (MP) gene, as described previously (67), or the MP gene was detected using an AgPath-ID One-Step RT-PCR Kit (Thermo Fisher Scientific) with primers and probes according to the diagnostic manual of the CSIRO Australian Animal Health Laboratory (68, 69). For virus isolation, media from nasal swabs that were virus-positive according to real-time PCR analysis were filtered (pore size, 0.45 μm; Millipore, Danvers, MA, USA) and inoculated into cultures of floating MDCK cells, 9- to 11-day embryonated chicken eggs, or primary cultures of porcine alveolar epithelial cells, as previously reported (70, 71). The supernatants of these cell cultures were used in HA assays (72) with guinea pig erythrocytes.

Genomic sequencing and phylogenetic analysis

All gene segments of isolated viruses were sequenced by using next-

generation sequencing; RNA was extracted from isolated viruses by using RNeasy Mini kits (Qiagen). cDNA libraries for next-generation sequencing were prepared by using an NEBNext Ultra RNA Library Prep Kit (Illumina, New England Biolabs, Ipswich, MA, USA) for Illumina. In total,10 pM of synthesized cDNA libraries was mixed with 10 pM of the PhiX control (Illumina) and sequenced by using a Miseq Reagent Kit version 2 (Illumina). Consensus sequences were generated and the HA and NA genes of each isolate were subtyped by using FluGAS software (World Fusion, Tokyo, Japan). The output pair-end reads from the MiSeq second-generation sequencer (Illumina) were mapped to reference sequences that were selected from a search of the Influenza Virus Database of the National Center for Biotechnology Information by using the FluGAS algorithm; this was followed by the construction of a consensus sequence when at least 3 reads were available. A single nucleotide was adopted when its representation exceeded 51% at that site, whereas mixed-base codes were adopted when multiple bases each accounted for at least 15% of the total coverage at the site. The nucleotide sequences of the IAVs-S analyzed here have been deposited in the Global Initiative on Sharing Avian Influenza Data (GISAID) EpiFlu database. For phylogenetic analyses, all H1 and H3 HA genes and N1 and N2 NA genes in the GISAID database were downloaded in September 2019. The sequences of the IAVs-S isolated here and the downloaded sequences from GISAID were aligned by using BioEdit (73) and MAFFT (74). Maximum likelihood (ML) trees based on aligned sequences (H1: 55,345; H3: 68,720; N1: 56,555; and N2: 70,938 strains) were constructed by using FastTree version 2.1.10 (75), and clusters containing Japanese IAVs-S with fast-global bootstrap values of 90 or greater were further analyzed.

To calculate molecular estimates of divergence times from ancestral IAVs for selected clusters containing HA and NA genes of IAVs-S, Maximum clade credibility (MCC) trees were constructed by using the BEAST package version 1.8.2 (76). Aligned sequences of genes were formatted by using the BEAUti at default settings, except for clock rate: the initial clock rate was set as 1.0×10^{-5} (substitutions/site/year) to fit the substitution rate of influenza viruses for constructing trees. Each calculation was set as 1×10^{8} to 1×10^{9} steps in length, where the number of steps was determined as that needed to obtain an effective sample size of more than 200.

Sequences for the polymerase basic protein (PB)1 genes of IAVs isolated from humans (55,504 strains) and swine (5,793 strains) were downloaded from the GISAID database, and nonredundant sets of human and swine sequences were produced by using CD-HIT software (77) at an identity threshold of 99.5%. Other gene segments of strains selected as described earlier (human, 1,475 strains;

swine, 2,056 strains) were used for constructing ML trees. A/swine/Gunma/10-1636/2016 (H1N1), which was isolated in the present study, was removed from the analysis because several gene segments included many mixed bases, indicating that this isolate can be considered a mixture of two IAVs-S.

Results

Subtyping and geographic distribution of IAV-S in Japan

The swabs collected through the active surveillance efforts in this study yielded 370 IAVs-S, giving an overall IAV-S isolation rate of 5.2%. In addition, 54 isolates were obtained from the specimens submitted for diagnosis during 2015 to 2019. Overall, 78 of the 424 total IAVs-S were subtyped as H1N1, 331 as H1N2, and 15 as H3N2. In addition, the lineages of the HA and NA genes were determined through phylogenetic analysis. Specifically, the H1 HA genes of 37 H1N1 and 319 H1N2 viruses belong to the 1A.1 classical swine lineage, whereas those of 41 H1N1 and 12 H1N2 viruses belong to the 1A.3.3.2 lineage [A(H1N1)pdm09] (Fig. 1). The H1 HA genes of the 1A.1 classical swine lineage share a common ancestor with the IAVs-S in Japan during the late 1970s, indicating that they have been circulating domestically for approximately 40 years (Fig. 2a).

All 15 of the H3N2 IAVs-S isolated here are located in a clade belonging to the human seasonal lineage (Fig. 1). These IAVs-S are related to the human influenza viruses that circulated during the 1999–2000 season, and their ancestral strain in swine, A/swine/Japan/KU-MD4/2013 (H3N2), was first isolated in 2013 (Fig. 2b). All 78 N1 genes of the H1N1 IAVs-S isolated here originated from A(H1N1)pdm09 viruses (Fig. 1), even though 37 of the H1N1 IAVs-S had H1 HA genes of the classical swine lineage. All 346 N2 NA genes of the 331 H1N2 IAVs-S and 15 H3N2 IAVs-S were classified into the human seasonal lineage (Fig. 1). However, a cluster consisting of N2 NA genes of the H1N2 IAVs-S was phylogenetically distinct from that of H3N2 IAVs-S. These H1N2 IAVs-S are related to the late-1960 human seasonal viruses, which were derived from Hong Kong H3N2 IAVs-S (Fig. 3a), whereas those of the H3N2 IAVs-S are related to the 1999–2000 seasonal influenza viruses, which correspond to the origin of their H3 HA genes (Fig. 3b).

The number of IAVs-S with various combinations of HA and NA genes and the number of IAV-S-positive farms in each prefecture and year indicate the breadth of distribution of IAVs-S in Japan and their persistence on some farms (Table 1). During 2015 to 2019, H1N1 IAVs-S with solely A(H1N1)pdm09-derived surface genes (P-P) were isolated from 18 farms in 9 prefectures. Reassortant H1N1 IAVs-S, carrying 1A.1 classical swine H1 and A(H1N1)pdm09-derived N1 NA genes (C-P), were found on 6 farms in 2 prefectures, and those harboring 1A.3.3.2 A(H1N1)pdm09 H1 HA and human seasonal N2 NA genes (P-H) were isolated from 2 farms in a single prefecture. H1N2 IAVs-S with 1A.1 classical swine H1 and human seasonal N2 NA genes

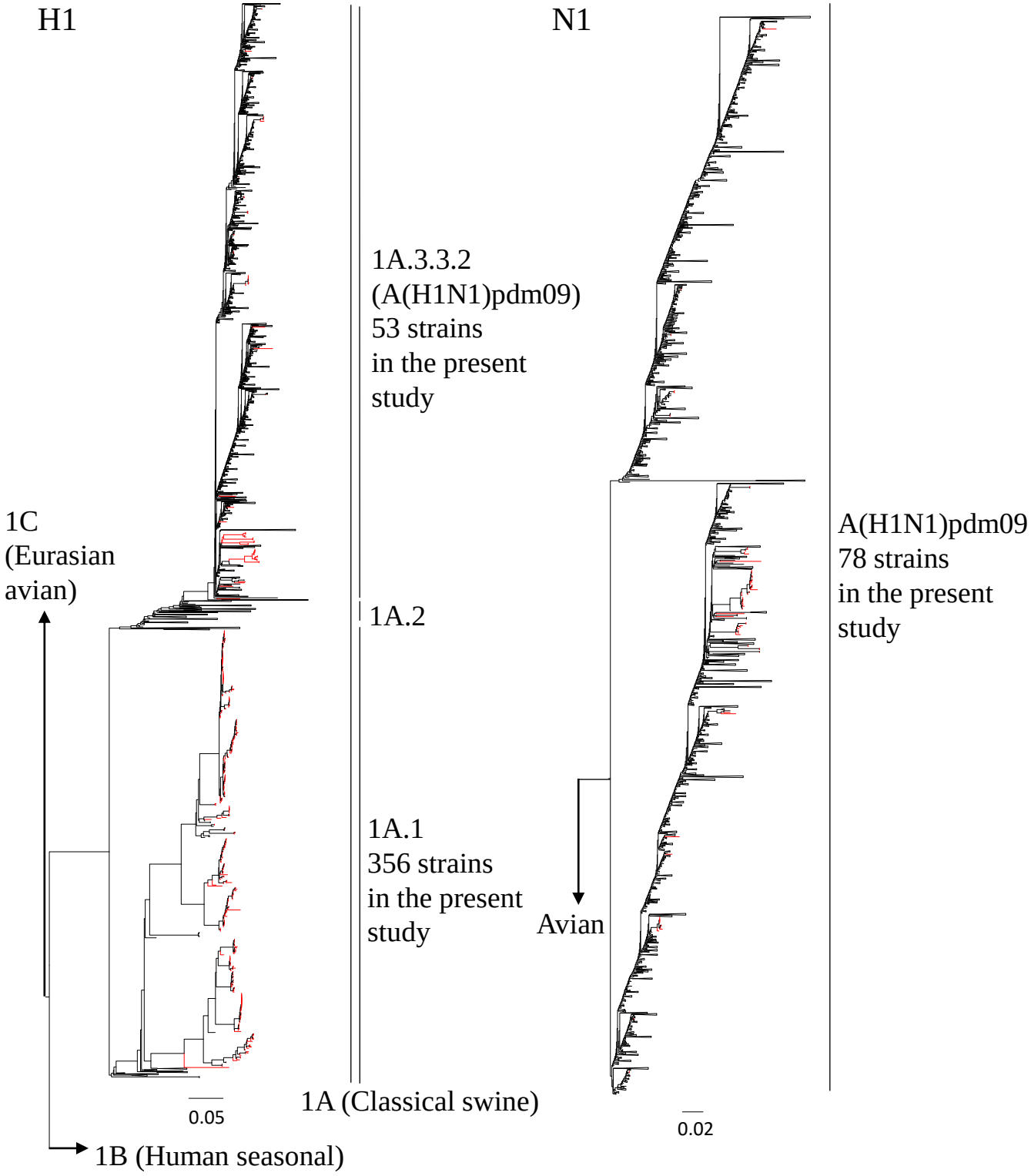

Fig. 1. Complete ML phylogenetic tree of the H1, H3, N1 and N2 genes. IAVs-S in the current study and were analyzed with data downloaded from the GISAID databases. Red branches indicate viruses isolated in the current study.

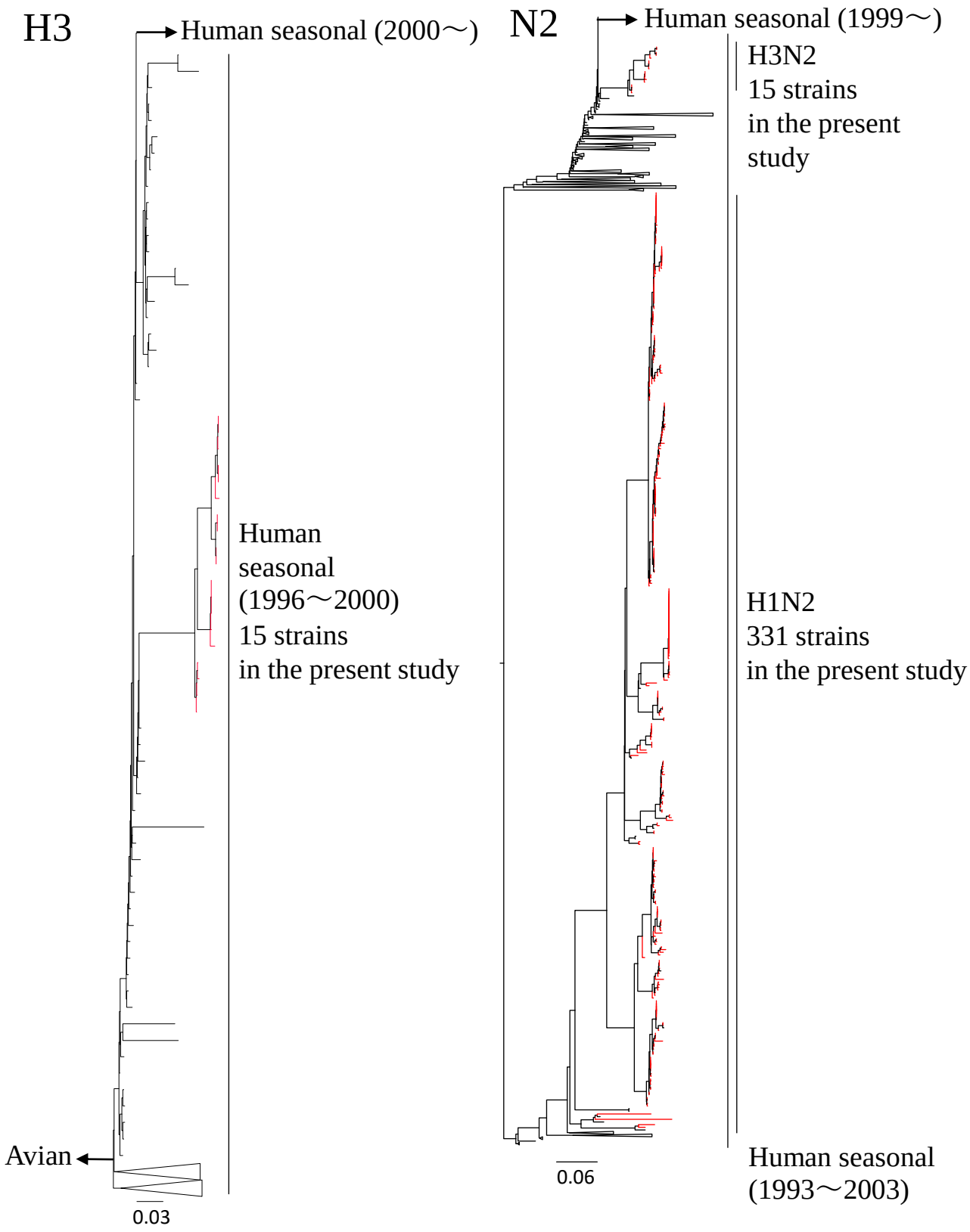

Fig. 1. Continued

Fig. 2. Detail of MCC trees of H1 (a) and H3 (b) genes in the 1A.1 classical swine lineage.

Red branches indicate viruses isolated in the present study. The divergence time at the branch is indicated by a black arrow, and the 95% highest posterior density for the divergence time is indicated by a gray box.

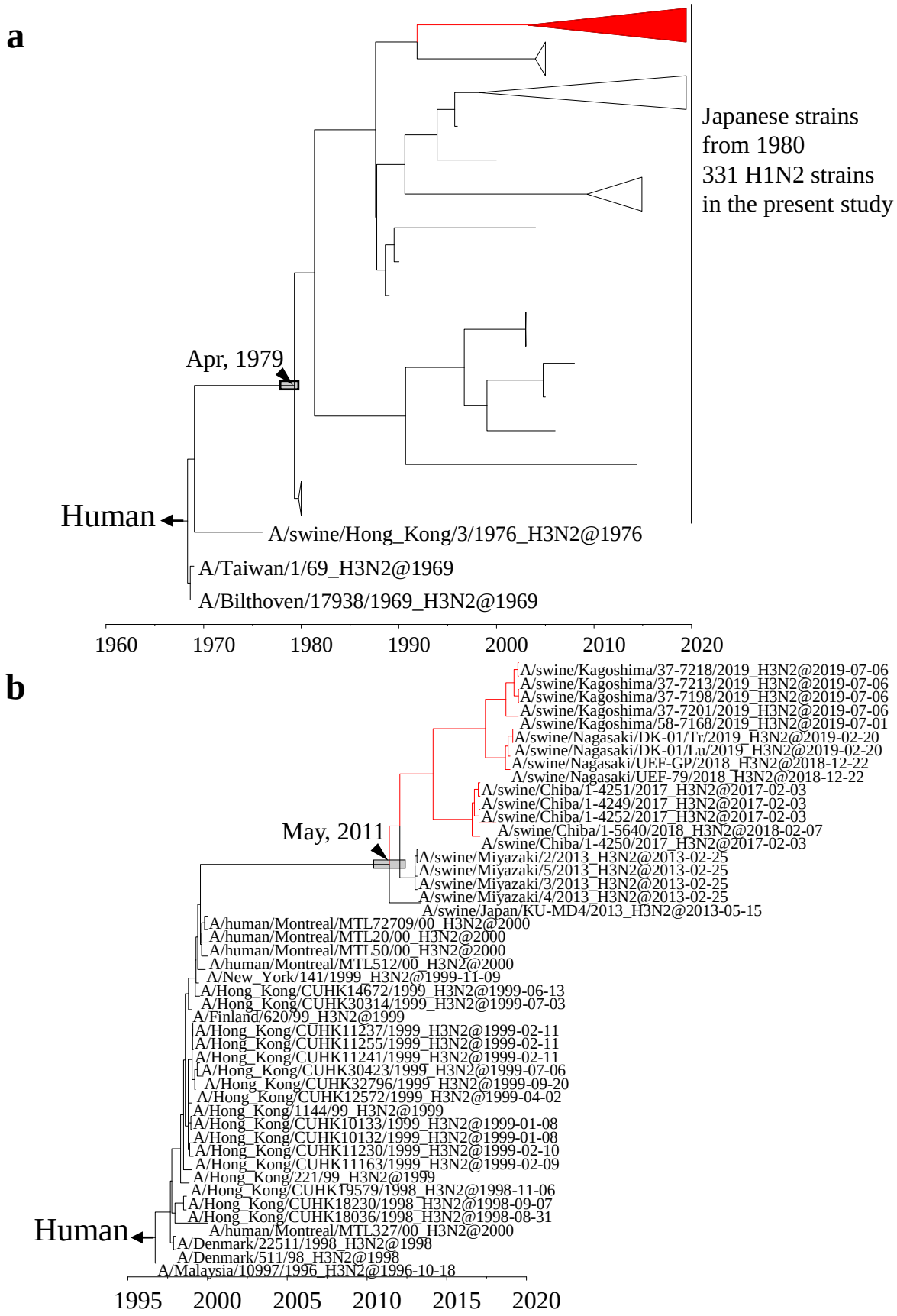

Fig. 3. Detail of MCC trees of N2 genes including H1N2 IAVs-S (a) and H3N2 IAVs-S (b) in the present study.

Red branches indicate viruses isolated in the present study. The divergence time at the branch is indicated by a black arrow, and the 95% highest posterior density for the divergence time is indicated by a gray box.

Table 1. Numbers of farms positive for IAVs-S during 2015–2019 according to prefecture.

	2015							2016							2017						
	No. of positive farms (no. of strains isolated)					Negative farms	No. of tested farms	No. of positive farms (no. of strains isolated)					Negative farms	No. of tested farms	No. of positive farms (no. of strains isolated)					Negative farms	No. of tested farms
	H1N1		H1N2		H3N2			H1N1		H1N2		H3N2			H1N1		H1N2		H3N2		
	(P-P)[a]	(C-P)	(P-H)	(C-H)	(H-H)			(P-P)	(C-P)	(P-H)	(C-H)	(H-H)			(P-P)	(C-P)	(P-H)	(C-H)	(H-H)		
Hokkaido	2(4)					2	4	1(1)					3	4						4	4
Tochigi																					
Ibaraki			1(1)			0	1														
Gunma	1(1)	3(5)	4(13)			1	8	1(9)	4(5)	8(129)			0	9			7(51)			5	12
Chiba		1(8)	3(3)			0	3		1(5)	1(21)			0	1		1(11)			1(4)	0	1
Niigata																	1(6)			0	1
Aichi								3(5)					12	15							
Tottori																					
Okayama																					
Nagasaki									1(2)				1	2							
Miyazaki								1(2)					1	2							
Kagoshima	1(1)					0	1						3	3	1(1)					0	1
Aomori																					
Iwate																					
Yamagata																					
Shizuoka																					
Hiroshima																					
Fukuoka																					
Saga																					
Oita													1	1							
Kumamoto													2	2							

[a]Surface genes derived from A(H1N1)pdm09 (P), 1A.1 classical swine (C), and human seasonal (H) viruses, respectively. For example, H1N1(C-P) indicates IAVs-S with 1A.1 classical swine HA and A(H1N1)pdm09 NA genes.

Table 1. Continued.

	2018							2019						
	No. of positive farms (no. of strains isolated)					Negative farms	No. of tested farms	No. of positive farms (no. of strains isolated)					Negative farms	No. of tested farms
	H1N1		H1N2		H3N2			H1N1		H1N2		H3N2		
	(P-P)[a]	(C-P)	(P-H)	(C-H)	(H-H)			(P-P)	(C-P)	(P-H)	(C-H)	(H-H)		
Hokkaido						4	4						1	1
Tochigi	1(1)			1(3)		1	3				2(2)		0	2
Ibaraki											1(1)		0	1
Gunma	2(5)			8(26)		1	10				8(59)		3	11
Chiba		1(3)		1(1)	1(1)	0	1				1(9)		1	1
Niigata			1(2)			0	1			2(4)			0	2
Aichi	1(1)					0	1							
Tottori	1(3)					0	1							
Okayama								1(1)					0	1
Nagasaki					1(2)	0	1					1(2)	0	1
Miyazaki													2	2
Kagoshima	2(4)					0	2					2(6)	1	3
Aomori													1	1
Iwate													1	1
Yamagata													1	1
Shizuoka													1	1
Hiroshima						1	1							
Fukuoka						1	1							
Saga													1	1
Oita														
Kumamoto														

[a]Surface genes derived from A(H1N1)pdm09 (P), 1A.1 classical swine (C), and human seasonal (H) viruses, respectively. For example, H1N1(C-P) indicates IAVs-S with 1A.1 classical swine HA and A(H1N1)pdm09 NA genes.

(C-H) were distributed on 14 farms in 4 prefectures. H3N2 IAVs-S with human seasonal H3 HA and N2 NA genes (H-H) were found on 5 farms in 4 prefectures.

The geographic distributions of the viruses corresponding to these 5 combinations of HA and NA genes revealed the endemicity of some subtypes in Japan (Fig. 4). Of the 21 prefectures where samples were collected during 2015 to 2019, C-H H1N2 IAVs-S were isolated from 4 prefectures around the center of Japan (Chiba, Gunma, Ibaraki, and Tochigi). P-P H1N1 IAVs-S were isolated from 9 prefectures: 3 on the southern island, Kyushu (Kagoshima, Miyazaki, and Nagasaki); 5 on the main island, Honshu (Aichi, Gunma, Okayama, Tochigi, and Tottori); and 1 on the northern island, Hokkaido. C-P H1N1 IAVs-S were isolated in Chiba prefecture, and P-H H1N2 IAVs-S were obtained in Niigata and Aichi prefectures. H-H H3N2 IAVs-S were isolated from 3 prefectures on Kyushu (Kagoshima, Miyazaki, and Nagasaki) and from Chiba prefecture.

Gene constellations and their numbers in the present study revealed all IAVs-S isolated here had at least 1 gene that was derived from an A(H1N1)pdm09 virus, except for a single strain isolated in Tochigi prefecture: A/swine/Tochigi/38-7119/2019 (H1N2) inherited all of its genes from Japanese pig isolates that circulated during the 1990s and 2000s (Fig. 5).

Genetic evolution of IAVs-S among pig populations on selected farms

During 2015 to 2019, active surveillance over prolonged periods yielded continuous isolation of IAVs-S on some farms (Table 2). Out of the 12 farms where IAVs-S were isolated twice or more through active surveillance, single genotype IAV-S was introduced and persisted at 4 farms (004, 034, 006, and 012), while 8 farms (001, 007, 009, 010, 011, 008, 035, and 040) experienced multiple introductions. In particular, farms 001, 006, 007, and 012 were IAV-S positive at least 15 times during 3 years or more. The evolutionary analyses of the HA genes of those isolates as well as their genetic constellations revealed that farms 001 (Fig. 6) and 007 [Figs. 7a for classical swine, 7b for A(H1N1)pdm09] had experienced multiple introductions of different genotypes whereas farms 006 (Fig. 8) and 012 (Fig. 9) had virus persistence, where viruses belonging to the single clade persisted for 3 or more years. All 4 farms applied farrow-to-finish operating systems and 300, 500, 1,000, and 2,000 sows were raised at farms 001, 006, 007, and 012, respectively.

On farm 001, H1N1 and its reassortant H1N2 IAVs-S (yellow green) were circulating from October 2015 to September 2016 (Fig. 6). Phylogenetically distinct H1N2 IAVs-S (orange) were sporadically isolated during the same period. Closely related but apparently distinct H1N2 IAVs-S (purple) emerged on the farm and circulated from March to October 2016; this was followed by

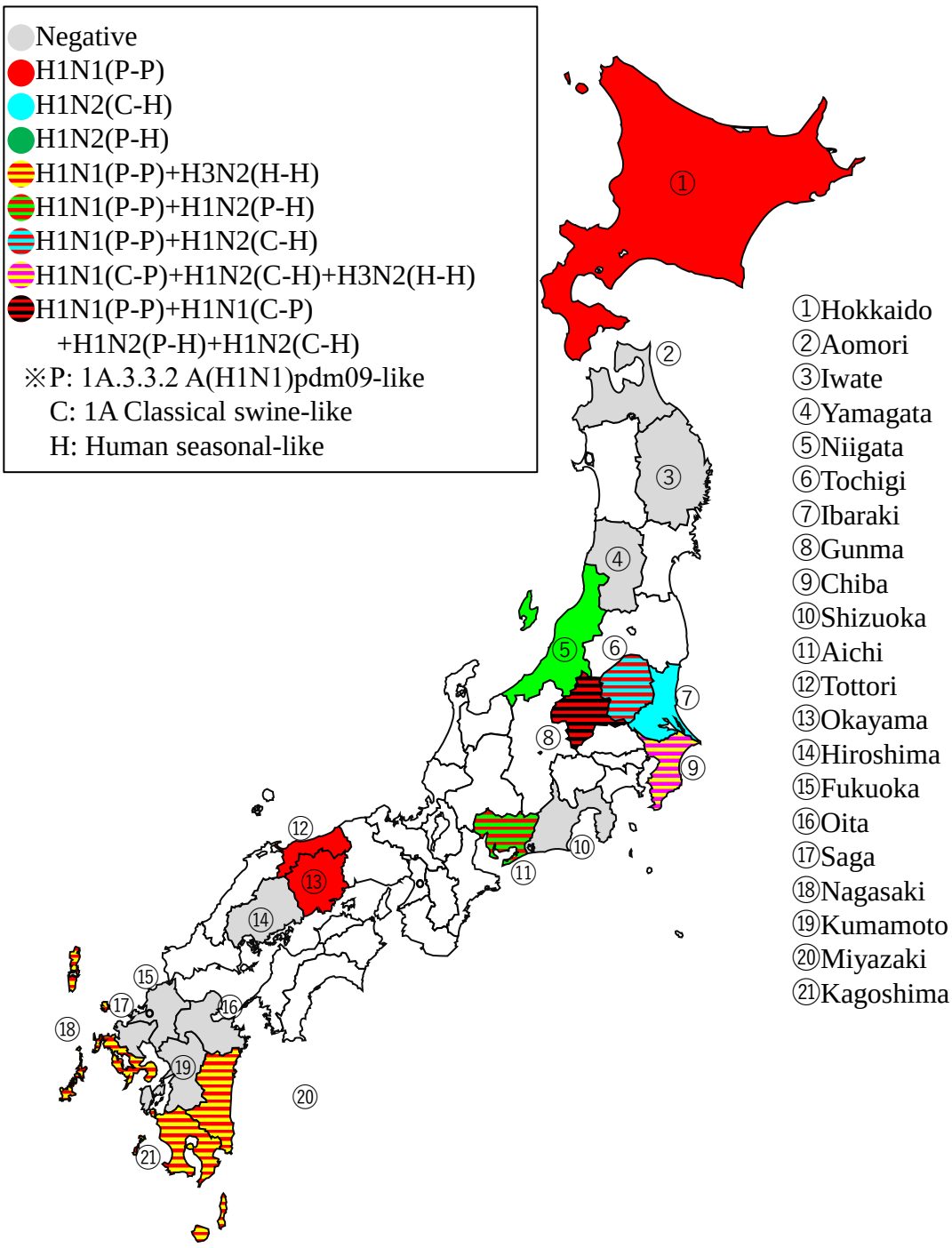

Fig. 4. Geographic distributions of the IAVs-S with various combinations of HA and NA genes.

Gray indicates prefectures where no IAVs-S were isolated; other colors indicate prefectures from which IAVs-S with various combinations of HA (1A.3.3.2 A(H1N1)pdm09 H1, 1A.1 classical swine H1, and human seasonal H3) and NA (A(H1N1)pdm09 N1 and human seasonal N2) were isolated.

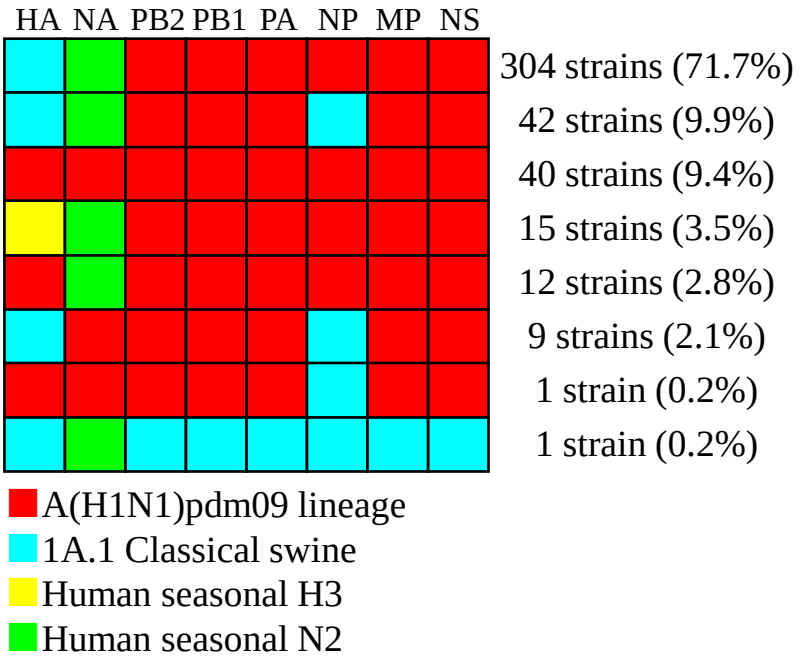

Fig. 5. Genetic constellations revealed by phylogenetic analyses.
Genes classified as A(H1N1)pdm09, 1A.1 classical swine, and human seasonal H3 and N2 were colored with red, light blue, yellow, and light blue, respectively. Detection rate according to total number of IAVs-S (424 strains) for each combination is shown in the right.

Table 2. Results of active surveillance activity regarding farms where samples were collected at least twice.

Prefecture	Farm No.	No. of samplings (IAVs-S-positive)						No. of IAVs-S-positive/ total no. of samplings (%)	No. of IAVs-S isolated	Duration of IAV-S persistence[a] (months)	Deduced number of introduction
		total	2015	2016	2017	2018	2019				
Gunma	007	20 (20)	2(2)	10(10)	4(4)	2(2)	2(2)	100.0	84	42	1 H1N1, 2 H1N2
Chiba	001	27 (20)	5(4)	12(9)	6(4)	2(2)	2(1)	74.1	67	42	6 H1N2, 1 H3N2
Gunma	012	20 (16)	2(2)	10(9)	4(2)	2(2)	2(1)	80.0	40	39	1 H1N2
Gunma	006	20 (15)	2(1)	10(7)	4(3)	2(2)	2(2)	75.0	69	42	1 H1N2
Gunma	010	13 (9)	2(1)	10(8)	1(0)	0	0	69.2	16	9	2 H1N2
Gunma	040	12 (9)	0	3(2)	5(4)	2(2)	2(1)	75.0	13	34	2 H1N1, 2 H1N2
Gunma	009	20 (8)	2(1)	10(5)	4(1)	2(1)	2(0)	40.0	19	25	1 H1N1, 2 H1N2
Gunma	011	13 (6)	2(1)	10(5)	1(1)	0	0	46.2	12	11	2 H1N2
Gunma	034	7 (5)	0	0	3(2)	2(1)	2(2)	71.4	8	24	1 H1N2
Gunma	008	13 (4)	2(0)	10(4)	1(0)	0	0	30.8	20	4	1 H1N1, 1 H1N2
Gunma	035	7 (4)	0	0	3(1)	2(2)	2(1)	57.1	11	24	2 H1N2
Hokkaido	004	6 (2)	1(1)	2(1)	2(0)	1(0)	0	33.3	2	12	1 H1N1
Kagoshima	043	2 (1)	0	0	0	2(1)	0	50.0	3		
Gunma	036	7 (1)	0	0	3(0)	2(0)	2(1)	14.3	4		
Hokkaido	003	6 (1)	1(1)	2(0)	2(0)	1(0)	0	16.7	3		
Kagoshima	037	3 (1)	0	0	1(0)	2(1)	0	33.3	2		
Gunma	045	2 (1)	0	0	1(0)	1(1)	0	50.0	1		
Hokkaido	002	6 (0)	1(0)	2(0)	2(0)	1(0)	0	0.0	0		
Hokkaido	005	6 (0)	1(0)	2(0)	2(0)	1(0)	0	0.0	0		
Kagoshima	013	4 (0)	0	4(0)	0	0	0	0.0	0		
Kagoshima	027	2 (0)	0	2(0)	0	0	0	0.0	0		

[a]: the longest period that IAV-S was repeatedly isolated in the farm, regardless of genotypes.

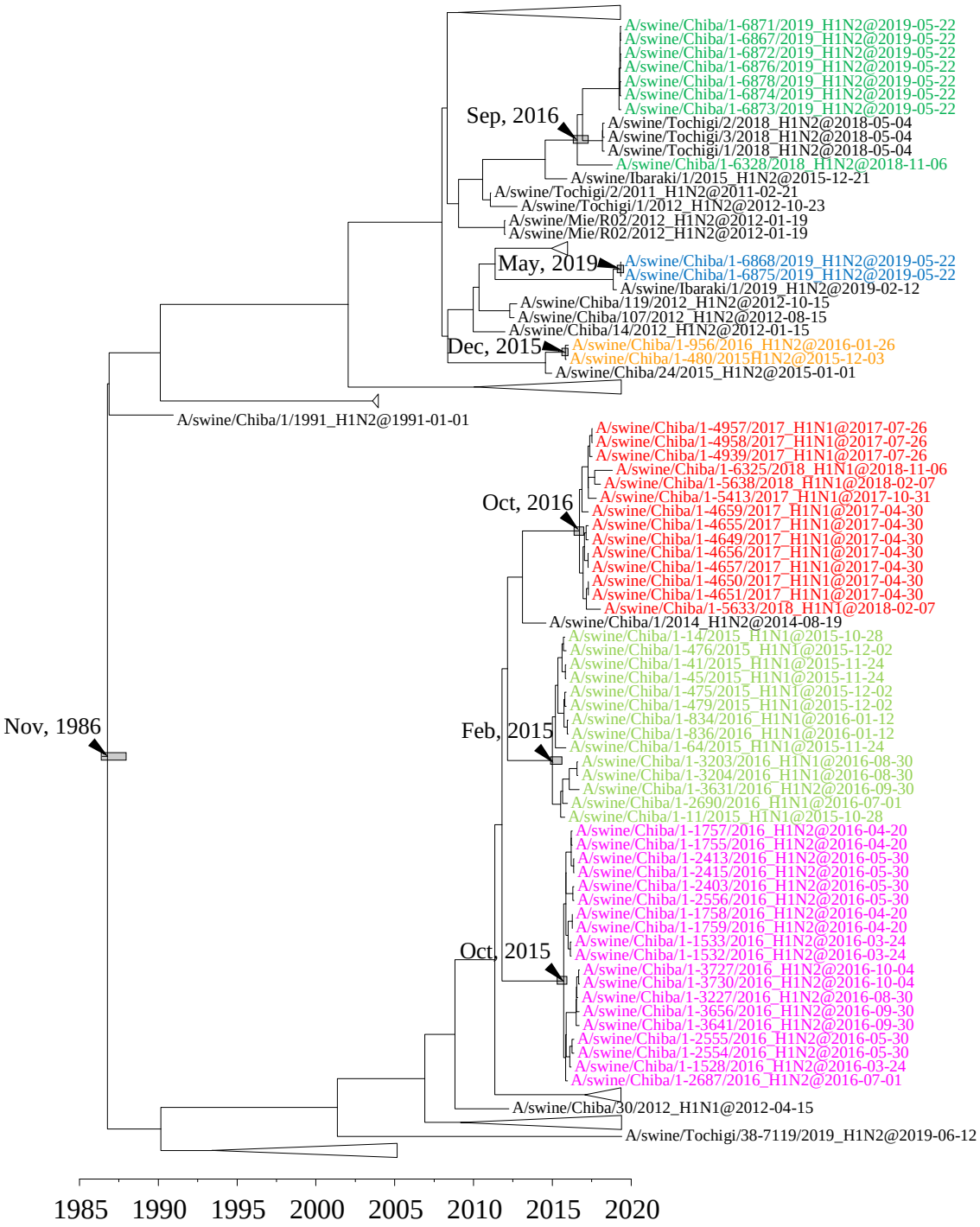

Fig. 6. Detail of MCC tree of H1 HA genes in the 1A.1 classical swine lineage. Colored text indicates H1N1 and H1N2 IAVs-S isolated at farm 001 as follows: H1N1 and its reassortant H1N2 IAVs-S circulating from October 2015 to September 2016, yellow green; phylogenetically distinct H1N2 IAVs-S sporadically isolated during the same period, orange; closely related but apparently distinct H1N2 IAVs-S circulated from March to October 2016, purple; other related H1N1 strains from April 2017 to November 2018, red; other H1N2 IAVs-S occurred since November 2018, dark green; phylogenetically distinct IAVs-S isolated in May 2019, blue.

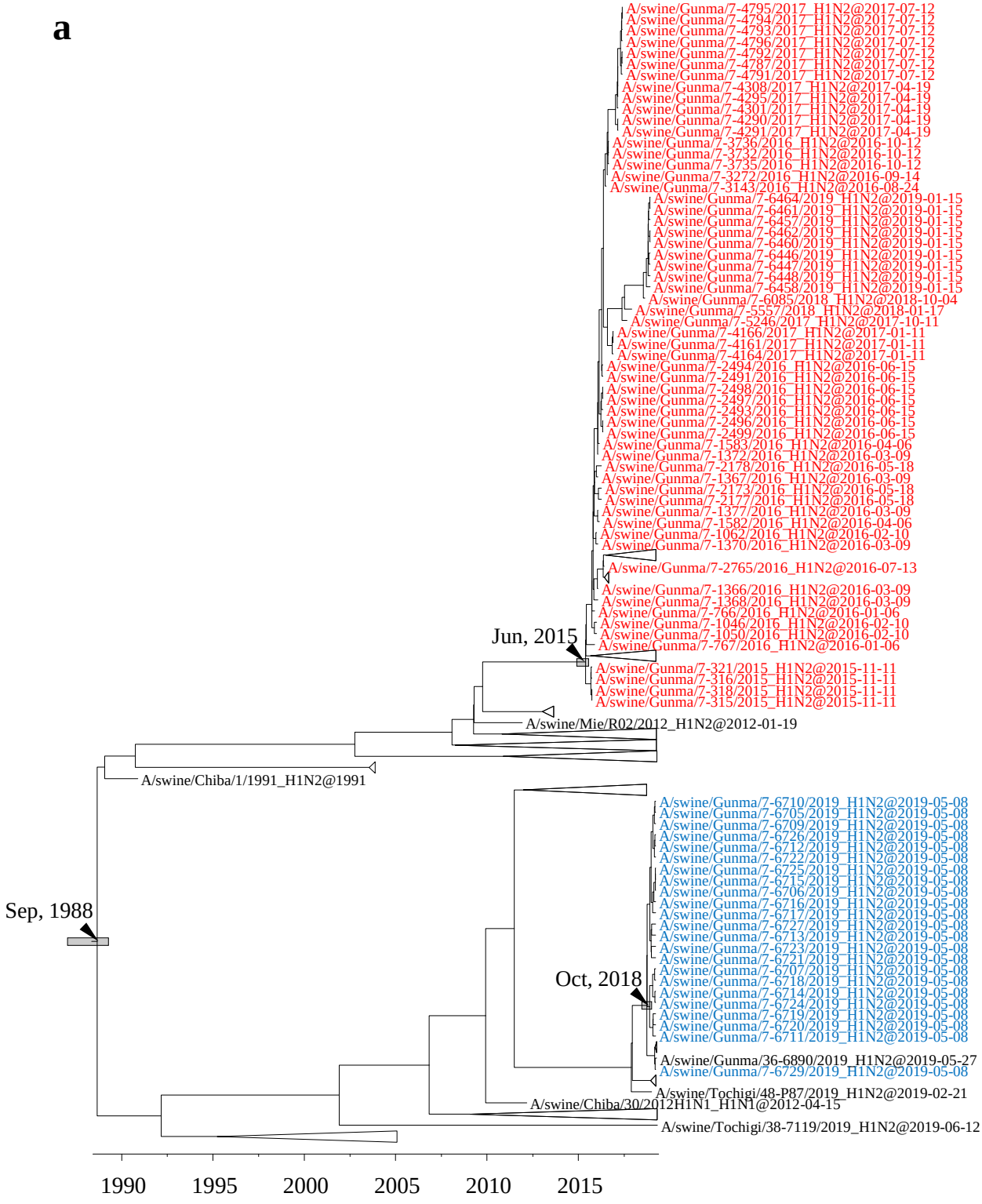

Fig. 7. Detail of MCC trees of H1 HA genes in the 1A.1 classical swine lineage (a) and 1A.3.3.2 A(H1N1)pdm09 lineage (b) (farm 007).
Colored text indicates H1N1 and H1N2 IAVs-S isolated at farm 007.

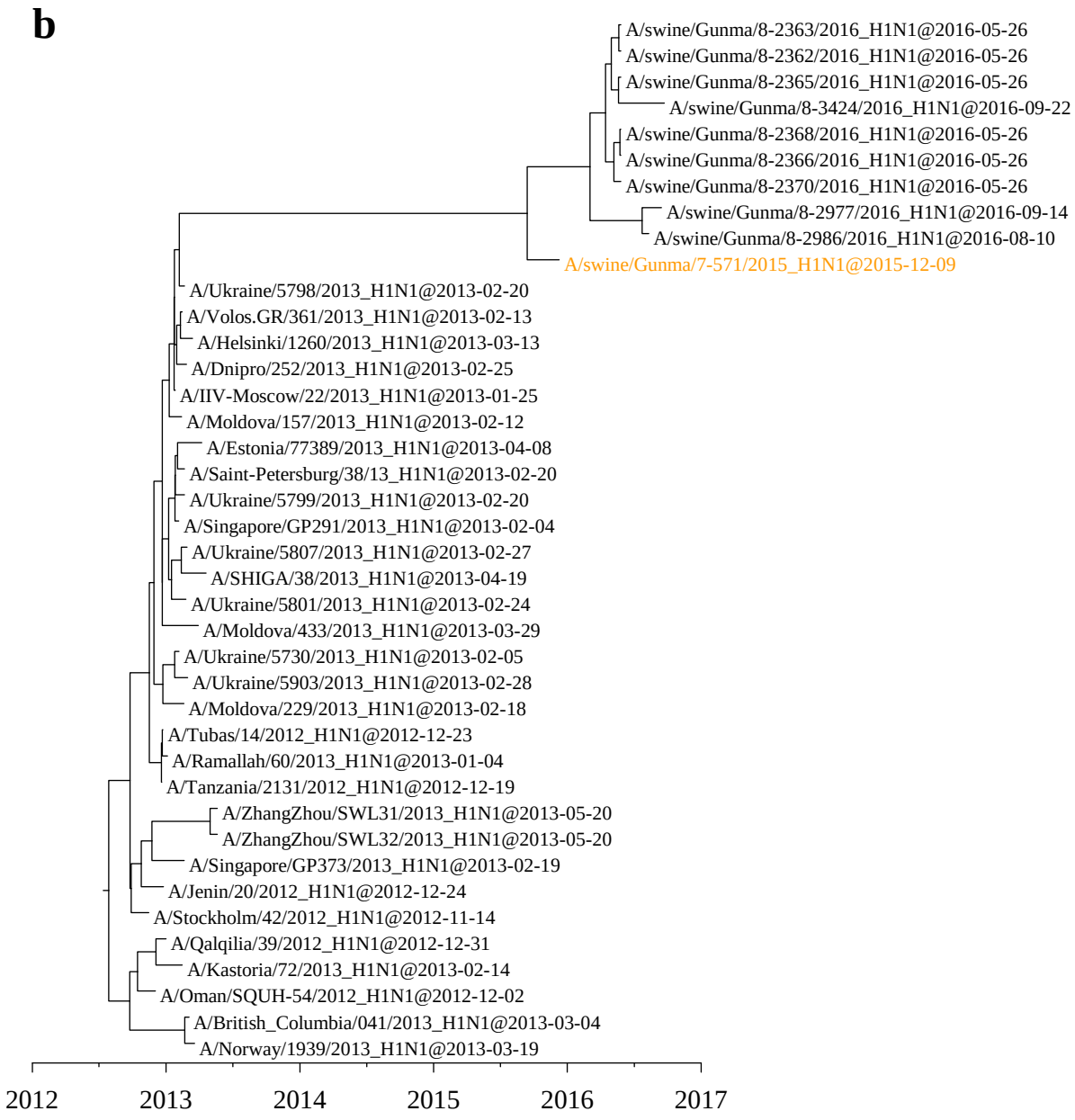

Fig. 7. Continued

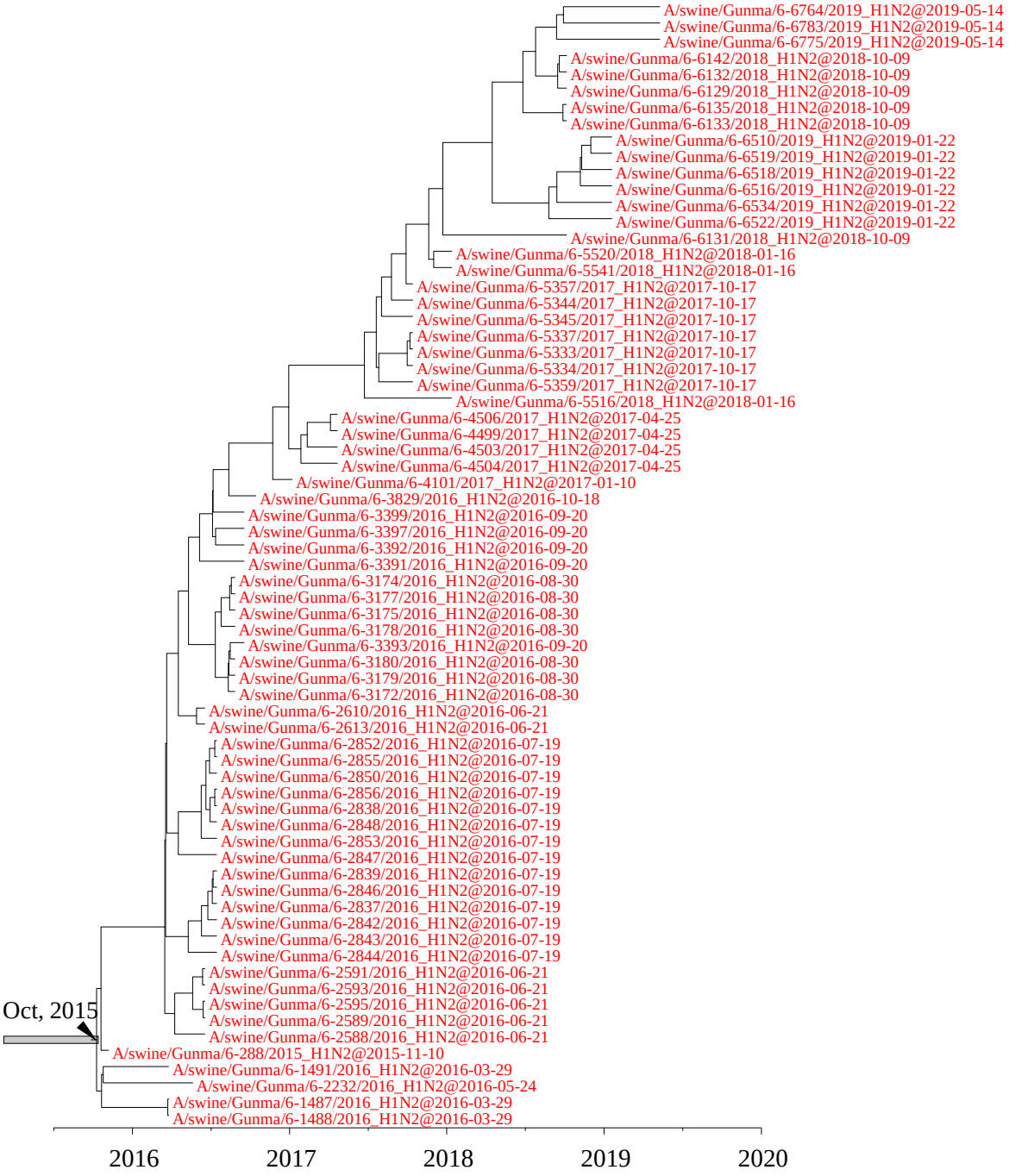

Fig. 8. Detail of MCC tree of H1 HA genes in the 1A.1 classical swine lineage (farm 006).

Red indicates H1N2 IAVs-S isolated at farm 006.

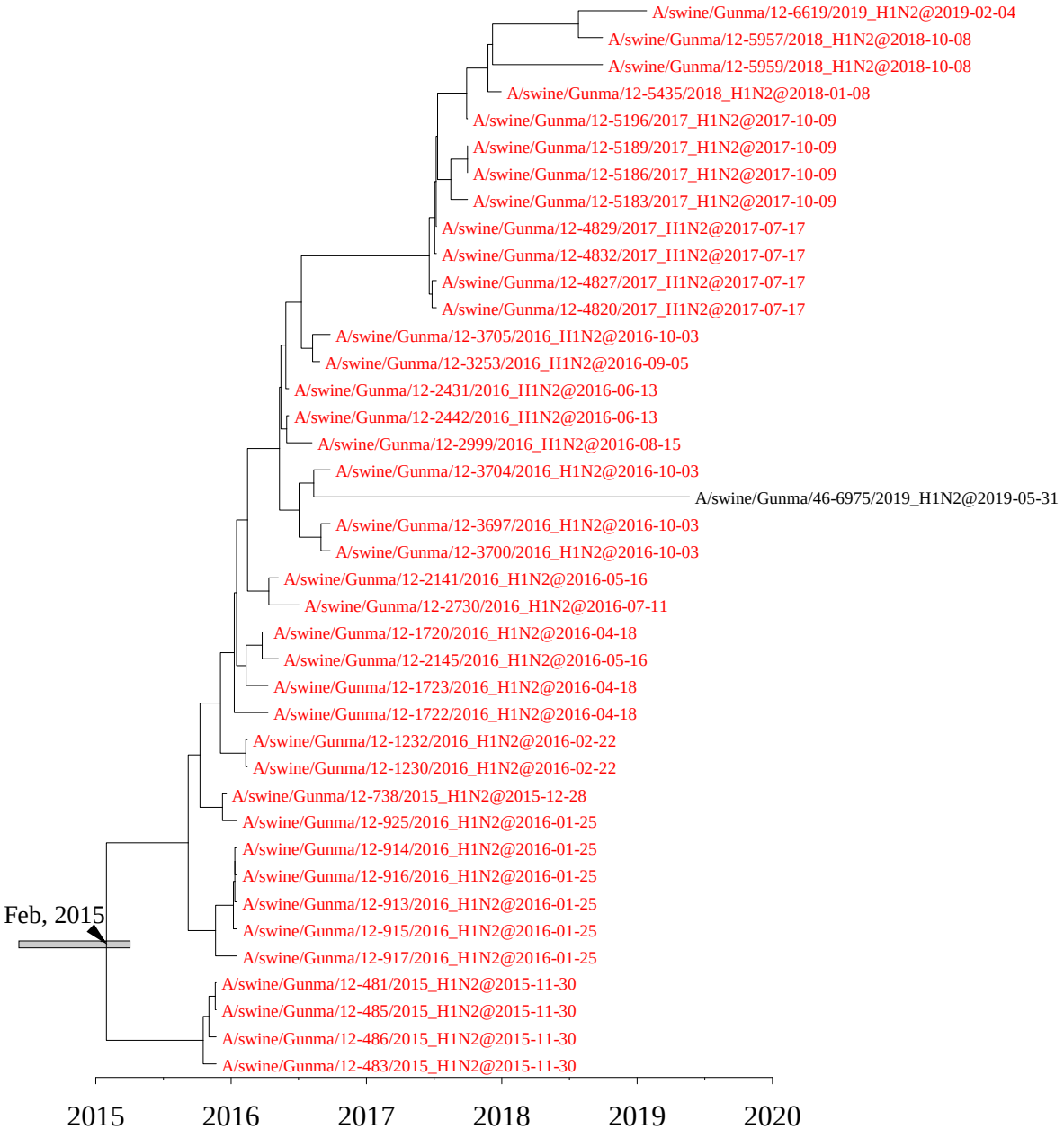

Fig. 9. Detail of MCC tree of H1 HA genes in the 1A.1 classical swine lineage (farm 012).

Red indicates H1N2 IAVs-S isolated at farm 012.

replacement by other related H1N1 strains (red) from April 2017 to November 2018. In February 2017, 4 H3N2 IAVs-S [A/swine/Chiba/1-4249/2017 (H3N2), A/swine/Chiba/1-4250/2017 (H3N2), A/swine/Chiba/1-4251/2017 (H3N2), A/swine/Chiba/1-4252/2017 (H3N2)] were isolated at the farm, and a progeny IAV-S [A/swine/Chiba/1-5640/2018 (H3N2)] was isolated 1 year later (Fig. 2b). Introduction of two other clusters of H1N2 IAVs-S occurred during 2018 to 2019. One cluster has been isolated since November 2018 (dark green), and another was first isolated in May 2019 (blue). The N2 NA genes of A/swine/Chiba/1-6328/2018 (H1N2) and 7 IAVs-S isolated in May 2019 were genetically distinguishable from the N2 NA genes of other H1N2 IAVs-S at the farm; the N2 NA genes of these viruses were phylogenetically distinct from those of the H3N2 IAVs-S. All internal genes of the H1N2 isolates were derived from A(H1N1)pdm09 viruses. In contrast, 5 of the internal genes (PB2, PB1, PA, MP, and NS) of the H1N1 IAVs-S were derived from A(H1N1)pdm09, but all of the NP genes were derived from 1A.1 classical swine H1 IAVs-S closely related to Japanese pig isolates during the 1990s and 2000s (Fig. 5). All of the internal genes of the H3N2 IAVs-S at the farm were A(H1N1)pdm09 in origin. However, the PB2, PB1, PA, and MP genes were phylogenetically distinguishable from those of H1 IAVs-S on the farm although NP and NS genes were shared with them, indicating the reassortment of H1 and H3 IAVs-S.

In the case of farm 007, two phylogenetically distinct 1A.1 classical swine H1 IAVs-S were introduced (Fig. 7a). One was first isolated in November 2015 and persisted until January 2019 (red); the other was isolated in May 2019 (blue). In addition to 1A.1 classical swine H1 IAVs-S, an 1A.3.3.2 H1 IAV-S that originated from an A(H1N1)pdm09 virus circulating within the human population during the 2012–2013 season was isolated in December 2015 (Fig.7b). Likewise, the NA genes of those isolates were phylogenetically classified into 3 groups: 2 groups derived from human seasonal-derived N2 NA genes and the remaining group from an A(H1N1)pdm09-derived N1 NA gene. All internal genes were derived from A(H1N1)pdm09 viruses and comprised 3 phylogenetically distinct groups.

At two farms, 006 and 012, H1N2 IAVs-S with 1A.1 classical swine H1 and human seasonal N2 NA genes derived from a single introduction had circulated for more than 3 years (Figs. 8 and 9). On farm 006, H1N2 IAVs-S were first isolated in November 2015, and they persisted until May 2019. At farm 012, H1N2 IAVs-S persisted from November 2015 to February 2019. An IAV-S genetically related to the strains on farm 012, A/swine/Gunma/46-6975/2019 (H1N2), was isolated at another farm in the same prefecture during May 2019. The N2 and internal genes of all IAVs-S isolated at farm 006 formed a single clade

in phylogenetic trees constructed for all genes, indicating that they were all derived from the single introduction. Likewise, all genes of the IAVs-S at farm 012 formed a single clade.

Discussion

The aims of this study were to illustrate the current situation of IAVs-S in pig populations in Japan and to show how IAVs-S genetically evolved at farms where they were isolated over a long period of time. The current phylogenetic analyses of HA genes revealed that 3 types of IAVs-S have been isolated in Japan. As reported previously (62-64), the 1A.1 classical swine H1 lineage in Japan has evolved uniquely in Japanese pig populations, as neither a human nor foreign isolate carrying an HA gene related to 1A.1 classical swine H1 HA genes of Japanese pig isolates has been reported since the late 1970s. Although triple-reassortant H3N2 viruses related to isolates in Canada were obtained in Japan during animal quarantine (78), they do not appear to have been introduced into the swine population in Japan. Instead, multiple introductions of 1A.3.3.2 A(H1N1)pdm09 viruses from humans have affected the Japanese swine population. As has been reported throughout the world, A(H1N1)pdm09 viruses have repeatedly been introduced into swine in Japan and then reassorted with endemic IAVs-S (32-43). Frequent introductions of 1A.3.3.2 A(H1N1)pdm09 viruses occurred on Hokkaido, mainland Japan, and Kyushu in the present study (Fig. 4). Consequently, 1A.3.3.2 A (H1N1)pdm09 viruses that have been introduced into the swine population and reassorted with Japanese endemic H1N2 IAVs-S were observed in Niigata prefecture (Fig. 4). All cases of the isolation of 1A.3.3.2 A(H1N1)pdm09 viruses were sporadic except for those from farms in Niigata prefecture, where H1N2 IAVs-S possessing 1A.3.3.2 A (H1N1)pdm09 HA genes persisted from May 2017 to May 2019. In a previous study, experimental infection of pigs with 5 IAVs-S of 3 subtypes (H1N1, H1N2, and H3N2), followed by co-housing, yielded H1N2 IAVs-S that were more viable than other subtypes (79). Although the epidemiologic and genetic background in the previous experiment differed from those in the current study, circulation in the pig population in Niigata prefecture might have selected H1N2 IAVs-S with increased stability and viability.

IAVs-S with an H3 HA gene of human seasonal strains have been reported sporadically in Japan (40, 60, 61), but the current situation differs from that during 1970 to 2013. H3N2 IAVs-S derived from human seasonal influenza viruses were isolated in Hokkaido in 1985, Ehime in 2002, and Osaka in 2007 (70). However, no descendent strains have been isolated subsequently, suggesting that these H3N2 IAVs-S have disappeared without being established within the Japanese pig population. In contrast, the remaining H3N2 IAVs-S that inherited the HA gene from the 1999–2000 human seasonal virus, including those collected in the current study, were also isolated in Kumamoto prefecture, Kyushu

[A/swine/Japan/KU-MD4/2013 (H3N2)] (60) and from diagnostic specimens submitted from Miyazaki prefecture, Kyushu in 2013. Subsequent strains carrying HAs of the same lineage were isolated in 2017, 2018, and 2019 in Kyushu and Chiba prefectures (Fig. 2b). These findings suggests that H3N2 IAVs-S harboring the earlier-mentioned lineage of the HA gene adapted to swine well enough to be established within the Japanese pig population. One possible mechanism of this adaptation is that these H3N2 IAVs-S acquired internal genes derived from A(H1N1)pdm09 viruses. A previous study demonstrated that an avian H9N2 influenza virus transmits better from pigs to pigs when the internal genes were replaced by those from A(H1N1)pdm09 viruses (80). This possibility should be further explored concerning the H3N2 IAVs-S currently circulating in Japan.

Vaccination is one of the most frequently implemented strategies to control IAV-S on farms. However, the vaccine will be ineffective when the vaccine strain and field strains differ in antigenicity; when mutations occur at antigenic sites of the HA gene in a field strain of IAV-S that is of the same lineage as a vaccine strain; or when a virus possessing HA of a different lineage from the vaccine strain circulates in the field (81). The vaccine strains available in Japan were derived from isolates in the 1960s to 1970s, which are phylogenetically distinct from IAVs-S currently circulating in Japan. Therefore, vaccine strains need to be updated to combat classical swine H1, human seasonal H3, and 1A.3.3.2 A(H1N1)pdm09 and thus effectively control the current IAV-S situation in Japan. However, it is essential to know the antigenicity of the current IAV-S in Japan to select the appropriate vaccine strain. Furthermore, current vaccination coverage against IAV-S of Japanese swine is at most about 10%. This is partially because swine influenza is not regarded as a critical or notifiable disease in Japan.

Multiple introductions of IAVs-S with the same subtype but different lineages of the HA genes might have contributed the long-term isolation of IAVs-S on farms 001 and 007. The level of immunity to a particular strain of IAV-S against experimentally infected IAVs-S might be high enough to hamper reinfection for approximately 100 days (82). If the same was true for farm levels, the herd immunity achieved against pre-existing IAVs-S could suppress the prevalence of pre-existing IAVs-S for several months. However, it could not prevent a newly introduced IAV-S, providing that the newly introduced virus expresses an HA protein of different antigenicity from that of the preexisting one. This mechanism might be a factor in the long-term isolation of IAVs-S from a farm, such as farms 001 and 007; however, the occurrence of substitutions that are considered to influence the antigenicity of the HA proteins at positions 155 (83, 84) and 185 (85) could be another persistence-associated factor. On farm 012,

glutamic acid 155 (Sa site) in the HA protein was shared by IAVs-S from November 2015 to July 2016 and then was replaced by glycine in the IAVs-S collected from October 2016 to February 2019 (data not shown). Likewise, along with one amino acid substitution at the antigenic site (168 on Ca1 site), aspartic acid at position 185 (Sb site) in the HA protein was shared among IAVs-S from November 2015 to April 2017 and then was replaced by asparagine in the IAVs-S from October 2017 to May 2019 on farm 006. Single mutations at positions 145, 155, 156, 158, 159, 189, and 193 that are adjacent to the receptor binding site of the human H3 HA protein greatly reduced reactivity against serum obtained from ferrets infected with a wild-type strain (86). Of these 7 mutations, the single mutation at position 145 on H3 HA protein among IAVs-S also reduced reactivity against serum obtained from pigs infected with a wild-type strain (87). Likewise, in the present study, the single mutation at position 155 on H1 HA protein, which corresponds to 158 on H3 HA protein, might be critical for the altered antigenicity, enabling the variant to evade immunity against the previous strain on the farm. However, demonstration of an effect of lineage replacement and substitution at the antigenic site on the antigenicity of the HA protein is necessary to prove this hypothesis.

In summary, phylogenetic analysis reveals the current situation of IAVs-S in Japan and the genetic evolution of IAVs-S on various farms. Whereas the 1A.1 classical swine H1 IAVs-S and human seasonal H3 IAVs-S have been established among pig populations in Japan, 1A.3.3.2 A (H1N1)pdm09 IAVs-S have been introduced repeatedly from the human population. Therefore, IAVs-S surveillance should be continued to understand the status of IAVs-S among the pig population in Japan and to support vaccine strategies compatible with the current situation in Japan.

Summary

To assess the current status of IAVs-S throughout Japan and to investigate how these viruses persisted and evolve on pig farms, IAVs-S isolated during 2015–2019 were genetically characterized. Nasal swab samples collected through active surveillance and lung tissue samples collected for diagnosis yielded 424 IAVs-S—comprising 78 H1N1, 331 H1N2, and 15 H3N2 viruses—from farms in sampled 21 prefectures in Japan. Phylogenetic analyses of surface genes revealed that the 1A.1 classical swine H1 lineage has evolved uniquely since the late 1970s among pig populations in Japan. During 2015–2019, A(H1N1)pdm09 viruses have been repeatedly introduced into farms and reassorted with endemic H1N2 and H3N2 IAVs-S. H3N2 IAVs-S isolated during 2015–2019 formed a single clade that originated from 1999–2000 human seasonal influenza viruses; this situation differs from previous reports, in which H3N2 IAVs-S derived from human seasonal influenza viruses were transmitted sporadically from humans to swine but then disappeared without becoming established within the pig population. At farms where IAVs-S were frequently isolated for at least 3 years, multiple introductions of IAVs-S with phylogenetically distinct HA genes occurred. In addition, at one farm, IAVs-S derived from a single introduction persisted for at least 3 years and carried no mutations at the deduced antigenic sites of the hemagglutinin protein except only one at the antigenic site (Sa). These results extend our understanding regarding the status of IAVs-S currently circulating in Japan and how they genetically evolve at the farm level.

Chapter II

Genetic and antigenic dynamics of influenza A viruses of swine on pig farms in Thailand

Introduction

Since the 1970s, the pig farming in Thailand has expanded rapidly to become a major livestock industry in the country; about 1,000,000 tons of pig meat were produced annually during the last decade (57). In Thailand, IAV-S strains of the H1N1 and H3N2 subtypes were first isolated during the 1970s (27, 88). After that, IAV-S strains of the H1N1, H1N2, and H3N2 subtypes have circulated in Thailand (18-20, 65). After the 2009 pandemic, A(H1N1)pdm09 viruses have become dominant, replacing classical swine H1N1 viruses, and the internal genes of H3N2 IAVs-S have been replaced by those of A(H1N1)pdm09 viruses (20, 39, 89-91). These viruses were generated through coinfection of IAVs-S in pigs followed by reassortment, as reported previously (21). Several longitudinal surveillance studies have revealed the dynamics of IAV-S from intrusion to extinction on swine farms (42, 92, 93). However, how IAVs-S might evolve to be retained within the pig population on a farm remains unclear.

In this study, five pig farms in Thailand were monitored from 2011 through 2017 to learn how IAV-S evolved within these populations. At the target farms, nasal swabs were collected from clinically healthy weaning pigs and sows for virus isolation followed by genetic and antigenic analyses. These analyses improve our understanding regarding how IAV-S evolve genetically and antigenically to be maintained longitudinally in the pig-farm setting.

Materials and Methods

Sample collection

Using the same techniques as previous study (65), nasal swabs were collected from clinically healthy weaning pigs (age, 3 to 10 weeks) and sows to elucidate the dynamics of IAVs-S reared on five pig farms (Table 3). Farms B and C are in Chonburi province, and farms D, O, and P are in Chachoengsao province; each of the farms had a different owner. Farms B and C adjoined each other, separated by a fence (Fig. 10). Beginning in 2011, nasal swabs were collected 12 times (February and July 2011; July 2012; May, August, and November 2013; March 2014; July 2015; February and July 2016; and February and July 2017) at farms B and C; nine times (February, July, and October 2011; July 2012; February, August, and November 2013; March 2014; and July 2015) at farm D; five times (July 2015, February and July 2016, and February and July 2017) at farm O; and four times (February and July 2016 and February and July 2017) at farm P (Table 4). The number of swabs collected from weaning piglets and sows enabled the detection of at least one IAV-S–infected pig with the probability of 0.95 if the prevalence rate was greater than 15% in each population (94).

Nasal swabs were promptly placed in transport media as described in chapter I and were kept on ice packs until transported to the National Institute of Animal Health in Thailand. Then, the swabs were removed, and the medium was aliquoted; several aliquots of each sample were stored at –80 °C as stocks. The remaining samples were stored at 4 °C until used for virus detection within 24 hours and for virus isolation within 48 hours, as described later.

Virus detection

RNA was extracted from swab samples by using RNeasy Mini Kits (Qiagen). The extracted RNA was reverse-transcribed to cDNA by using Superscript III (Thermo Fisher Scientific) and universal primers for IAV (66). cDNA was used as the template for real-time PCR analysis by using SYBR Premix Ex Taq (Takara Bio) with primers specific for the MP gene, as described previously (67).

Virus isolation

For virus isolation, media from nasal swab samples that were positive according to real-time PCR analysis were filtered (pore size, 0.45 μm; Millipore) and inoculated into the allantoic cavities of 10-day-old embryonated chicken eggs and cultures of MDCK cells in Minimum Essential Media (Sigma-Aldrich) containing penicillin (100 units/ml) (Thermo Fisher Scientific), streptomycin

Table 3. Characteristics of the farms surveyed in this study.

Farm	General information			Number of pigs						Workers					
	Country	Province	Operation type	Suckling piglets (0–3 wk)	Weaning piglets (4–10 wk)	Fattening piglets (11 wk–6 mo)	Sows (1–3 yr)	Gilts	Boars	Number of workers	Workers' living quarters	Shower facilities	Wears worn while working	Boots worn while working	Masks worn while working
B	Thailand	Chonburi	Farrow to Finish	700	4,000	10,000	2,000	50	40	100	Inside the farm	Yes	Yes	Yes	No
C	Thailand	Chonburi	Farrow to Finish	700	3,500	5,000	1,500	90	30	50	Inside the farm	Yes	Yes	Yes	No
D	Thailand	Chachoengsao	Farrow to Finish	1,900	4,000	3,500	1,300	-	20	36	Inside the farm	Yes	Yes	Yes	No
O	Thailand	Chachoengsao	Weaning to Finish	-		20,000	-	-	-	86	Outside the farm	Yes	Yes	Yes	No
P	Thailand	Chachoengsao	Farrow to Weaning	800	1,000	-	100	-	15	8	Outside the farm	Yes	Yes	Yes	Yes

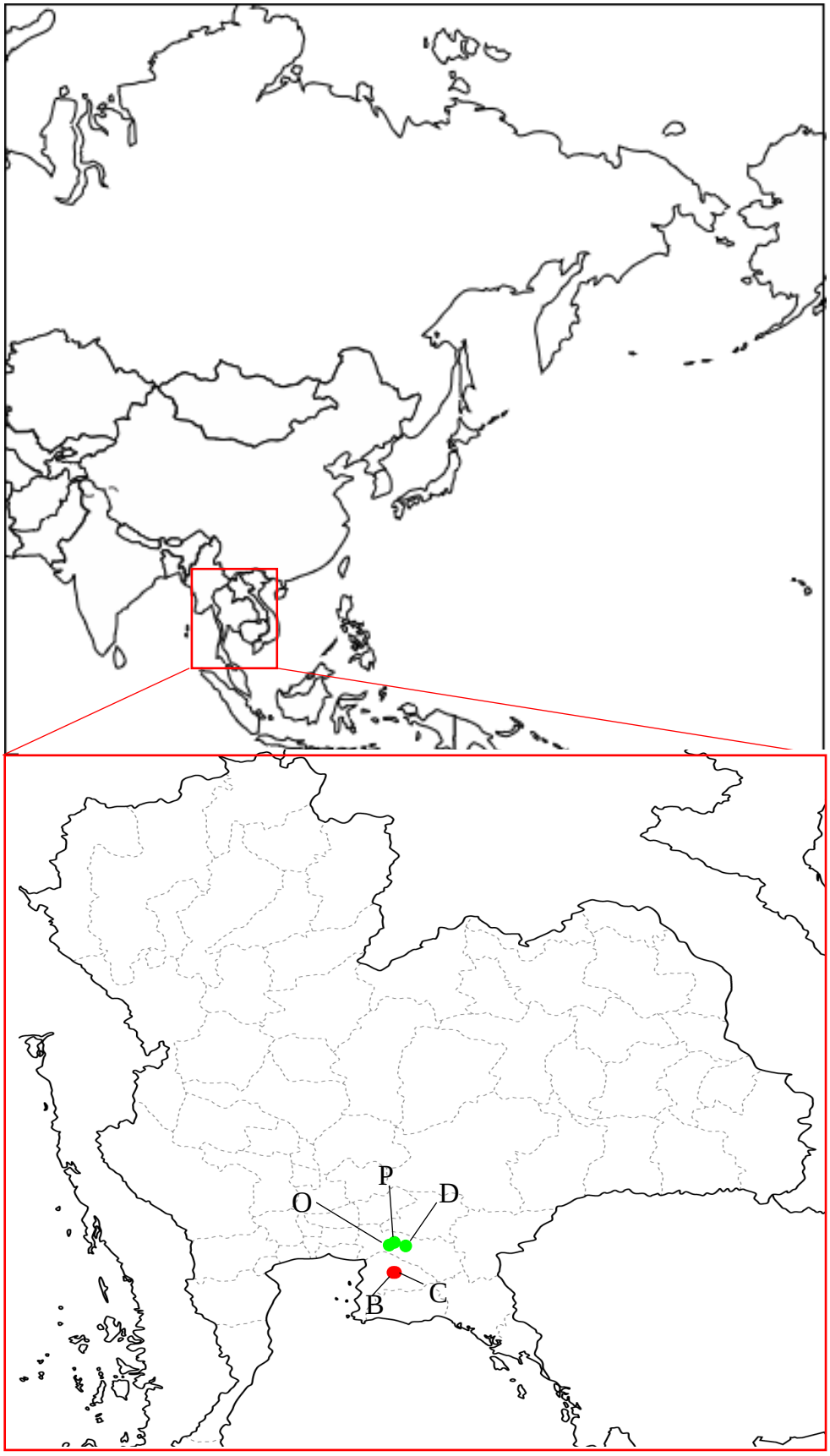

Fig. 10. Geographic locations of farms where nasal swab samples were collected.
Red indicates B and C farms in Chonburi province and green indicates D, O, and P farms in Chachoengsao province.

Table 4 Surveillance schedule and numbers of nasal swabs collected in this study.

Farm	Collection date	2011			2012	2013				2014	2015	2016		2017	
		Feb	Jul	Oct	July	Feb	May	Jul	Nov	Mar	Jul	Feb	Jul	Feb	Jul
B	Sow	20	20	-	20	-	20	45	45	45	45	45	45	45	45
	Weaning piglets	40	40	-	40	-	40	56	56	56	56	56	56	56	56
C	Sow	20	20	-	20	-	20	45	45	45	45	45	45	45	45
	Weaning piglets	40	40	-	40	-	40	56	56	56	56	56	56	56	56
D	Sow	20	20	20	45	45	-	45	45	45	45	-	-	-	-
	Weaning piglets	40	40	40	55	56	-	56	56	56	56	-	-	-	-
O	Sow	-	-	-	-	-	-	-	-	-	-	-	-	-	-
	Weaning piglets	-	-	-	-	-	-	-	-	-	101	101	101	101	101
P	Sow	-	-	-	-	-	-	-	-	-	45	45	45	45	45
	Weaning piglets	-	-	-	-	-	-	-	-	-	56	56	56	56	56

(100 μg/ml) (Thermo Fisher Scientific), amphotericin B (2.5 μg/ml) (Thermo Fisher Scientific), gentamicin (25 μg/ml) (Thermo Fisher Scientific), 3× Minimum Essential Media Vitamin Solution (Thermo Fisher Scientific), 1× GlutaMAX (Thermo Fisher Scientific), 0.4% bovine serum albumin (Sigma-Aldrich), and 0.5 to 3.0 μg/ml trypsin (Thermo Fisher Scientific). After 4 days of incubation at 37 °C in the presence of 5% CO_2, the supernatants of these cell cultures were used in HA assays (72) with guinea pig erythrocytes.

Genomic sequencing and phylogenetic analysis

Each gene segment of isolated viruses was sequenced by using Sanger or next-generation sequencing. Sanger sequencing was performed as described in previous reports (18, 21). The complete genome sequences of viruses isolated after July 2016 were obtained through next-generation sequencing as described in chapter I. Consensus sequences were generated using FLUGAS software (World Fusion). The nucleotide sequences and isolation information for the viruses analyzed have been deposited in the GISAID EpiFlu database.

For phylogenetic analysis, complete sequences of each genome (PB2, 46,130 sequences; PB1, 34,052; PA, 48,692; H1 HA, 35,983; H3 HA, 32,481; NP, 46,441; N1 NA, 34,502; N2 NA, 34,264; MP, 61,853; and NS, 48,857) were downloaded from the GISAID databases in January 2017. Sequences of the isolates obtained during this study and all downloaded sequences were aligned using BioEdit and MAFFT. After alignment, sequences with ambiguous nucleotide bases were removed; remaining sequences were used for phylogenetic analysis in MEGA-CC with 100 bootstrap replicates, using the ML method in a general time-reversible model (95).

In addition, MCC trees were constructed to calculate molecular estimates of substitution rates and divergence times for the viruses. MCC trees were constructed using the BEAST method. Alignments of each gene were formatted using the Bayesian Evolutionary Analysis Utility at the default settings, except for clock rate; the initial clock rate was set as 1.0×10^{-5} (substitutions/site/year) to fit substitution rate of influenza viruses for constructing trees. Calculation was set as 1×10^8 to 1×10^9 steps in length, where the number of steps was that needed to obtain an effective sample size of more than 200. Substitution rates and Ka/Ks ratios of genes were calculated as mentioned earlier and were expressed using the Tracer function of BEAST (96).

Antigenic analysis

HI tests were performed using 0.5% (vol/vol) guinea pig erythrocytes according to the standard method (72). Post-infection ferret sera against the

human H3N2 viruses, A/Wuhan/359/95 (H3N2)(Wuh95), A/Sydney/5/97 (H3N2) (Syd97), A/Panama/2007/99 (H3N2) (Pan99), A/Wyoming/3/2003 (H3N2) (Wyo03), A/New York/55/2004 (H3N2) (NY04), A/Hiroshima/52/2005 (H3N2) (Hir05), and A/Uruguay/716/2007 (H3N2) (Uru07) (provided by the National Institute of Infectious Diseases); hyperimmune chicken sera against the swine H3N2 IAVs-S A/swine/Chachoengsao/2003 (H3N2) (Cha03) and A/swine/Saraburi/107725-28/2008 (H3N2) (Sar08) (generated through animal experiments under approval number 10-111, 29 March 2011); and hyperimmune chicken sera against the H1N1 IAVs-S A/swine/Narita/aq21/2011 (H1N1) (Nar11) and California/04/2009 (H1N1) (Cal09)(provided by the National Institute of Infectious Diseases) were used for antigenic analysis. Swine sera collected at farm C during May and December 2014 and July 2015 were used in HI tests against viruses isolated in this study. To remove nonspecific inhibitors of hemagglutination, all sera and antisera were treated with receptor-destroying enzyme from *Vibrio cholerae* (Denka Seiken, Tokyo, Japan) according to the manufacturer's protocol. Subsequently, each mixture was adsorbed to packed guinea pig erythrocytes for 60 min at room temperature.

Results

Sample collection and virus isolation

In total, the 3,790 swabs collected from the five farms in this study yielded 169 IAV-S isolates comprising 82 H1N1 and 87 H3N2 isolates during the monitoring period (2011 through 2017). No influenza virus isolates were obtained from farm P, giving an overall IAV-S isolation rate of 4.5% (Table 5).

From farm B in Chonburi province, 36 H1N1 and 34 H3N2 viruses were isolated (isolation rate, 6.7%). Two H3N2 (H3_ChoB11.2) viruses were isolated in February 2011 and two H1N1 viruses (H1_ChoB12.7) in July 2012. After the first isolation of these two subtypes, H1N1 viruses in May 2013 (H1_ChoB13.5), July 2015, July 2016, and February 2017; H3N2 viruses were isolated in May 2013, August 2013, and March 2014.

From farm C in Chonburi province, two H1N1 and three H3N2 viruses were isolated (isolation rate, 0.5%). No virus was isolated until July 2015, when samples yielded two H3N2 (H3_Cho15.7) isolates. After July 2015, two H1N1 (H1_ChoC16.2) and one H3N2 (H3_ChoC17.2) viruses were isolated in February 2016 and February 2017, respectively.

From farm D in Chachoengsao province, 45 H1N1 and 5 H3N2 viruses were isolated (isolation rate, 6.4%). These viruses comprised H1N1 viruses isolated in February 2011, October 2011, July 2012, February 2013, August 2013, November 2013, and March 2014 and H3N2 IAVs-S isolated in July 2012, February 2013, and July 2015.

From farm O in Chachoengsao province, where monitoring started in July 2015, 44 H3N2 viruses were isolated (isolation rate, 10.9%). Eighteen H3N2 isolates (H3_ChaO16.7) were isolated in July 2015, followed by another 26 H3N2 isolates (H3_ChaO17.7) in July 2017.

Genetic evolution of IAVs on the tested pig farms

To investigate the genetic evolution of the IAV-S isolates obtained in the current study, entire genome sequences of all isolates were determined and then individual segments were phylogenetically analyzed. The HA gene of the Thai H1N1 viruses isolated in this study originated from A(H1N1)pdm09 viruses, classified as 1A classical swine lineage 3.3.2 (97), and these formed three distinct clusters with bootstrap values of more than 60%, designated respectively as 3.3.2a, 3.3.2b, and 3.3.2c in the current study (Fig. 11).

The HA genes belonging to 3.3.2a consisted of the H1N1 viruses from farms B and C from 2012 through 2017 (Fig 12a). Those genes originated from A(H1N1)pdm09 viruses isolated from humans and swine in Asia (including

Table 5. Gene constellations of IAVs-S isolated in this study.

Farm	Group name	Subtype	Isolation rate (%)	Number of isolated viruses	Sampling date	Gene constellation[a]							
						HA	NA	PB2	PB1	PA	NP	M	NS
B	H3_ChoB11.2	H3N2	3.3	2	2011/2/7	Hl-a	Hl-a	3.3.2a	3.3.2a	3.3.2a	3.3.2ab	3.3.2ab	3.3.2ab
	H1_ChoB12.7	H1N1	3.3	2	2012/7/19	3.3.2a	3.3.2a	3.3.2a	3.3.2a	3.3.2a	3.3.2ab	3.3.2ab	3.3.2ab
	H3_ChoB13.5	H3N2	8.3	2	2013/5/27	Hl-a	Hl-a	3.3.2a	3.3.2a	3.3.2a	3.3.2ab	3.3.2ab	3.3.2ab
	H1_ChoB13.5	H1N1		3	2013/5/27	3.3.2a	3.3.2a	3.3.2a	3.3.2a	3.3.2a	3.3.2ab	3.3.2ab	3.3.2ab
	H3_ChoB13.8	H3N2	1.0	1	2013/8/19	Hl-a	Hl-a	3.3.2a	3.3.2a	3.3.2a	3.3.2ab	3.3.2ab	3.3.2ab
	H3_ChoB14.3	H3N2	28.7	29	2014/3/13	Hl-a	Hl-a	3.3.2a	3.3.2a	3.3.2a	3.3.2ab	3.3.2ab	3.3.2ab
	H1_ChoB15.7A	H1N1	3.0	3	2015/7/1	3.3.2a	3.3.2a	3.3.2a	3.3.2a	3.3.2a	3.3.2ab	3.3.2c	3.3.2ab
	H1_ChoB15.7B	H1N1	11.9	12	2015/7/1	3.3.2a	3.3.2a	3.3.2b	3.3.2a	3.3.2a	3.3.2ab	3.3.2ab	3.3.2ab
	H1_ChoB16.7	H1N1	1.0	1	2016/7/27	3.3.2a	3.3.2a	3.3.2a	3.3.2a	3.3.2a	3.3.2ab	3.3.2ab	3.3.2ab
	H1_ChoB17.2	H1N1	14.9	15	2017/2/9	3.3.2a	3.3.2a	3.3.2a	3.3.2a	3.3.2a	3.3.2ab	3.3.2ab	3.3.2ab
C	H3_ChoC15.7	H3N2	2.0	2	2015/7/1	Hl-b	Hl-a	3.3.2a	3.3.2a	3.3.2a	3.3.2ab	3.3.2ab	3.3.2ab
	H1_ChoC16.2	H1N1	2.0	2	2016/2/24	3.3.2a	3.3.2a	3.3.2b	3.3.2a	3.3.2a	3.3.2ab	3.3.2ab	3.3.2ab
	H3_ChoC17.2	H3N2	1.0	1	2017/2/8	Hl-b	Hl-a	3.3.2a	3.3.2a	3.3.2a	3.3.2ab	3.3.2ab	3.3.2ab
D	H1_ChaD11.2	H1N1	10.0	6	2011/2/3	3.3.2b	3.3.2b	3.3.2b	3.3.2b	3.3.2b	3.3.2ab	3.3.2ab	3.3.2ab
	H1_ChaD11.10	H1N1	1.7	1	2011/10/19	3.3.2b	3.3.2b	3.3.2b	3.3.2b	3.3.2b	3.3.2ab	3.3.2ab	3.3.2ab
	H1_ChaD12.7	H1N1	3.0	1	2012/7/10	3.3.2b	3.3.2b	3.3.2b	3.3.2b	3.3.2b	3.3.2ab	3.3.2ab	3.3.2ab
	H3_ChaD12.7	H3N2		2	2012/7/10	Hl-a	Hl-a	3.3.2c'	3.3.2c'	3.3.2c'	3.3.2c'	3.3.2c'	3.3.2c'
	H1_ChaD13.2	H1N1	9.9	8	2013/2/6	3.3.2c	3.3.2c	3.3.2c	3.3.2c	3.3.2c	3.3.2c	3.3.2c	3.3.2c
	H3_ChaD13.2	H3N2		2	2013/2/6	Hl-a	Hl-a	3.3.2c'	3.3.2c'	3.3.2c'	3.3.2c'	3.3.2c'	3.3.2c'
	H1_ChaD13.8	H1N1	3.0	3	2013/8/7	3.3.2c	3.3.2c	3.3.2c	3.3.2c	3.3.2c	3.3.2c	3.3.2c	3.3.2c
	H1_ChaD13.11	H1N1	4.0	4	2013/11/20	3.3.2c	3.3.2c	3.3.2c	3.3.2c	3.3.2c	3.3.2c	3.3.2c	3.3.2c
	H1_ChaD14.3	H1N1	21.8	22	2014/3/17	3.3.2c	3.3.2c	3.3.2c	3.3.2c	3.3.2c	3.3.2c	3.3.2c	3.3.2c
	H3_ChaD15.7	H3N2	1.0	1	2015/7/2	Hl-a	Hl-a	3.3.2c	3.3.2c	3.3.2c	3.3.2c	3.3.2c	3.3.2c
O	H3_ChaD16.7	H3N2	17.8	18	2016/7/15	Hl-b	Hl-a	3.3.2a	3.3.2a	3.3.2a	3.3.2c	3.3.2ab	3.3.2ab
	H3_ChaD17.7	H3N2	25.7	26	2017/7/5	Hl-b	Hl-a	3.3.2a	3.3.2a	3.3.2a	3.3.2c	3.3.2ab	3.3.2ab

[a]Each color means the genetic group as follows; Hl-a, green; Hl-b, yellow; 3.3.2a, light red; 3.3.2b, pink; 3.3.2c(3.3.2c'), blue; 3.3.2ab, dark pink

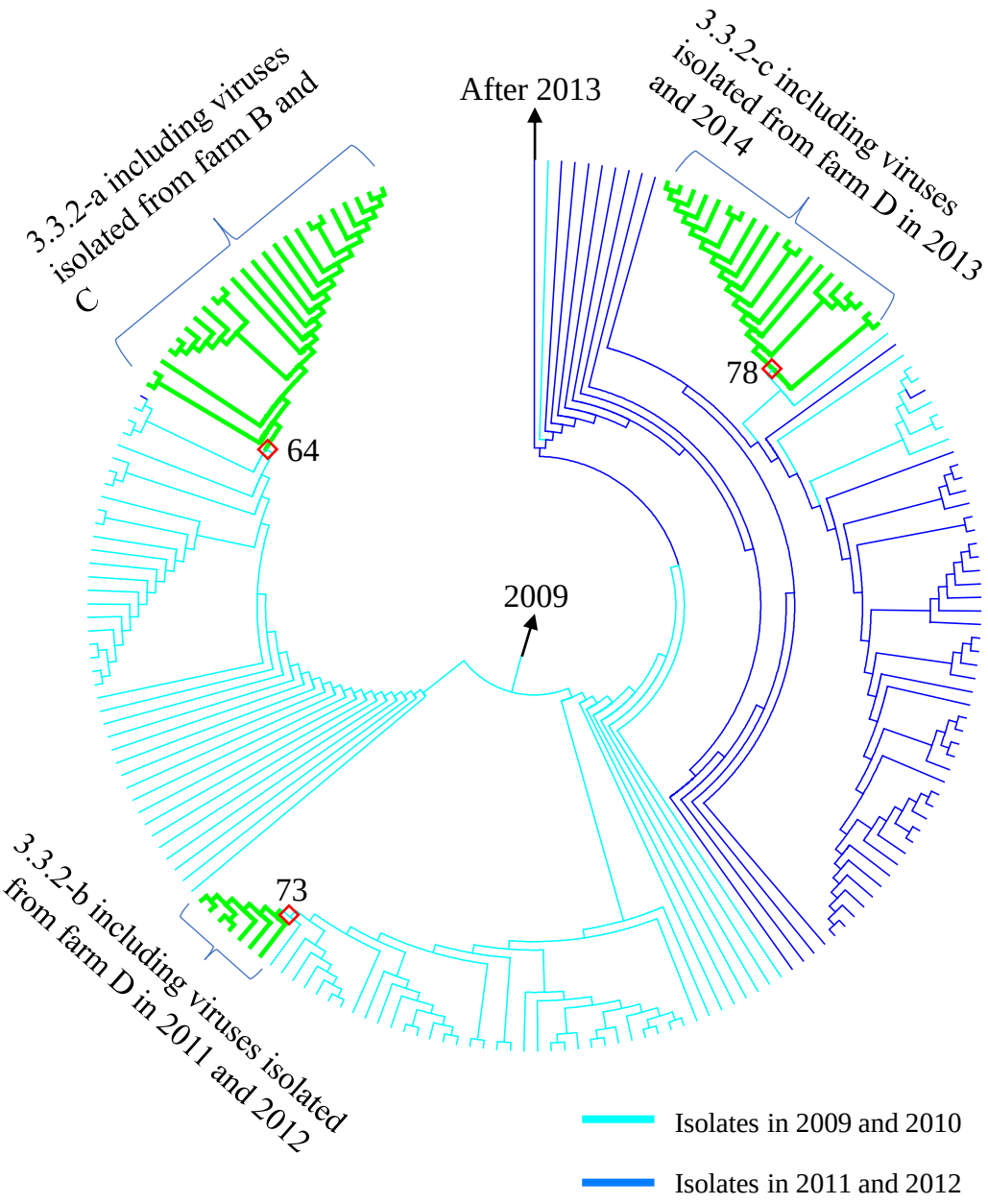

Fig. 11. Detail ML tree of isolates from this study that display H1 HA genes and those originating from A(H1N1)pdm09 viruses between 2009 and 2013.

IAVs isolated in 2009 and 2010 are shown in light blue; those isolated in 2011 and 2012 are in dark blue. Genetic groups 3.3.2a, 3.3.2b, and 3.3.2c are all shown in green. Bootstrap values at the root of each genetic group are indicated by red squares.

Fig. 12. Detail trees from the entire H1 HA MCC tree made of the genes of viruses isolated in this study and downloaded from the GISAID databases.
Genetic groups 3.3.2a, 3.3.2b, and 3.3.2c are shown in lines colored with light red (a), pink (b), and blue (c), respectively, in each panel. Strain names of isolates from farms B, C, and D are shown in red, orange, and blue, respectively. The gray box in each tree indicates the divergence time estimated by using BEAST.

b

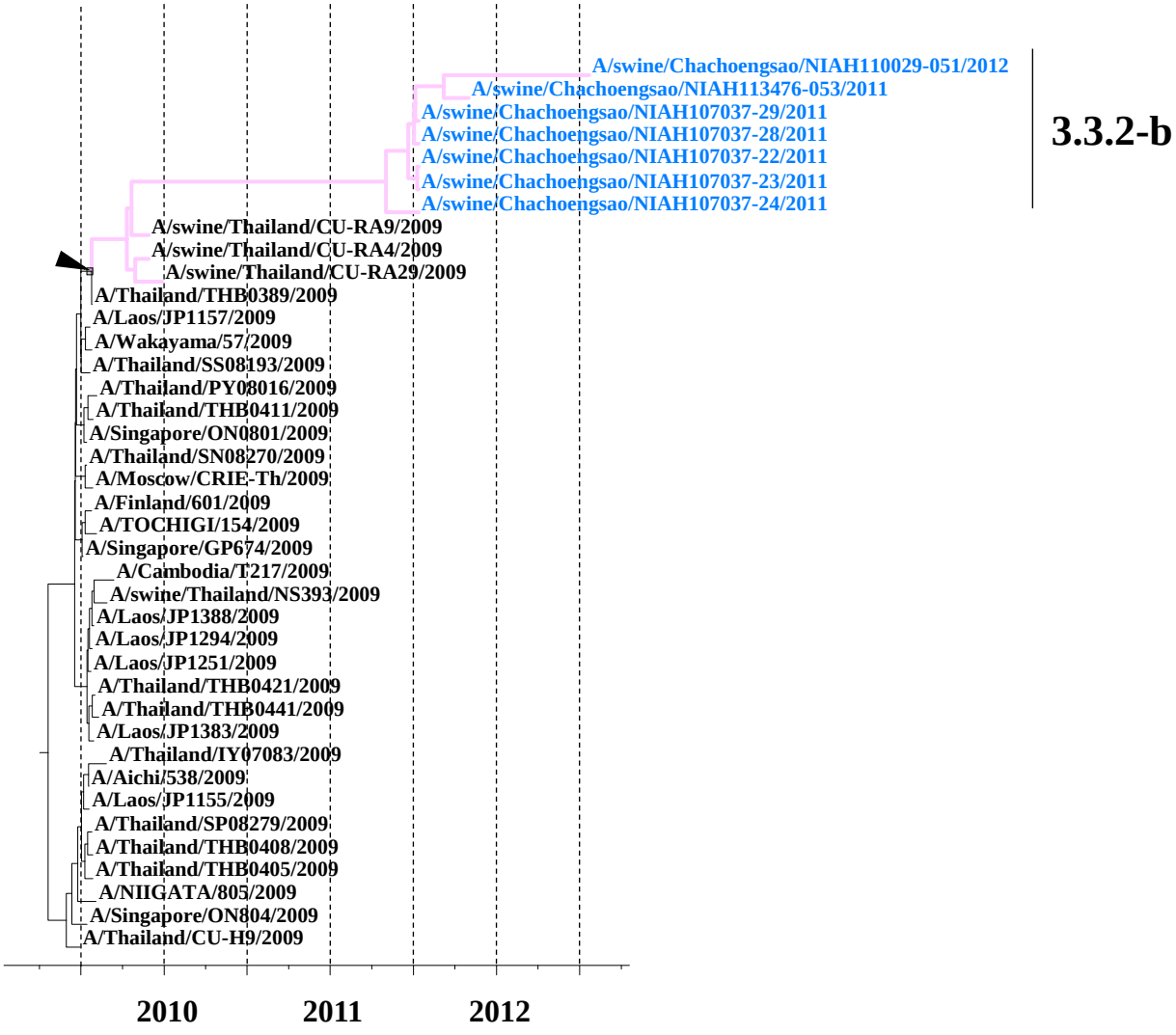

Fig. 12. Continued

c

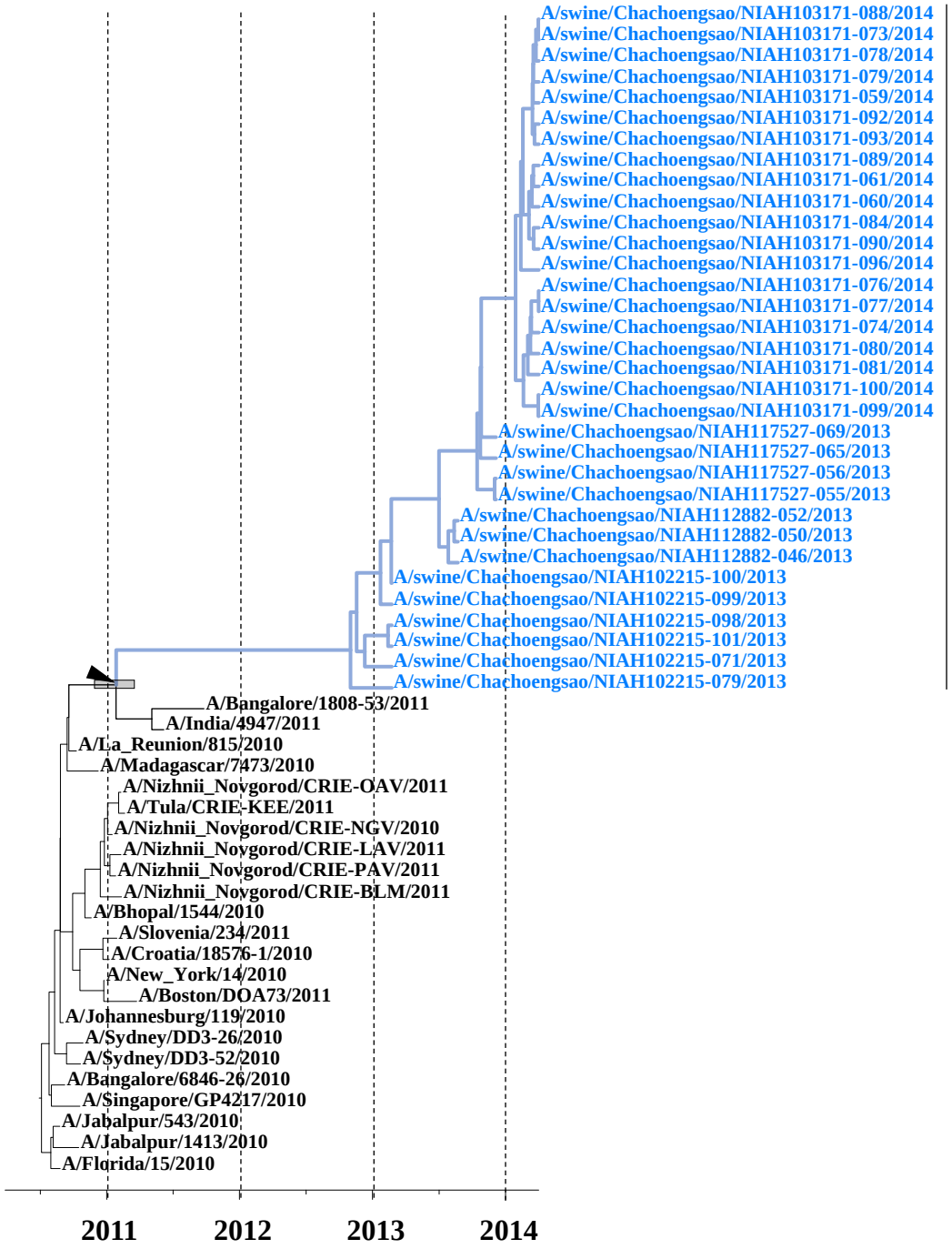

Fig. 12. Continued

Thailand) in 2009, and shared a putative common ancestor with A/swine/Saraburi/NIAH116627-24/2009 (H1N1) and A/Thailand/SS08208/2009 (H1N1). 3.3.2a genes were estimated to diverge as a phylogenetic group on 17 January 2010 (95% HPDV, 20 October 2009 to 22 April 2010; black arrow, Fig. 12a).

Clusters 3.3.2b of the H1 HA genes consisted of the viruses obtained in 2011 and 2012, and 3.3.2c of the H1 HA genes consisted of the viruses obtained in 2013 and 2014, respectively, from farm D (Figs. 12b and 12c). The HA genes of 3.3.2b originated from A(H1N1)pdm09 viruses isolated from humans and swine in Asia in 2009, and a group of Thai IAV-S isolates including A/swine/Thailand/CU-RA9/2009 (H1N1), formed an out-group of this cluster. The HA genes of 3.3.2b were estimated to diverge from human isolates on 25 July 2009 (95% HPDV, 12 July 2009 to 25 July 2009; black arrow in Fig. 12b). In contrast, genes of 3.3.2c originated from human viruses in 2010 to 2011, and a putative ancestral strain of 3.3.2c was estimated to diverge from those viruses on 25 January 2011 (95% HPDV, 18 October 2010 to 4 April 2011; black arrow, Fig. 12c).

The H3N2 viruses isolated in this study had the HA genes of the human-like IAV-S strains circulating among swine populations in Thailand (Fig. 13). They were divided into two distinguishable clades with bootstrap values of 98%, designated as human-like-a and human-like-b. The human-like-a clade consisted of those viruses isolated from farms B and D, and the human-like-b viruses were those from farms C and O. Both human-like-a and human-like-b originated from a seasonal influenza virus during 1996–1998, and they diverged as human-like-a and human-like-b in the late 1990s (95% HPDV, 1 January 1997 to 4 February 2001; black arrow, Fig. 13). No previous Thai IAV-S isolate that belonged to the human-like-a cluster has been recognized, whereas IAVs-S belonging to the human-like-b in this study were related to Thai H3N2 IAV-S isolates from 2005 to 2014, and they diverged around 2011 (95% HPDV, 8 November 2010 to 21 November 2011; red arrow, Fig. 13) from the human-like-b Thai IAVs-S.

The N2 NA genes of H3N2 viruses isolated from four of the five farms in this study originated from a seasonal influenza virus in the mid-1990s (Fig. 14a), and their patterns of divergence were similar to that of human-like-a H3 genes. HA and NA genes of IAVs-S were retained within Thai pig populations for approximately 20 years after the intrusion from humans, suggesting these genes gradually evolved to be endemic in pig populations.

The internal genes of the viruses isolated in this study originated from A(H1N1)pdm09 viruses and were divided into groups 3.3.2a, b, and c, as for the H1 genes. This pattern typically was seen for the PB1 genes. 3.3.2a originated

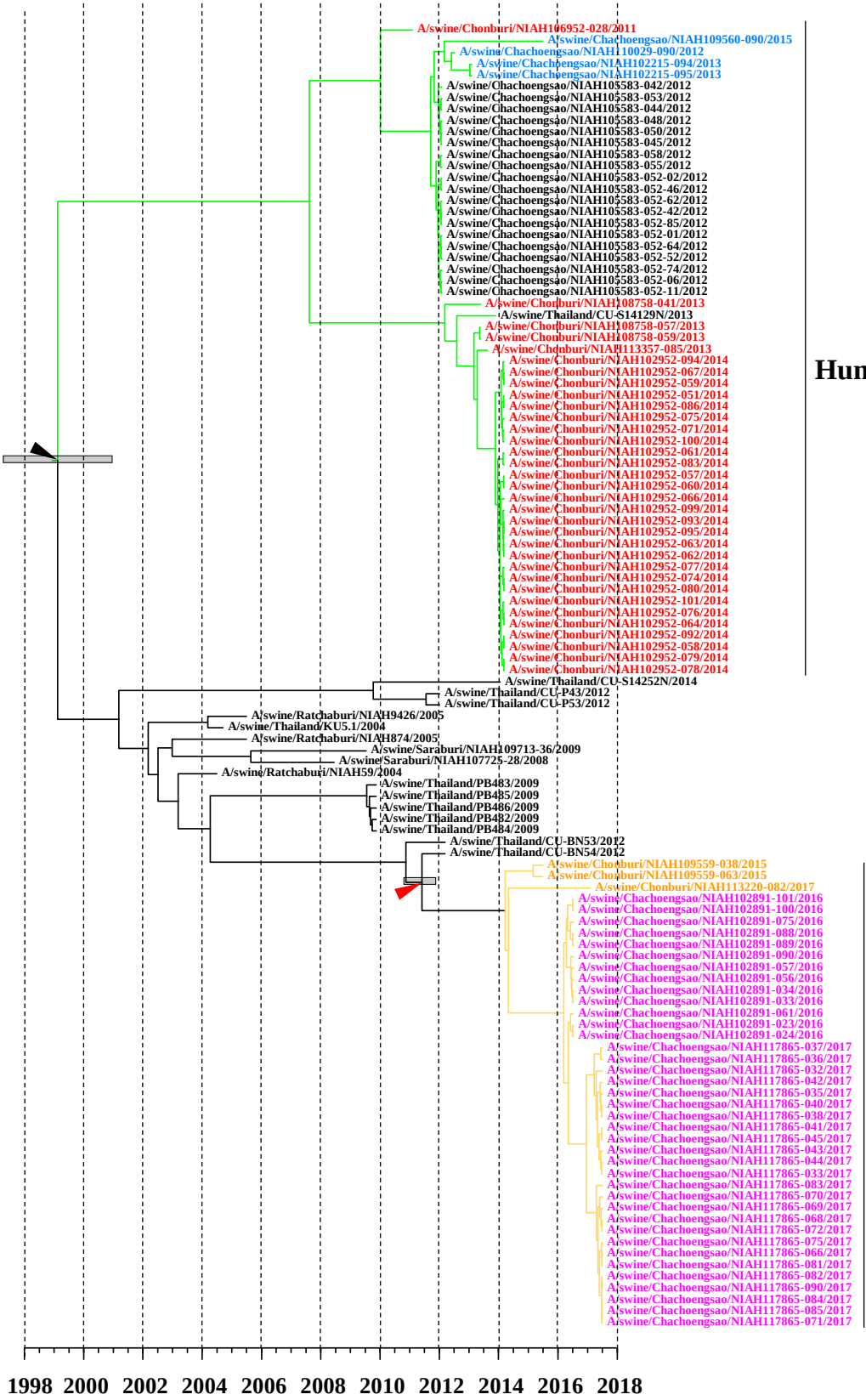

Fig. 13. Detail trees from the entire H3 HA MCC tree of the genes of viruses isolated in this study and downloaded from the GISAID databases.

Genetic group Human-like-a is shown in lines colored with green, and Human-like-b is in yellow. Strain names isolated from farms B, C, D, and O are shown in red, orange, blue, and purple, respectively. Gray boxes indicated the divergence time estimated by using BEAST.

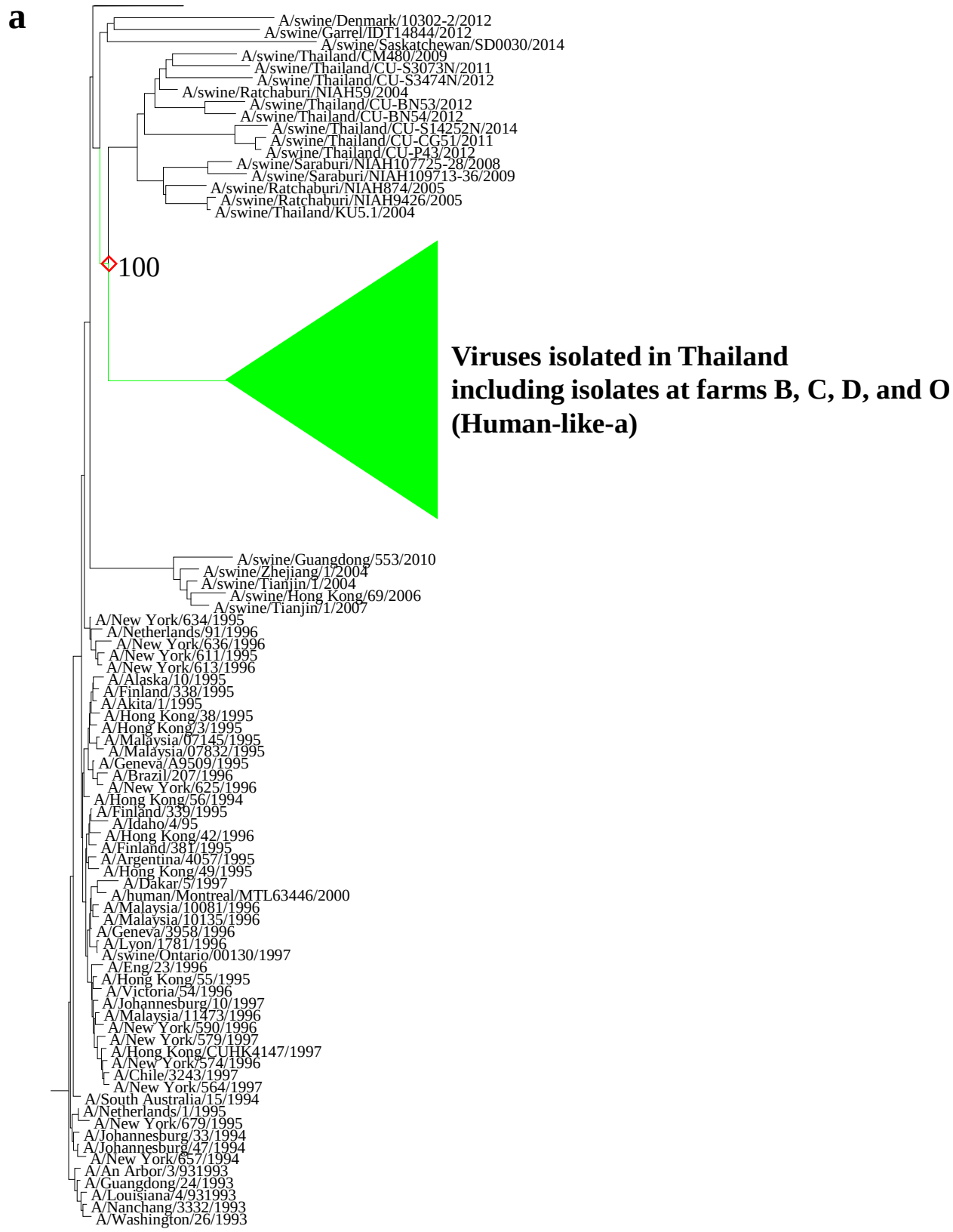

Fig. 14. ML tree (a) and MCC tree (b) of the N2 NA genes displayed by the H3N2 isolates in this study.

The genetic group Human-like-a is in green. In (a), bootstrap values at the root of each genetic group are indicated by red squares. Strain names of isolates from farms B, C, D, and O are shown in red, orange, blue, and purple, respectively in (b).

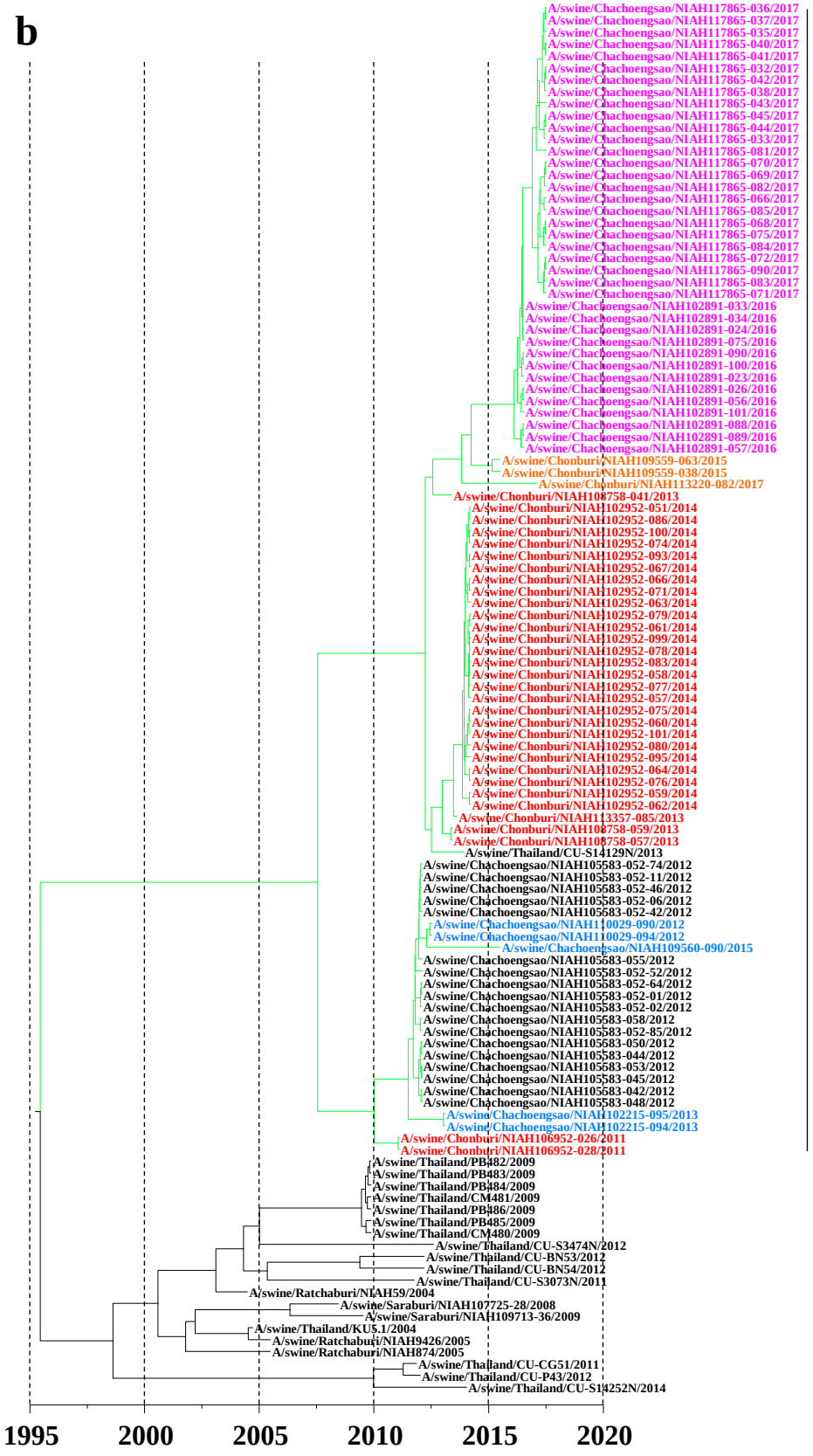

Fig. 14. Continued

from A(H1N1)pdm09 viruses isolated from humans and swine in Asia (Fig. 15a). 3.3.2b originated from another group of A(H1N1)pdm09 viruses isolated from humans and swine in Asia (Fig. 15b). 3.3.2c originated from a group of A(H1N1)pdm09 viruses isolated from humans and swine from various areas during 2010 to 2011 (Fig. 15c). In addition, 3.3.2c formed a further outgroup, designed as 3.3.2c′. Like 3.3.2c, 3.3.2c′ originated from A(H1N1)pdm09 viruses isolated from humans in Thailand in 2010 (red arrow, Fig 15c). The topology of the N1 NA, PB2, and PA genes of the Thai IAV-S isolates in this study were similar to those of the H1 HA and PB1 genes. However, the sequences of the NP, MP, and NS genes of the viruses were so closely related between 3.3.2a and b that they were not phylogenetically distinguishable (bootstrap value, <60%), therefore they were designated as 3.3.2ab (Fig. 16).

Because the divergence pattern was similar between the H1 HA and PB1 genes, as described, their estimated divergence times were compared (Table 6). Whereas the time of divergence differed by only 1 month between the H1 HA and PB1 genes in 3.3.2a, the dates of divergence for 3.3.2b and 3.3.2c of PB1 genes were at least 4 and 6 months earlier than those of H1 HA genes. However, such deviations might reflect differences of the numbers of full-length genes registered in the database.

Next, the genetic constellations of the viruses were scrutinized at each farm based on the genetic designation described earlier (Table 5). On farm B, except for two cases (H1_ChoB15.7A and B), the constellation of H1N1 IAVs-S remained the same throughout the monitoring period—the viruses in the constellation carried the HA, NA, PB2, PB1, and PA genes of 3.3.2a and the NP, MP, and NS genes of 3.3.2ab until July 2017. The two exceptional cases arose in July 2015, when the isolates at that time had the PB2 of 3.3.2b or MP of 3.3.2c. These data suggest that, before July 2015, new viruses carrying the PB2 gene originated from humans in 2009 and/or the MP gene that originated in 2010 to 2011 was introduced into farm B, where these viruses reassorted with those that had circulated but had not been established on the farm. Although the first isolates from farm B were H3N2 viruses in February 2011, the constellations of the internal genes described earlier were shared by both H1N1 and H3N2 IAVs-S viruses, suggesting that H1N1 viruses carrying the original gene constellations might have been circulating on farm B before February 2011.

On farm C, the gene constellations of the H1N1 viruses, H1_ChoC16.2, were the same as for the exceptional H1N1 viruses isolated on farm B in July 2015, H1_ChoB15.7B. Although the origin of the H3 HA genes on farm C differed from that of farm B, that of the internal and NA genes of the H3N2 viruses, H3_ChoC15.7 and H3_ChoC17.2, were the same as that of those isolated

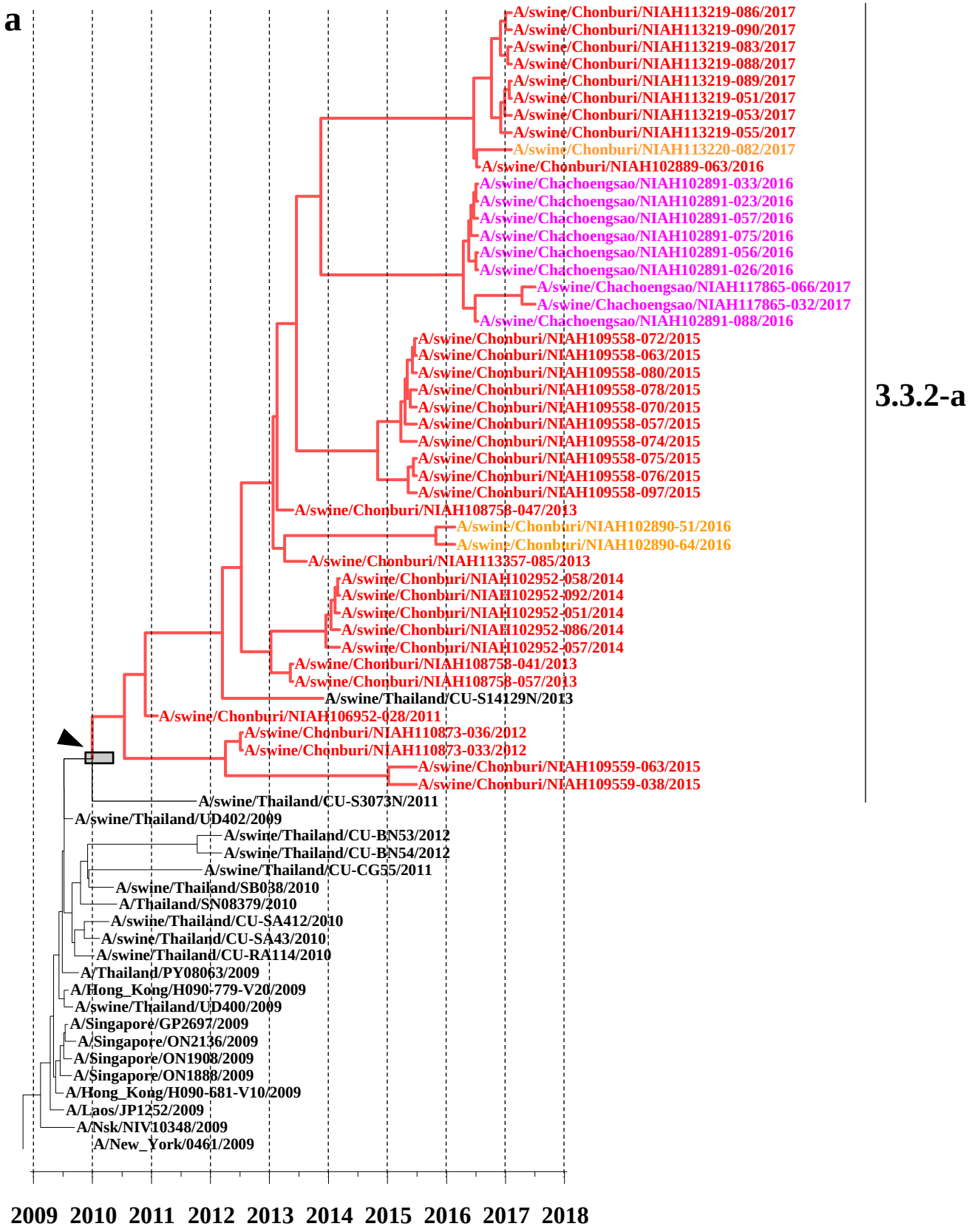

Fig. 15. MCC trees of the PB1 genes of the isolates in this study.
The genetic groups 3.3.2a, 3.3.2b, and 3.3.2c are colored light red (a), pink (b), and blue (c), respectively. Strain names of isolates from farms B, C, D, and O are shown in red, orange, blue, and purple, respectively. Gray boxes indicate the divergence time estimated by using BEAST.

b

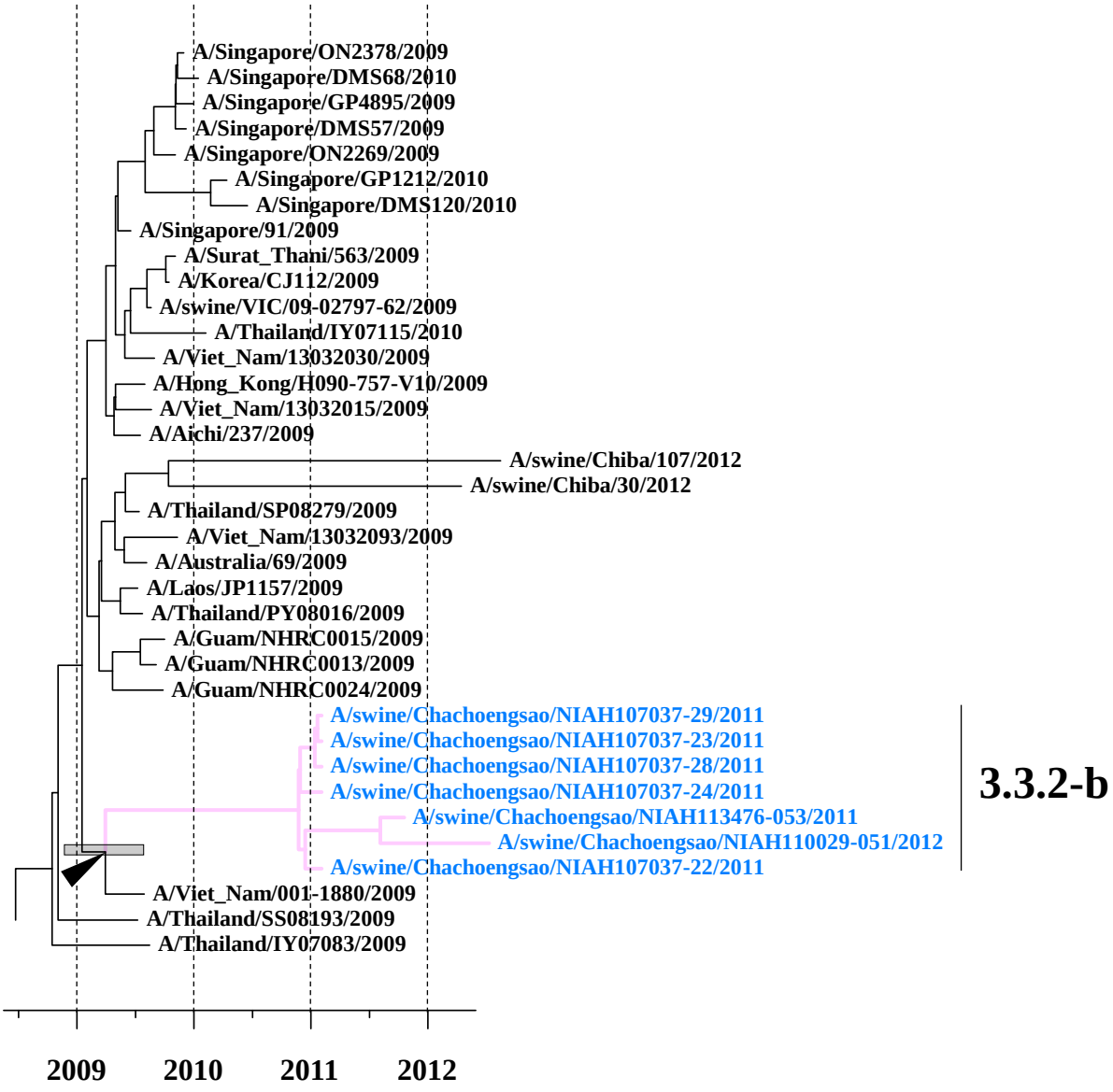

Fig. 15. Continued

Fig. 15. Continued

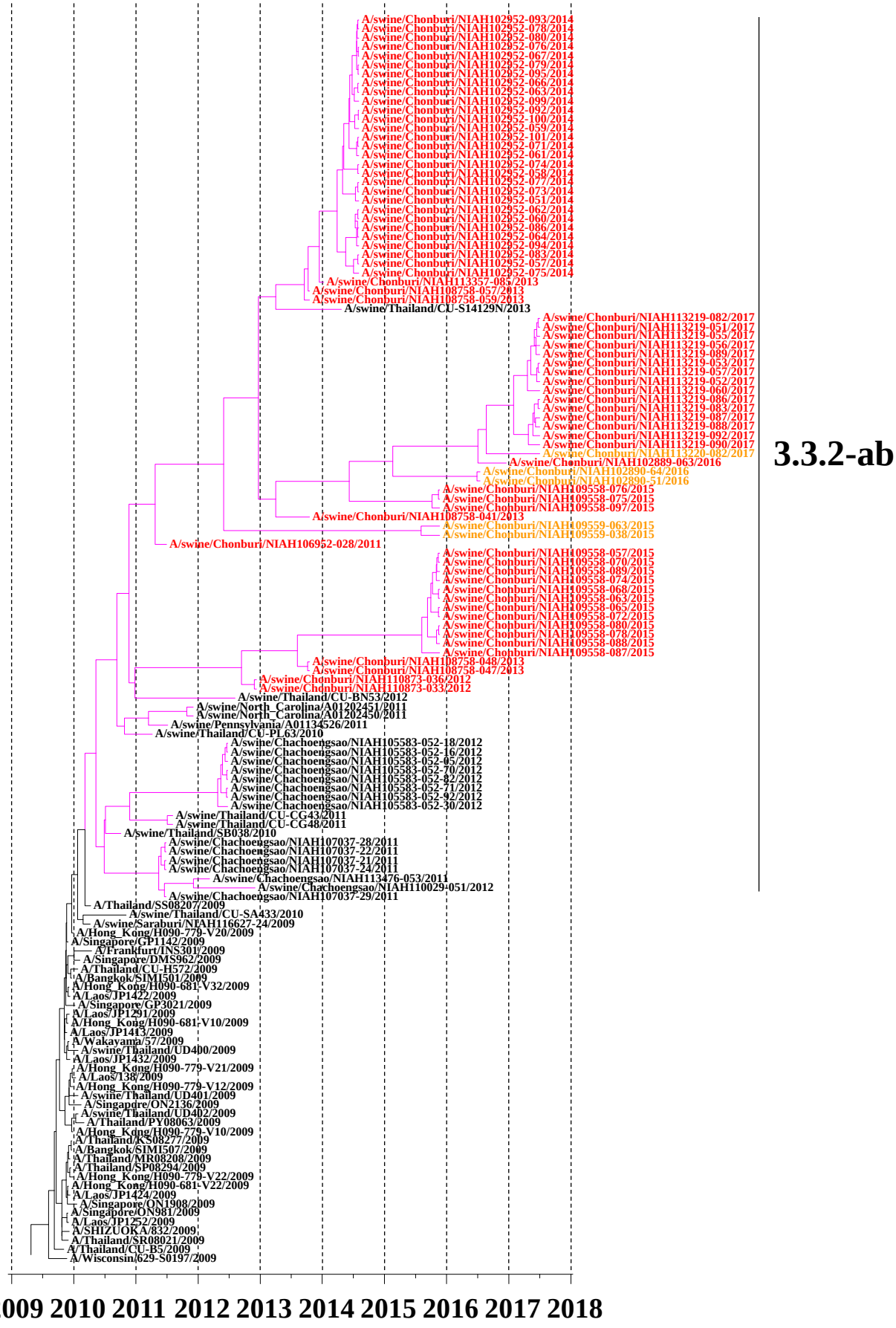

Fig. 16. MCC trees of NP genes, including the isolates in this study.
The genetic group 3.3.2ab is colored bright purple. Strain names of isolates from farms B and C are shown in red and orange, respectively.

Table 6. Estimated divergence time of the HA and PB1 genes in each genetic group.

Gene group	H1 HA		PB1	
	Branch node	95% HPDV[a]	Branch node	95% HPDV
3.3.2a	17 Jan 2010	20 Oct 2009 - 22 Apr 2010	19 Feb 2010	19 Oct 2009 - 19 Jun 2010
3.3.2b	25 Jul 2009	12 Jul 2009 - 25 Jul 2009	29 Mar 2009	5 Nov 2008 - 19 Jul 2009
3.3.2c	25 Jan 2011	18 Oct 2010 - 4 Apr 2011	2 July 2010	4 Apr 2010 - 31 August 2010

[a]Highest posterior density value

on farm B (Table 3). H3N2 viruses with the same gene constellations were retained on farm C for at least 1.5 years (July 2015 through February 2017).

On farm D, H1N1 viruses that had the same gene constellation as H1_ChoD11.2 persisted until July 2012. Then, in February 2013, other H1N1 viruses emerged, of which all of the gene segments originated from 3.3.2c A(H1N1)pdm09 viruses, thus indicating another introduction of A(H1N1)pdm09 viruses into farm D. H3N2 viruses isolated after July 2012 carried the same internal genes as H1N1 viruses that circulated after February 2013. However, the origin of the internal genes of H3_ChaD12.7 and H3_ChaD13.2 differed from that of H3_ChaD15.7, as illustrated by the PB1 phylogeny (Fig. 15c). Like the situation on farm B, although the first viruses carrying genes of 3.3.2c on farm D were H3N2 viruses in July 2012, H1N1 viruses carrying all genes of 3.3.2c might have been circulating before July 2012, reassorting with the H3N2 strains to yield H3_ChoD12.7.

On farm O, H3N2 viruses with the same gene constellation had persisted for at least one year (July 2016 to July 2017).

Antigenic analyses of the Thai isolates

HI assays were performed to ascertain whether antigenic differences were present among the IAVs-S isolated in the current study. All viruses isolated in this study reacted with hyperimmune chicken sera raised against Cal09 with HI titers within 2-fold lower than that of the homologous virus (Table 7). In contrast, viruses isolated on farms B and D showed 4-fold different reactivity with the other 2 hyperimmune chicken sera. Among the A(H1N1)pdm09 viruses isolated from pigs at farm B, whose H1 HA genes phylogenetically belonged to 3.3.2a, H1_ChoB12.7 showed higher reactivity with hyperimmune chicken sera raised against Nar11 and H1_ChoC16.2, whereas H1_ChoB17.2 showed a 4-fold lower titer, suggesting gradual antigenic drift among the A(H1N1)pdm09 viruses isolated from farm B. Among the A(H1N1)pdm09 viruses isolated from pigs at farm D, H1_ChaD11.2, H1_ChaD11.10, and H1_ChaD12.7, whose H1 HA genes belonged to 3.3.2b, reacted with hyperimmune chicken sera raised against H1_ChoC16.2 at titers of 160 or 320, whereas H1_ChaD13.2, H1_ChaD13.8, H1_ChaD13.11, all of which carried H1 HA genes of 3.3.2c, reacted at the titer of 640. In addition, the latest H1_ChaD14.3 that had H1 HA genes of 3.3.2c showed 4-fold lower reactivity than H1_ChaD13.2, H1_ChaD13.8, and H1_ChaD13.11 viruses.

Antigenic changes were present among H3 isolates obtained from the same farm as well as among those obtained from different farms (Table 8). The reactivity of H3_ChoB11.2 with anti-Sar08 hyperimmune chicken sera was

Table 7. HI titers against the H1 viruses.

		HI titer with antisera[a]						
		Hyperimmune chicken sera			Sera from 20-week-old swine at farm C[b]			
Antigen	Farm	Cal09	Nar11	H1_ChoC16.2	no. 1	no. 2	no. 3	no. 4
Nar09		2,560	1,280	640	320	160	320	80
Cal09		**2,560**	1,280	640	160	160	640	160
Nar11		2,560	**1,280**	320	160	160	640	160
H1_ChoB12.7		2,560	1,280	640	160	320	640	160
H1_ChoB13.5		1,280	640	640	320	320	320	160
H1_ChoB15.7A	B	2,560	640	640	160	160	320	80
H1_ChoB15.7B		2,560	640	320	320	160	320	80
H1_ChoB16.7		2,560	1,280	320	160	160	320	80
H1_ChoB17.2		1,280	320	160	80	80	160	40
H1_ChoC16.2	C	2,560	640	**640**	320	160	320	80
H1_ChaD11.2		2,560	640	160	160	80	320	80
H1_ChaD11.10		1,280	640	320	160	160	320	160
H1_ChaD12.7		2,560	640	160	80	40	160	40
H1_ChaD13.2	D	1,280	160	640	20	80	80	<20
H1_ChaD13.8		1,280	160	640	20	80	80	20
H1_ChaD13.11		1,280	640	640	40	80	80	<20
H1_ChaD14.3		1,280	320	160	40	80	40	<20

[a]Homologous HI titers are underlined.

[b]Timepoints for collection of swine sera are as follows; no.1, May 2014; nos. 2 and 3, December 2014; no. 4, July 2015.

Table 8. HI titers against the H3 viruses.

		HI titer with antisera raised against the strains below[a]														
		Hyperimmune chicken sera				Post-infection ferret sera							Sera from 20-week-old swine at farm C[b]			
Strain	Farm	H3_ChaD15.7	H3_ChoC15.7	Sar08	Cha03	Wuh95	Syd97	Pan99	Wyo03	Ny04	Hir05	Uru07	no. 1	no. 4	no. 5	no. 6
H3_ChoB11.2	B	320	640	5,120	<20	160	80	40	80	20	<20	<20	320	80	40	160
H3_ChoB13.5		160	320	160	20	40	20	20	40	<20	<20	<20	320	320	160	160
H3_ChoB13.8		80	160	80	<20	40	20	20	40	<20	<20	<20	160	320	320	320
H3_ChoB14.3		160	160	80	<20	40	20	20	40	<20	<20	<20	<20	320	320	80
H3_ChaD12.7	D	160	160	320	<20	320	<20	<20	80	<20	<20	<20	<20	160	40	20
H3_ChaD13.2		160	160	320	<20	320	20	20	80	20	<20	<20	20	320	20	40
H3_ChaD15.7		**640**	160	2,560	<20	40	20	20	20	20	<20	<20	160	80	20	80
H3_ChoC15.7	C	160	**640**	640	40	160	20	20	40	<20	<20	<20	640	<20	160	160
H3_ChoC17.2		320	640	640	40	320	20	40	80	20	<20	<20	640	<20	320	320
H3_ChaO16.7	O	160	320	640	40	80	<20	20	20	<20	<20	<20	320	<20	80	160
H3_ChaO17.7		160	640	640	40	160	20	20	40	<20	<20	<20	640	<20	160	320
Sw/Sar/08		160	320	**5,120**	<20	160	40	80	40	<20	<20	<20	320	<20	40	80
Sw/Cha/03		<20	<20	40	**1,280**	<20	<20	<20	<20	<20	<20	<20	<20	<20	<20	<20
Wuh95		<20	160	2,560	40	**640**	80	80	80	20	<20	<20	160	20	20	80
Syd97		<20	640	2,560	20	1,280	**320**	640	640	80	80	80	320	160	80	320
Pan99		<20	40	2,560	<20	80	40	**640**	320	<20	<20	<20	80	<20	<20	20
Wyo03		<20	160	2,560	<20	160	160	320	**2,560**	1,280	80	320	320	<20	<20	20
Ny04		<20	<20	40	<20	20	20	20	320	**2,560**	160	640	20	40	<20	<20
Hir05		<20	20	40	20	40	40	80	160	640	**640**	640	40	80	160	80
Uru07		<20	<20	20	<20	<20	20	<20	80	640	160	**1,280**	40	<20	40	<20

[a]Homologous HI titers are underlined.

[b]Timepoints for collection of swine sera are as follows: nos. 1 and 5, May 2014; no. 6, December 2014; no. 4, July 2015.

clearly distinguishable from those of H3_ChoB13.5, H3_ChoB13.8, and H3_ChoB14.3. H3_ChoB11.2 reacted with anti-Sar08 hyperimmune chicken sera at the titer of 5120, which was the same titer obtained with the homologous antigen; H3_ChoB13.5, H3_ChoB13.8, and H3_ChoB14.3 reacted with 32-, 64-, and 64-fold lower titers, respectively. Similar but less extensive changes in reactivity were recognized when anti-serum against H3_ChoC15.7 was used. The titers of both H3_ChaD12.7 and H3_ChaD13.2 against anti-Sar08 hyperimmune chicken sera were 16 times lower than the titer of the homologous antigen, whereas H3_ChaD15.7 maintained its titer; similar results were obtained with anti-H3_ChaD15.7 hyperimmune serum. The H3N2 isolates from farms C and O, both belonging to the human-like-b cluster, showed similar reactivity against the four hyperimmune sera used. In addition, the H3N2 IAV-S isolates from all four farms showed low reactivity to post-infection ferret sera against seasonal human strains from 1995 through 2003 and did not react at all to those from after 2005.

To ascertain whether the antigenic differences observed with hyperimmune chicken and post-infection ferret sera could be detected by naturally infected host animals in the field, sera collected from 20-week-old swine at farm C were used. Specifically, 25 sera obtained from 20-week-old pigs, which were considered to be unaffected by maternal antibodies, in HI tests. Of these 2 sera, nos. 1 and 4, reacted at titers of 160 or more to several H1N1 and H3N2 isolates, and both were used for HI tests. For HI tests with the H1N1 strains, two sera, nos. 2 and 3, were added, because they reacted at the two highest titers, except for nos. 1 and 4, to any of the H1N1 strains examined. Sera nos. 5 and 6 were selected for HI testing with the H3N2 strains for the same reason as the H1 strains. H1_ChoB17.2 showed a 4-fold lower titer than H1_ChoB12.7 to swine sera 2 and 4, suggesting that the antigenic drift observed among H1N1 isolates on farm B by using hyperimmune sera could be recognized by serum antibodies in naturally infected pigs. H1_ChoC16.2 reacted similarly to H1_ChoB15.7B with the pig sera. A correlation between antigenicity and phylogenic grouping was evident among the viruses from farm D in regard to sera 1, 3, and 4. H1_ChaD11.2, H1_ChaD11.10, and H1_ChaD12.7, which belonged to 3.3.2b, reacted well with sera 1, 3, and 4, but those belonging to 3.3.2c—H1_ChaD13.2, H1_ChaD13.8, H1_ChaD13.11, and H1_ChaD14.3—were less reactive. Regarding H3 viruses, H3_ChoB11.2 showed low reactivity to sera 4 and 5, whereas newer strains showed more than 4-fold higher titers. At farm D, H3_ChaD15.7 showed high reactivity to serum no. 1, whereas older strains were 8 times less reactive.

To examine the correlation between antigenic changes and amino acid substitutions in the HA protein, the amino acid substitutions among the H1 (Table

9) and H3 (Table 10) were compared. Among the H1N1 viruses, several substitutions within predicted antigenic sites deduced by previous studies (98-100) occurred between isolates that showed different antigenicities in the HI tests. Among the five amino acid substitutions in the HA protein of H1_ChoB17.2 relative to that of H1_ChoB12.7, two within predicted antigenic sites possibly contributed to the gradual antigenic drift observed in the HI test. Likewise, any of the four substitutions within the predicted antigenic sites between older strains (H1_ChaD11.2, H1_ChaD11.10, and H1_ChaD12.7) and recent strains (H1_ChaD13.2, H1_ChaD13.8, H1_ChaD13.11, and H1_ChaD14.3) are likely to be related to the different reactivities against swine serum no. 4. Because the H3N2 isolates demonstrated many substitutions even within the antigenic sites deduced in a previous report (101), it was difficult to identify which substitution correlated to antigenic difference. Compared with H3_ChoB11.2, the H3N2 isolates from farm B after 2013, H3_ChoB13.5, H3_ChoB13.8, and H3_ChoB14.3, which showed different reactivity to hyperimmune sera against Sar08 and swine sera 4 and 5, shared 14 substitutions within the predicted antigenic sites (Table 10). Among the isolates from farm D, five substitutions within the predicted antigenic sites were present between older strains (H3_ChaD12.7 and H3_ChaD13.2) and the most recent (H3_ChaD15.7) that showed different reactivities to antisera against Sar08 and Whu95 and swine serum no. 1. Compared with H3_ChoB11.2 of human-like-a, the H3N2 isolates of human-like-b (H3_ChoC15.7, H3_ChoC17.2, H3_ChaO16.7, and H3_ChaO17.7) shared more than 18 substitutions within predicted antigenic sites.

To assess whether the HA protein of the H1 isolates from farm B had undergone selection pressure for evading host immune surveillance, the ratio of nonsynonymous to synonymous nucleotide substitution rates (Ka/Ks ratios) (102) of their HA genes were compared. Because internal genes appear to be less vulnerable to such selection pressure than HA and NA genes, Ka/Ks ratios of their PB1 genes were calculated for comparison (Table 11). The Ka/Ks ratios of the H1 HA genes were significantly higher than those of their PB1 genes (*t*-test, $P < 0.01$). In addition, the substitution rates within these viruses were significantly higher for the HA genes (4.9×10^{-3} substitutions/site/year; 95% HPDV, 3.5×10^{-3} to 6.3×10^{-3}) than for the PB1 genes (2.6×10^{-3} substitutions/site/year; 95% HPDV, 1.8×10^{-3} to 3.4×10^{-3}; $P < 0.01$). Ka/Ks ratios and mutation rates of the H3N2 IAVs-S from farm D were similarly calculated because they also had evolved as a single lineage with antigenic change. The Ka/Ks ratios and substitution rates of their H3 HA genes were significantly higher than those of their own PB1 genes ($P = 0.03$ and $P < 0.01$, respectively). These results suggest that selection pressure, possibly due to immune pressure, in the pig population

may have driven the antigenic drift of the HA genes of these viruses within the same farm.

Table 9. Deduced amino acid residues in HA1 of H1 viruses used in this study.

		Antigenic site[a]																																				
								Ca2	Ca2	Ca2		Sb	Sa	Sa	Ca1	Ca2	Sb	Sb	Sb			Ca1	Ca1		Ca2			Ca1											
		Amino acid position in HA1																																				
		45[b]	83	94	97	120	128	137	138	142	152	156	157	161	168	183	185	190	195	197	202	203	205	211	216	222	223	234	235	260	262	272	289	293	298	321
Strain	Farm	54[c]	91	101	104	Del	132	140	141	145	155	159	160	164	171	186	188	193	198	200	205	206	208	214	219	225	226	237	238	263	265	274	291	295	300	323
Nar09		R	S	D	D	T	S	P	H	K	V	N	S	L	D	S	S	S	A	A	G	S	R	K	I	D	Q	V	E	N	G	V	S	Q	I	V
Cal09		-	P	-	-	-	-	-	-	-	-	D	-	-	-	P	-	-	-	T	-	-	-	-	-	-	-	-	-	-	-	-	-	-	-	I
Nar11		-	-	-	N	-	-	-	-	-	-	-	-	-	-	-	T	-	-	-	W	T	-	-	-	-	-	-	-	-	-	-	-	-	-	-
H1_ChoB12.7		-	-	-	-	-	P	-	-	R	-	-	-	-	N	-	-	-	-	-	-	-	-	-	-	G	-	-	-	-	-	-	N	H	T	-
H1_ChoB13.5	B	-	-	-	-	-	P	S	-	-	-	-	-	-	N	-	-	-	-	-	-	-	-	-	-	-	R	-	-	-	E	-	N	H	T	-
H1_ChoB15.7A		-	-	-	-	-	P	S	-	-	-	-	-	I	N	-	-	T	-	-	-	-	-	-	-	N	-	-	G	-	E	-	N	H	T	-
H1_ChoB15.7B		-	-	-	-	-	P	S	-	-	-	-	-	-	N	P	-	-	E	-	-	-	-	-	-	N	-	-	G	-	E	-	N	H	T	-
H1_ChoB16.7		-	-	-	-	-	P	S	-	-	-	-	-	-	N	-	-	-	-	-	-	-	K	-	-	-	-	-	-	-	E	-	N	H	T	-
H1_ChoB17.2		-	-	-	-	-	P	-	-	-	I	-	-	-	N	-	-	-	-	-	-	-	K	-	-	G	-	L	-	-	E	-	N	H	T	-
H1_ChoC16.2	C	-	-	-	-	-	P	S	-	-	-	-	-	-	N	-	-	-	-	-	-	-	K	-	-	-	R	-	-	-	E	-	N	H	T	-
H1_ChaD11.2		-	-	-	-	A	-	-	-	-	-	-	L	-	-	-	-	-	-	-	-	T	-	-	-	-	-	-	-	D	-	-	-	-	-	-
H1_ChaD11.10		-	-	-	-	A	-	-	-	-	-	-	L	-	-	-	-	-	-	-	-	T	-	-	-	-	-	-	-	D	-	-	-	-	-	-
H1_ChaD12.7		-	-	-	-	-	-	-	-	-	-	-	L	-	-	-	-	-	-	-	-	T	-	-	-	-	-	-	-	D	-	-	-	-	-	-
H1_ChaD13.2	D	K	-	V	-	A	-	-	L	R	-	-	-	-	-	-	T	-	-	-	-	T	-	E	K	-	-	-	-	-	A	-	-	-	I
H1_ChaD13.8		-	-	V	-	A	-	-	L	R	-	-	-	-	-	-	T	-	-	-	-	T	-	E	K	-	-	-	-	-	A	-	-	-	I
H1_ChaD13.11		-	-	V	-	A	-	-	L	R	-	-	-	-	-	-	T	-	-	-	-	T	-	E	K	-	-	-	-	-	A	-	-	-	I
H1_ChaD14.3		-	-	V	-	A	-	-	L	R	-	-	-	-	-	-	T	-	-	-	-	T	-	E	K	-	-	-	-	-	A	-	-	-	I

[a]Antigenic sites of H1
[b]H1 HA numbering
[c]H3 HA numbering

Table 10. Deduced amino acid residues of the HA1 protein of H3 viruses used in this study.

Strain	Farm	Antigenic site[a]																														
									C	C	C	C			E	E			C			A	A	A	A	A	A	A	A	B	B
		Amino acid position in the HA1																														
		3	4	9	10	31	39	45	48	50	53	54	56	57	62	78	79	88	92	96	105	122	131	133	137	138	143	144	145	155	157
H3_Cho11.2	B	L	P	S	K	N	A	S	I	E	N	S	H	R	G	G	F	V	E	D	H	D	A	N	Y	A	S	I	K	H	L
H3_Cho13.5		-	-	-	-	-	-	-	-	-	-	-	-	-	E	S	-	-	-	-	-	-	T	-	-	S	Y	V	N	Y	S
H3_Cho13.8		-	-	-	-	-	-	-	-	-	-	-	-	-	E	S	-	-	-	-	-	-	T	-	-	S	Y	V	N	Y	S
H3_Cho14.3		-	-	-	-	-	-	-	-	-	-	-	-	-	E	S	-	-	-	-	-	-	T	-	-	S	Y	V	N	Y	S
H3_Cha12.7	D	-	-	-	-	-	-	-	-	-	-	-	Y	Q	-	-	-	-	-	-	-	-	-	-	-	S	-	-	N	-	-
H3_Cha13.2		-	-	-	-	-	-	-	-	-	-	-	Y	Q	-	-	-	-	-	-	-	-	-	-	-	S	-	-	N	-	-
H3_ChaD15.7		-	-	-	-	-	-	-	T	-	-	-	Y	Q	-	D	-	-	-	-	-	-	-	-	-	S	-	-	-	-	-
H3_ChoC15.7	C	H	F	T	T	D	S	-	T	R	D	G	-	-	K	-	L	I	G	N	Y	S	-	D	N	S	-	V	-	-	-
H3_ChoC17.2		H	F	T	T	D	-	-	T	R	D	G	-	-	K	-	L	I	G	N	Y	S	-	D	N	S	-	V	-	-	-
H3_ChaO16.7	O	H	F	T	T	D	-	N	T	R	D	G	-	-	K	-	L	I	G	N	Y	S	-	D	N	S	-	V	-	-	-
H3_ChoO17.7		H	F	T	T	D	-	N	T	R	D	G	-	-	K	-	L	I	G	N	Y	S	-	D	N	S	-	V	-	-	-
Sar08		-	S	T	T	D	-	-	T	R	D	-	-	-	E	-	-	I	Q	-	Y	N	-	D	N	S	-	V	-	-	-
Cha03		-	-	N	T	S	-	-	M	K	D	-	-	-	A	R	-	I	K	N	Y	N	T	-	N	-	P	D	S	Y	S
Wuh95		-	-	-	T	-	-	-	T	R	D	-	-	-	K	-	-	-	K	N	Y	N	-	D	-	-	-	V	-	-	-
Syd97		I	-	-	T	-	-	-	T	R	D	-	-	-	E	-	-	-	K	N	Y	N	-	-	-	-	-	-	-	-	-
Pan99		-	-	-	T	-	-	-	T	R	D	-	-	Q	E	-	-	-	K	N	Y	N	-	-	S	-	-	N	N	-	-
Wyo03		-	-	-	T	-	-	-	T	G	D	-	-	Q	E	-	-	-	K	N	Y	N	T	-	S	-	-	N	-	T	-
NY04		-	-	-	T	-	-	-	T	G	D	-	-	Q	E	-	-	-	K	N	Y	N	T	-	S	S	-	N	N	T	-
Hir05		-	-	-	T	-	-	-	T	G	D	-	-	Q	E	-	-	-	K	N	Y	N	T	-	S	-	-	N	N	T	-
Uru07		-	-	-	T	-	-	-	T	-	D	-	-	Q	E	-	-	-	K	N	Y	N	T	-	S	S	-	N	N	T	-

[a]Antigenic sites of H3 were classified into five groups as described previously (101).

Table 10. Continued.

Strain	Farm	Antigenic site[a]																														
		B	B	D	B	B	B		D	D		D	D	D	D																	
		Amino acid position in the HA1																														
		158	159	172	186	189	193	197	208	209	214	219	220	223	230	238	239	242	257	261	262	267	268	272	273	274	280	282	300	304	312
H3_Cho11.2	B	E	Y	E	S	S	S	Q	R	G	I	S	R	V	M	K	S	V	Y	R	N	I	M	A	P	M	E	I	V	A	S
H3_Cho13.5		G	H	-	G	-	-	-	-	S	-	-	-	-	V	-	-	I	-	-	S	-	-	-	S	I	-	V	-	-	-
H3_Cho13.8		G	H	-	G	-	-	-	-	S	-	-	-	-	V	-	-	I	-	-	S	V	-	-	S	I	-	V	-	-	-
H3_Cho14.3		G	H	-	G	-	-	-	G	S	-	-	-	-	V	-	-	I	-	-	S	-	-	-	S	I	-	V	-	-	-
H3_Cha12.7	D	-	-	-	-	-	-	-	-	-	-	-	-	-	-	-	-	-	-	-	-	-	I	-	-	-	-	-	-	-	-
H3_Cha13.2		-	-	-	-	-	-	-	-	-	T	-	-	-	-	-	-	-	-	-	-	-	I	-	-	-	-	-	-	-	-
H3_ChaD15.7		-	H	-	-	-	-	H	-	-	-	-	K	-	-	-	-	-	-	-	-	-	I	-	-	-	-	-	-	-	-
H3_ChoC15.7	C	D	-	D	-	N	N	-	-	S	-	Y	-	-	I	N	P	I	-	Q	S	-	-	T	-	I	G	-	I	P	N
H3_ChoC17.2		D	-	D	-	N	N	-	-	S	-	Y	-	-	I	N	P	I	F	Q	-	-	-	T	-	I	G	-	I	P	N
H3_ChaO16.7	O	D	-	D	-	N	N	-	-	S	-	Y	-	I	I	N	P	M	-	Q	S	-	-	T	-	I	G	-	I	P	N
H3_ChoO17.7		D	-	D	-	N	N	-	-	S	-	Y	-	I	I	N	P	M	-	Q	S	-	-	T	-	I	G	-	I	P	-
Sar08		N	-	D	-	-	N	-	-	S	V	-	-	-	I	-	-	I	-	-	S	-	I	-	L	I	-	-	I	-	N
Cha03		G	T	D	-	R	N	-	-	S	S	P	-	I	I	-	P	T	-	H	T	-	-	-	-	I	-	-	I	-	T
Wuh95		-	-	D	-	-	-	-	-	S	-	-	-	-	I	-	P	I	-	-	S	-	-	-	-	I	-	-	I	-	N
Syd97		K	-	D	-	-	-	-	-	S	-	-	-	-	I	-	P	I	-	-	S	-	-	-	-	I	-	-	I	-	N
Pan99		K	-	-	-	-	-	-	-	S	-	-	I	-	I	-	P	I	-	-	S	-	-	-	-	I	-	-	I	-	N
Wyo03		K	-	-	V	-	-	-	-	S	-	Y	-	-	I	-	P	I	-	-	S	-	-	-	-	I	-	-	I	-	N
NY04		K	F	-	V	N	R	-	-	S	-	-	-	-	I	-	P	I	-	-	S	-	-	-	-	I	-	-	I	-	N
Hir05		K	F	-	V	N	F	-	-	S	-	-	-	-	I	-	P	I	-	-	S	-	-	-	-	I	-	-	I	-	N
Uru07		K	F	-	G	N	F	-	-	S	-	-	-	-	I	-	P	I	-	-	S	-	-	-	-	I	-	-	I	-	N

[a]Antigenic sites of H3 were classified into five groups as described previously (101).

Table 11. Ka/Ks ratio and substitution rates of H1N1 and H3N2 viruses used in this study.

			Ka/Ks[a]		Substitution rate		
Virus	Subtype	Segment	Ratio	*P*[c]	Rate	95% HPDV[b]	*P*
H1_ChoB12.7 H1_ChoB13.5 H1_ChoB15.7A H1_ChoB15.7B H1_ChoB16.7 H1_ChoB17.2	H1N1	HA	0.64	< 0.01	4.9×10^{-3}	3.5×10^{-3}-6.3×10^{-3}	< 0.01
		PB1	0.57		2.6×10^{-3}	1.8×10^{-3}-3.4×10^{-3}	
H3_Cha12.7 H3_Cha13.2 H3_ChaD15.7	H3N2	HA	0.72	0.03	5.5×10^{-3}	3.5×10^{-3}-7.7×10^{-3}	< 0.01
		PB1	0.65		3.2×10^{-3}	1.7×10^{-3}-4.6×10^{-3}	

[a]Nonsynonymous substitutions per non-synonymous site / synonymous substitutions per synonymous site
[b]Highest posterior density value
[c]Student's t-test

Discussion

To investigate the evolution of IAVs-S within a farm, longitudinal studies were conducted at five pig farms in Thailand, which yielded 169 IAVs-S consisting of H1N1 and H3N2 IAVs-S. Phylogenetic and antigenic analyses demonstrated the dynamics of various IAV-S strains due to accumulation of mutations, multiple introductions of viruses, and reassortment events in the pig farm setting. Through surveillance at these farms, the presence of antigenic drift were confirmed over several years due to the accumulation of amino acid substitutions in the HA protein, and multiple introductions of viruses followed by reassortment events that generated the observed genetic and antigenic diversity were documented. Both events could contribute to the maintenance of IAV-S on a pig farm and to the generation of new viruses.

Regarding the dynamics of a particular subtype of IAV-S on a farm, IAVs-S with similar antigenicity persisted on a farm for approximately 1 year and then became undetectable, followed by an approximately 1-year interlude and then resurgence of a virus with the same subtype but different antigenicity. Antigenic alteration at the time of resurgence was caused by either antigenic drift or the introduction of a virus belonging to another sublineage. Sun et al. (82) demonstrated that IAV-S expanded easily and rapidly on a farm, thus raising the herd immunity level against the IAV-S within 100 days after the first infection sufficiently high to prevent virus shedding at the second infection. Given the similar dynamics that occurred within the swine population at farm B, rapid expansion of viruses likewise could have elevated herd immunity, thus restricting the prevalence of a circulating virus to below the detection limit. This high immune pressure might have led to the antigenic drift in the H1N1 viruses from farm B such that, for example, H1_ChoB12.7 accumulated substitutions for 3 years and resurged as H1_ChoB15.7A/B, followed by H1_ChoB16.7 and H1_ChoB17.2. Over 4 years, these viruses gradually became less reactive to naturally infected pig sera, as typically seen with sera no. 4, suggesting that IAVs-S evolve to evade immune pressure in a farm setting. It is unclear whether such antigenic drift under immune pressure actually occurred at the farm level in this study, although previous reports have demonstrated using experimentally infected animals that antigenic drift can occur under immune pressure in a pig (103, 104). Other researchers have demonstrated that selection pressure is more intense on the HA gene than on internal genes and have hypothesized that IAVs behave as though they are trying to outrun their immune pursuers (105). Rambaut et al. (106) demonstrated that the antigenic drift of human IAVs due to such selection pressure is a global event, and thus new variants are spread. In the current study,

in a farm setting, non-synonymous substitutions with higher substitution rates in the HA gene than in the PB1 gene resulted in the emergence of a drifted virus that differed from the strain that had circulated previously in the pig population. However, it remains to be determined whether the drift was a consequence of escape from herd immunity against the strain that had previously been circulating on the farm.

It is interesting to note that, regardless of the farm sampled, phylogenetically distinct groups showed remarkably different reactivity to swine serum no. 4. Although serum no. 4 did not react with the isolates from farms C and O that carried human-like-b H3 HA genes, it reacted with the H3N2 viruses carrying human-like-a H3 HA genes isolated from the other two farms. Considering that serum no. 4 was collected at farm C in July 2015, IAV-S strains that carried human-like-b H3 HA genes might have emerged because of the lack of immunity to them on farm C. Isolates from farms C and O reacted similarly with sera 1, 5, and 6. Taken together, analysis of the Thai isolates in the present study indicated that both hyperimmune antisera and naturally infected swine sera revealed antigenic differences not only between phylogenetically distinct groups but also within each group (that is, antigenic drift).

In addition, introductions of viruses of the same subtype but with different antigenicity were another key for evading immune pressure, as seen in the H3N2 viruses on farm B and H1N1 viruses on farm D. Through a 1-year longitudinal study of farrow-to-wean farms, Diaz et al. (42) documented multiple introductions of H1N1, H1N2, and H3N2 IAV-S on individual farms, with some IAV-S strains retained and others replaced by phylogenetically distinct groups on individual farms. Current 5-year longitudinal study demonstrated that such introduced viruses can establish themselves on a farm only when the new IAV-S differs in antigenicity from the pre-existing IAV-S strains on that farm.

The isolation from four Thai pig farms of A(H1N1)pdm09 viruses and of H3N2 viruses whose internal genes were replaced by those of A(H1N1)pdm09 viruses demonstrates interspecies transmission from humans to swine and subsequent reassortment in pigs, as reported previously (21, 39, 107, 108). The three epidemic peaks of A(H1N1)pdm09 virus in the human population in Thailand—August 2009, February 2010, and September 2010—were followed by another peak in 2014, and few cases of A(H1N1)pdm09 infection in humans were recorded between 2011 and 2013 (109, 110). The genetic analysis of IAV-S isolates of A(H1N1)pdm09 origin revealed a close genetic relationship between the IAV-S strains from the pig farms and human epidemic strains. 3.3.2a and 3.3.2b of H1 HA genes were estimated to diverge in October 2009 and July 2009, respectively, suggesting that they were introduced into pig farms around the first

epidemic peak in the human population in Thailand. Likewise, 3.3.2c of H1 HA genes was estimated to diverge in September 2010, coinciding with the third epidemic peak in the human population. This finding suggests that the magnitude of an epidemic in the human population might promote interspecies transmission of IAVs to the pig population. Studying the timing of influenza outbreaks in human and pig populations is important for revealing the mechanisms underlying the introduction of a human epidemic influenza virus into pig farms.

During the active surveillance, IAV-S were detected on multiple occasions on farms B, C, D, and O, whereas no IAV-S was detected during any of the four sampling events on farm P. A previous report showed that farms with more than 1,000 pigs are at increased risk for IAV-S positivity (71). In that regard, each of the five farms in the present study had more than 1,000 pigs, thus ruling out the possibility that the different isolation rates were due to differences in the number of pigs on the surveyed farms. In addition, the farms in the present study maintained similar animal husbandry practices, mandating workers to wear dedicated clothes and boots and to shower before and after handling pigs. The only husbandry practice that differed between farm P and the other four farms that might have resulted in their differing hygiene status was that workers on farm P wore masks when handling pigs. Wearing masks might reduce the pigs' exposure to aerosolized infectious influenza virus from humans, thus decreasing the risk of transmission of human seasonal influenza virus on the farm. However, the small sample size precludes the demonstration of a significant correlation between the presence of IAV-S and the wearing of masks by workers. Further investigation of the ability of masks to prevent human-to-pig transmission is needed.

In summary, continuous longitudinal surveillance was conducted to show how IAV-S generated genetic and antigenic diversity over several years in the pig farm setting; antigenic drift due to the accumulation of substitutions at antigenic sites in the HA gene contributed to the evolution of IAVs-S. In addition, the introduction of viruses with different antigenicity was confirmed. At the farm level, both of these events appeared to be important for the evasion of host immunity and subsequent circulation and resurgence of IAV-S. One remarkable feature of the present study is that it indicates that both multiple introductions of IAV-S and accumulation of substitutions in the HA proteins had occurred, resulting in the antigenic evolution and long-term circulation of IAV-S within a farm. Although evidence of multiple introductions into and resurgence of viruses on the pig farms were found, additional clues regarding how such introductions occurred would help to prevent similar introductions and to control IAV infections in pigs.

Summary

Surveillance studies of IAV-S have accumulated information regarding IAVs-S circulating in Thailand, but how IAV-S evolves within a farm remains unclear. In the present study, 82 A(H1N1)pdm09 and 87 H3N2 IAVs-S were isolated from four farms through active surveillance from 2011 to 2017; then isolates were phylogenetically and antigenically analyzed to elucidate their evolution within each farm. Phylogenetic analyses demonstrated multiple intrusions of A(H1N1)pdm09 viruses that coincided with epidemic A(H1N1)pdm09 strains in humans in Thailand, and they reassorted with H3N2 viruses as well as other A(H1N1)pdm09 viruses. Antigenic analyses revealed that the viruses acquired antigenic diversity either by accumulating substitutions in the HA protein or through the introduction of IAV-S with different antigenicity. These results, obtained through continuous longitudinal surveillance, revealed that IAVs-S can be maintained in a pig farm over several years through the generation of antigenic diversity due to the accumulation of mutations, intrusion of viruses, and reassortment events.

Chapter III

Genetics and pathogenicity of H5N6 highly pathogenic avian influenza viruses isolated from wild birds and a chicken in Japan during winter 2017-2018

Introduction

During winter 2017–2018, there were outbreaks of HPAI in both Asia and Europe caused by H5N6 HPAIVs with the H5 HA gene of clade 2.3.4.4.B (111). In Europe, the first report of the H5N6 HPAIV outbreak occurred at a Dutch duck farm in December 2017 (112), after which H5N6 and H5N8 HPAIVs were isolated from both domestic poultry and wild birds. On the other side of the Eurasian continent, Korea experienced an outbreak due to H5N6 HPAIVs on a duck farm in North Jeolla province during November 2017. This was followed by outbreaks in poultry farms from Gyeonggi province in the north to South Jeolla province in the south and concurrent isolation of H5N6 HPAIVs from wild birds from Gyeonggi province in the north to Jeju province in the south (111, 113, 114). The H5 HA gene of the HPAIVs isolated from ducks in Korea during November 2017 were genetically similar to those of the December 2017 isolates in the Netherlands, and the N6 NA gene was phylogenetically related with an H3N6 AIV isolated from a barnacle goose in the Netherlands during 2014 (113, 115). In addition, H5N6 HPAIVs affected a chicken farm as well as wild birds in Japan, including several species of wild birds in Shimane during November 2017, a northern goshawk in Tokyo on 5 January 2018, a broiler chicken farm in Kagawa on 10 January 2018, and jungle crows in Hyogo during March 2018. Furthermore, the H5N8 HPAIVs isolated in Shimane carried HA and NA genes related to both the Netherlands and Korean strains (115).

In the current study, the H5N6 HPAIVs that affected Japan during winter 2017–2018 were phylogenetically compared with gene sequences deposited in the GISAID database and the repositories to investigate the origins of these H5N6 HPAIVs. In addition, the H5N6 HPAIV isolates from a chicken, a northern goshawk, and a jungle crow were characterized to assess whether pathogenicity to chickens differed between poultry and wild bird isolates.

Materials and Methods

Virus isolation and whole-genome sequencing

Tracheal or cloacal swabs collected from chickens on a farm in Kagawa prefecture with suspected HPAIV infections were inoculated into embryonated chicken eggs for virus isolation at the diagnostic laboratories of the livestock health center in Kagawa prefecture. Allantoic fluid that showed HA activity against chicken red blood cells was submitted to the National Institute of Animal Health of Japan for diagnosis, as were swab samples from dead wild birds in Tokyo and Hyogo prefectures. The whole genomes of the 43 isolated viruses were obtained by using next-generation sequencing as described in Chapter I. Consensus sequences were generated by using Workbench software (version 9.5.3, Qiagen) or FluGAS software (World Fusion). The sequences of the viruses isolated during this study are deposited in the GISAID databases.

Phylogenetic analysis

For phylogenetic analysis, sequences of all AIVs were downloaded from the GISAID database in 25 December 2018; the number of sequences downloaded for each gene was: PB2, 69,552 sequences; PB1, 51,793; PA, 71,568; H5, 10,685; NP, 69,775; N6, 3,693; MP, 87,318; and NS, 72,176. BioEdit and MAFFT were used to align the GISAID sequences with those of AIVs at the National Institute of Animal Health, Japan, and sequences shared by the Federal Research Center of Fundamental and Translational Medicine, Russia which is the collaborator of National Institute of Animal Health, Japan. After alignment, sequences with ambiguous nucleotide bases were removed, after which MAFFT was used to align the remaining sequences in order of decreasing identity with A/chicken/Kagawa/1C-1/2018 (H5N6). Sequences that were most highly related to the A/chicken/Kagawa/1C-1/2018 (H5N6) were phylogenetically analyzed by using MEGA-CC with 1,000 bootstrap replicates according to the ML method in a general time-reversible model.

Tanglegrams were constructed from pairs of the above-mentioned ML trees by using Dendroscope 3 (116). Taxa in adjacent trees were connected with those in the tree of H5 HA genes when the taxa in the two trees corresponded with each other.

MCC trees were constructed to calculate molecular estimates of divergence times from the ancestral AIVs for the PB2, PB1, PA, NP, N6, MP, and NS genes of the H5N6 HPAIVs isolated in Europe and Asia during winter 2017–2018. MCC trees were constructed by using the BEAST package version 1.8.2 as described in Chapter I to estimate divergence times.

Animal experiments

A/chicken/Kagawa/1T-1/2018 (H5N6) (Kagawa strain; isolated through 2-egg passage from a tracheal swab), A/Northern Goshawk/Tokyo/1301B003T/2018 (H5N6) (Tokyo strain; isolated through 2-egg passage from a tracheal swab), and A/Jungle crow/Hyogo/2803E023C/2018 (H5N6) (Hyogo strain; isolated through 1-egg passage from a cloacal swab) were used for animal experiments. White leghorn chickens (L-M-6 strain; specific pathogen free; age, 4 weeks) were obtained from Nisseiken (Tokyo, Japan). Animal experiments were conducted in Biosafety Level 3 facilities at the National Institute of Animal Health, Japan, and were approved by the institutional committee for Ethics of Animal Experiments (approval numbers; 17-076, 15 January 2018, 17-082, 2 March 2018, 17-086, 6 April 2018). For survival analysis, virus doses of 10^2, 10^4, 10^5, and 10^6 fifty percent egg infectious dose (EID_{50})/100 μL were inoculated intranasally into groups of 4 to 6 chickens. The chickens were observed for 14 days after inoculation. For virus titration, tracheal and cloacal swabs were collected at 1, 2, 3, 5, 7, 10, and 14 days after inoculation or at death. The swabs were put and mixed into MEM (Sigma-Aldrich) containing 0.5% bovine serum albumin (Sigma-Aldrich), 25 mg/mL amphotericin B (Thermo Fisher Scientific), 1,000 units/mL penicillin and 1,000 mg/mL streptomycin (Thermo Fisher Scientific), 0.01 M HEPES (Sigma-Aldrich), and 8.8 mg/mL $NaHCO_3$ (Thermo Fisher Scientific); the swab was removed from the medium and then the media were stored at –80°C until titration. To investigate tissue dissemination of the virus in chickens, 3 chickens were inoculated intranasally with 10^6 EID_{50}/100 μL of Kagawa, Tokyo, and Hyogo strains. Three chickens were euthanized at 3 days post-inoculation and pancreas, spleen, pectoral major muscle, liver, trachea, lung, kidney, heart, brain, duodenum, rectum, blood, tracheal swab, cloacal swab, and conjunctiva swab were collected. Tissues were minced using a Precellys homogenizer (Bertin Technologies, Ile-de-France, France) to prepare a 10 % (w/v) emulsion, and the emulsion supernatant was stored at –80 °C until titration by egg inoculation. Frozen samples were thawed and centrifuged in 3,000g at 4°C; the supernatant underwent viral titration by EID_{50}. Student's *t*-test was applied for statistical comparison and *P* value of less than 0.05 was considered as significant.

For the transmission study, 1 or 3 chickens were inoculated with 10^6 EID_{50}/100 μL of Kagawa strain; beginning at 18 h after inoculation, 6 or 4 chickens, respectively, were cohoused with the inoculated chicken(s) and then observed for 14 days thereafter. Tracheal and cloacal swabs for virus titration were collected at 1, 3, 5, 7, 10, and 14 days after inoculation or at death. To verify

viral infection in surviving chickens, blood samples were collected at the end of the observation period, and antibodies against IAV were detected by using an influenza A virus antibody test kit (IDEXX Laboratories, Westbrook, ME, USA).

Results

Outbreaks due to H5N6 strains in Japan during winter 2017–2018

In Japan, 47 reports (1 outbreak in poultry farm and 46 cases in wild birds) due to H5N6 HPAIVs were reported across 4 prefectures between 5 November 2017 and 25 March 2018 (Fig. 17). The first case involved a dead mute swan in Shimane prefecture; this was followed by cases in 5 tufted ducks and 1 black-headed gull. On January 5, a dead northern goshawk was collected in Tokyo prefecture and an H5N6 HPAIV was isolated. Six days after the report of the northern goshawk, an outbreak occurred on a broiler farm in Kagawa prefecture and approximately 90,000 broilers were euthanized to prevent disease spread. Subsequently, H5N6 HPAIVs killed multiple jungle crows in Hyogo prefecture during 1 March through 25 March 2018.

Phylogenetic analysis of the Japanese isolates

The ML trees constructed for the H5 HA gene revealed that the HA genes of the Japanese H5N6 HPAIVs during winter 2017–2018 belonged to clade 2.3.4.4.B and thus were related to the H5N8 HPAIVs in Europe during winter 2016–2017 (Fig. 18a). The Kagawa strain formed a cluster with the Korean HPAIVs of December 2017, sharing a common ancestor with the H5N6 HPAIVs that caused outbreaks in Europe during the same season. However, the isolates from wild birds in Japan formed another cluster with the Korean HPAIVs of November 2017 and the Taiwanese HPAIV from December 2017. The nucleotide identity between the Japanese wild bird isolates and the Kagawa strain was 98.2% to 98.3%.

The ML tree of the N6 NA genes demonstrated that NA genes of Japanese H5N6 HPAIVs isolated from poultry and wild birds during winter 2017–2018 were related to AIVs isolated in European countries, including Croatia, Georgia, the Netherlands, and in Moscow and Novosibirsk, Russia (Fig. 18b). The Kagawa strain showed low identity (94.5% to 94.7%) with the isolates from wild birds in Japan and formed a cluster with the Korean HPAIVs from December 2017, which differed from the cluster containing isolates from wild birds in Japan, Korean HPAIVs isolated in November 2017, and the Taiwanese HPAIV of December 2017. All of the internal genes of the Japanese H5N6 HPAIVs were derived from clade 2.3.4.4.B H5N8 HPAIVs isolated in Europe during winter 2016–2017, and almost all of them were most related to isolates in Eastern Europe (Fig. 19). As with the HA and NA genes, the internal genes of the Kagawa strain and the wild bird isolates in Japan formed different clusters and identities between Kagawa strain and wild bird isolates were as follows: PB2, 98.9% to 99.0%; PB1,

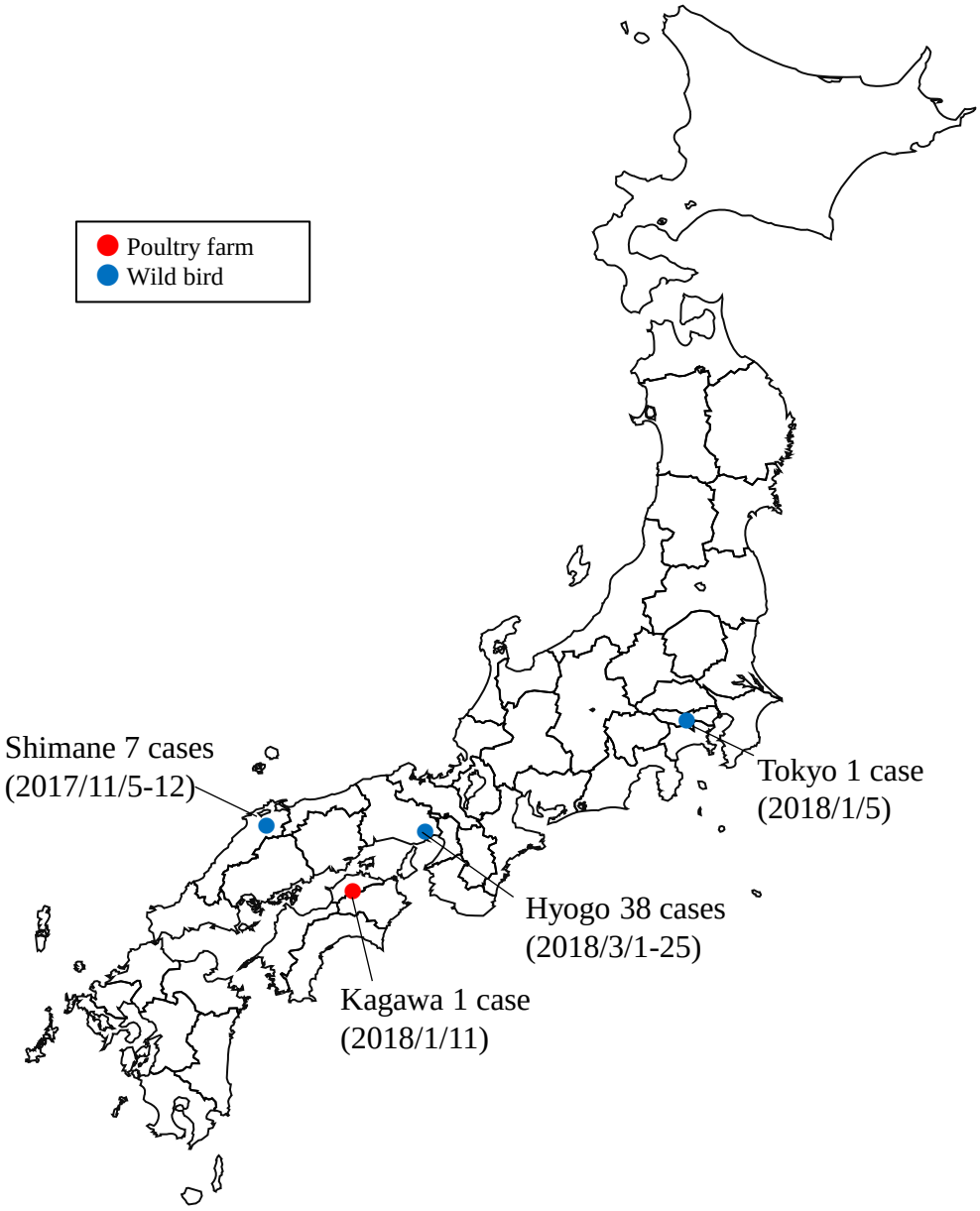

Fig. 17. Geographic locations of the H5N6 HPAI outbreaks affecting 1 poultry farm and 46 wild birds in Japan during the 2017–2018 season. Numbers of reported cases and sample collection dates are shown in parentheses.

Fig. 18. Details of ML trees based on the H5 HA (a) and N6 NA (b) genes.

The Kagawa strain is shown in red, and strains isolated from wild birds are blue. Bootstrap values of 60 or higher are shown.

b

Fig. 18. Continued

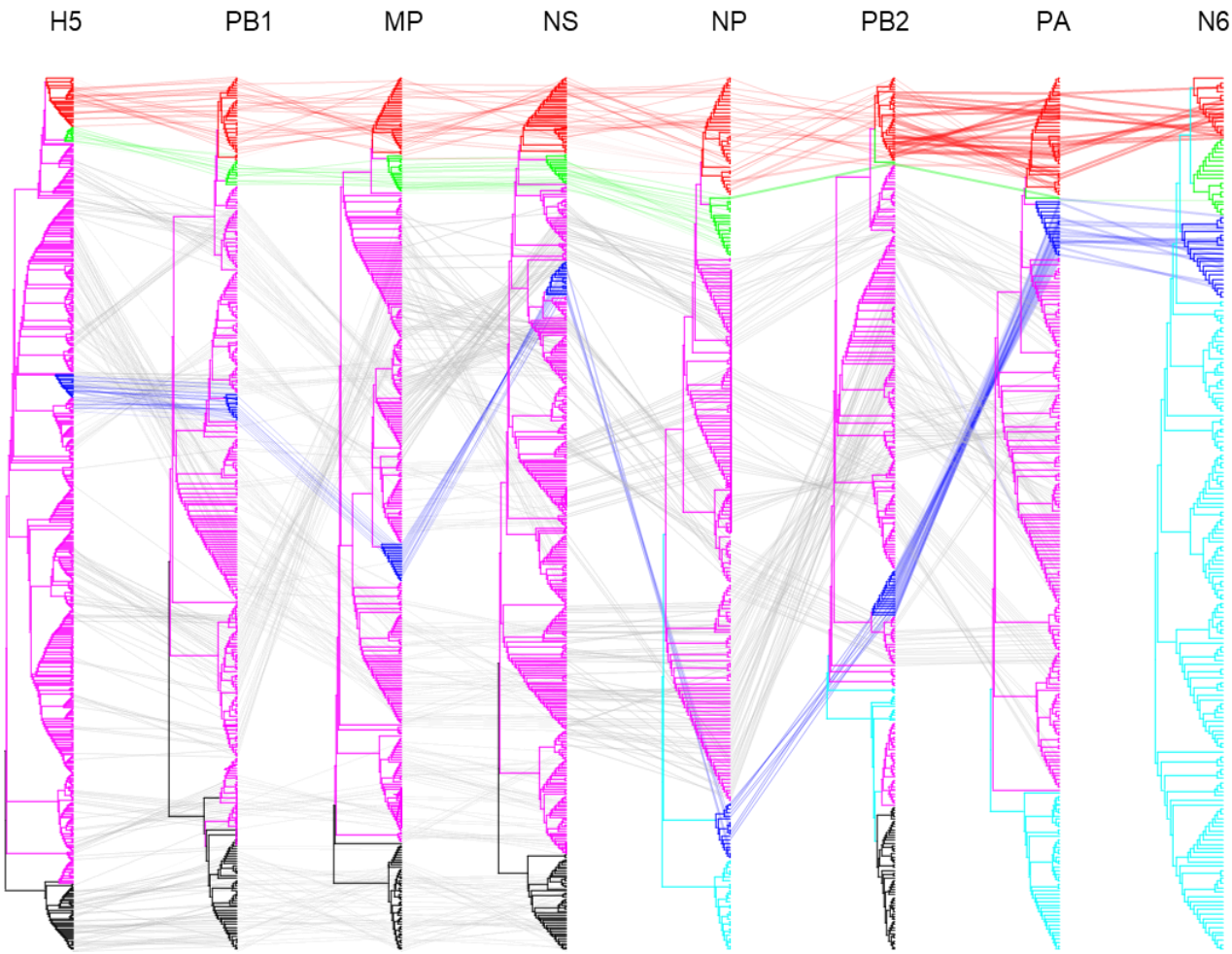

Fig. 19. Tanglegrams constructed from the ML trees of strains containing the individual gene most related to that of the Kagawa strain.
Colors of taxa and lines are as follows: black, isolates of clade 2.3.4.4.B H5N8 HPAIVs isolated in China and Russia during May 2016; purple, H5N8 HPAIVs isolated during the 2016–2017 season; red, Kagawa strain and Korean strains of December 2017; green, H5N6 HPAIVs isolated in Europe during the 2017–2018 season; blue, H5N6 HPAIVs isolated from wild birds in Japan and Korean HPAIVs during November 2017 and the Taiwanese HPAIV of December 2017; light blue, not HPAIVs. Corresponding taxa in adjacent trees are connected by lines.

98.2% to 98.3%; PA, 98.5% to 98.7%; NP, 98.8% to 99.0%; MP, 97.9% to 98.1%; and NS, 97.6% to 98.0%.

According to the MCC tree that was constructed by using N6 sequence data (Fig. 20), the cluster including the Kagawa strain was estimated to have diverged from that containing the wild bird isolates on 15 September 2016 (95% HPD: 17 August to 26 October 2016). Furthermore, the subcluster composed of the Kagawa and Korean strains was estimated to have diverged from the subcluster of European H5N6 HPAIVs on 14 August 2017 (95% HPD: 10 June to 21 September 2017). These results suggest that the H5N6 HPAIVs in the Kagawa–Korean cluster shared a common ancestor during summer 2017 and had been disseminated to both Asia and Europe by December 2017. The cluster including the wild bird isolates in Japan was estimated to have diverged from Greek strains on 30 October 2016 (95% HPD: 16 October to 14 December 2016), thus indicating that the strains diverged from a common ancestor during Autumn 2016. In contrast, Taiwanese and Japanese strains were estimated to have diverged from each other during summer 2017 (16 August 2017; 95% HPD: 16 May to 5 October 2017).

Then the dates on which various genes of the H5N6 HPAIVs in Japan during winter 2017–2018 had diverged from an ancestral (non-HPAIV) AIV were estimated (Table 12). The divergence times of the PB1 and MP genes of the Japanese H5N6 HPAIVs of winter 2017–2018, which shared deduced ancestors with the H5N8 HPAIVs in Europe during winter 2016-2017 that were related to H5N8 HPAIVs in China and Russia during May 2016, were 3 October 2015 (95% HPD: 14 September 2015 to 29 January 2016) and 13 October 2015 (95% HPD: 2 February to 10 November 2015), respectively, thus indicating that these viruses diverged during summer 2015. The H5 and NS genes of Japanese H5N6 HPAIVs during winter 2017–2018 shared an ancestor with H5N8 HPAIVs in Europe during 2016-2017 that were related to A/duck/Eastern China/S1109/2014 (H5N8) as well as the H5N8 HPAIVs in China and Russia in May 2016; the divergence times from AIVs (excluding HPAIVs) were 1 October 2014 (95% HPD: 30 July to 7 November 2014) and 28 July 2014 (95% HPD: 15 June to 7 November 2014), respectively. The PB2, PA, and NP genes, the origins of which were considered to be H5N8 HPAIVs in Europe during winter 2016-2017 that were different from the H5N8 HPAIVs in China and Russia during May 2016, were estimated to have diverged on 22 April 2016 (95% HPD: 2 April to 14 June 2016), 19 May 2016 (95% HPD: 11 January to 10 June 2016), and 24 June 2016 (95% HPD: 13 April to 4 August 2016), respectively, indicating that they all diverged from an ancestral AIV during summer 2016. Except for A/Black-headed Gull/Netherlands/29/2017 (H5N6), the PB2 and PA genes of H5N6 HPAIVs in Europe during winter 2017–

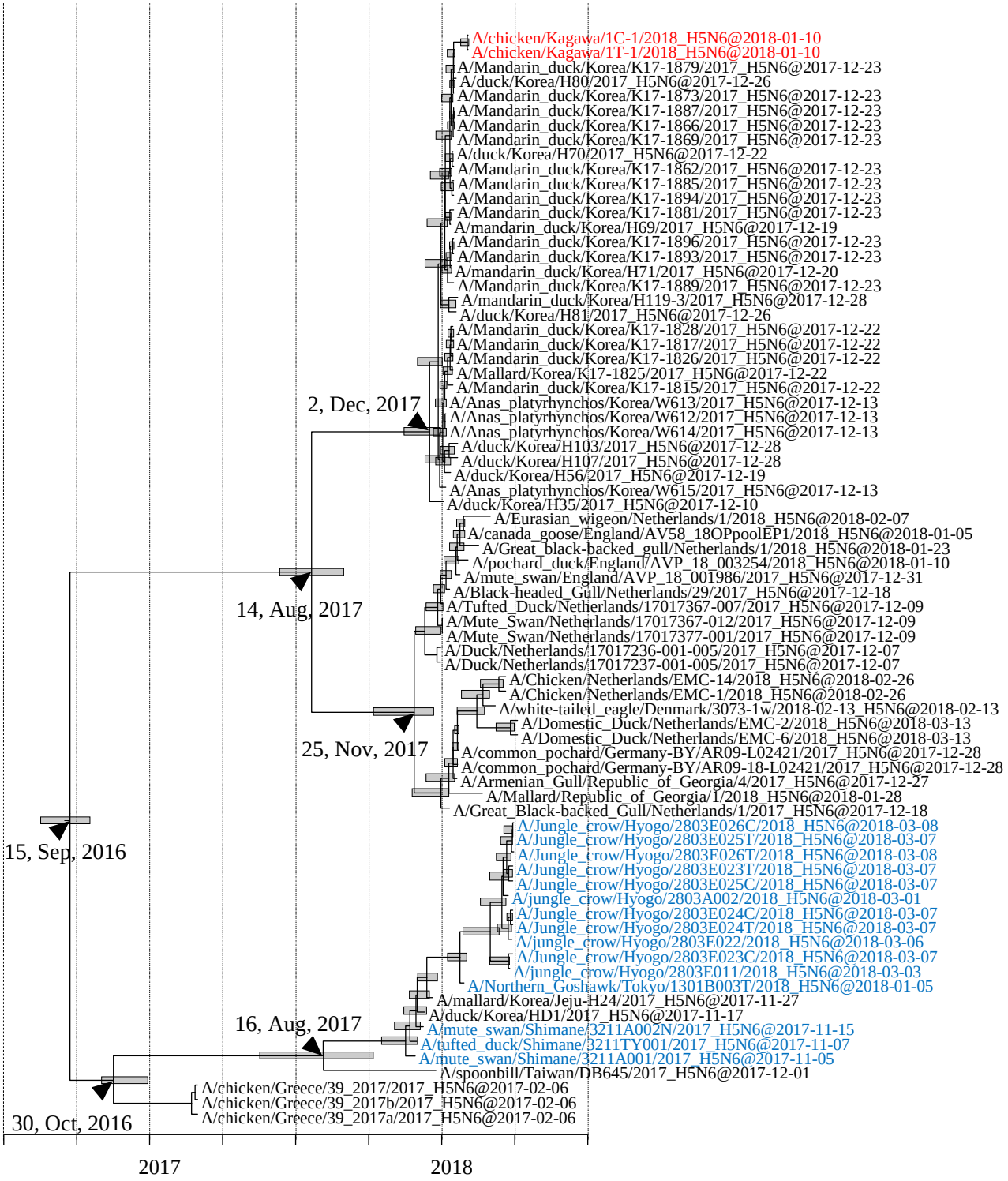

Fig. 20. Detail of the MCC tree of the N6 NA genes.
The divergence time at the branch is indicated by a black arrow, and the 95% highest posterior density for the divergence time is indicated by a gray box. The Kagawa strain and strains isolated from wild birds are red and blue, respectively.

Table 12. Estimated divergence time of each gene of H5N6 HPAIVs during Winter 2017–2018 from the most recent AIVs (except HPAIVs).

Gene	Estimated time (95% HPD interval)		
	H5N6 HPAIVs in Asia (including Kagawa strain)	H5N6 HPAIVs in Asia (including Tokyo and Hyogo strain)	H5N6 HPAIVs in Europe
PB2	23 June, 2016 (21 April to 7 July, 2016)	23 June, 2016 (21 April to 7 July, 2016)	29 June, 2017 (24 February to 29 September, 2017)
PB1	13 September, 2015 (11 July to 28 November, 2015)	13 September, 2015 (11 July to 28 November, 2015)	13 September, 2015 (11 July to 28 November, 2015)
PA	17 June, 2016 (6 April to 4 August, 2016)	17 June, 2016 (6 April to 4 August, 2016)	23 August, 2016 (10 April to 6 October, 2016)
NP	18 July, 2016 (7 April to 6 August, 2016)	18 July, 2016 (7 April to 6 August, 2016)	18 July, 2016 (7 April to 6 August, 2016)
N6	14 August, 2017 (10 June to 21 September, 2017)	30 October, 2016 (16 October to 14 December, 2016)	14 August, 2017 (10 June to 21 September, 2017)
MP	7 August, 2015 (2 February to 10 November, 2015)	7 August, 2015 (2 February to 10 November, 2015)	7 August, 2015 (2 February to 10 November, 2015)
NS	12 October, 2014 (17 June to 7 November, 2014)	12 October, 2014 (17 June to 7 November, 2014)	12 October, 2014 (17 June to 7 November, 2014)

2018 were not related to the H5N6 HPAIVs in Asia during 2017–2018 but instead were descended from AIVs in Europe, with estimated divergence dates of 19 May 2017 (95% HPD: 29 December 2016 to 11 September 2017) and 30 September 2016 (95% HPD: 5 May to 10 October 2016), respectively.

The time-measured phylogenetic analysis suggests that these reassortments might have occurred as depicted in Fig. 21. The PB1, HA, MP, and NS genes of the H5N6 HPAIVs in Asia and Europe during winter 2017–2018 were derived from the H5N8 HPAIVs in China and Russia during May 2016. The Tokyo and Hyogo strains acquired the PB2, PA, NP, and N6 NA genes during summer 2016. In contrast, the Kagawa strain acquired the PB2, PA, and NP genes during summer 2016 and then N6 during summer 2017. The identities of the PB2, PA, and NP genes between the Kagawa strain and the Japanese wild bird isolates (98.9% to 99.0%, 98.5% to 98.7%, and 98.8% to 99.0%, respectively) are higher than those of PB1, MP, and NS (98.2% to 98.3%, 97.9% to 98.1%, and 97.6% to 98.0%, respectively), supporting the notion that the origins of PB2, PA, and NP genes were distinct from PB1, MP, and NS genes. European H5N6 HPAIVs obtained their PA and NP genes during summer 2016 and their PB2 and N6 NA genes during summer 2017.

Pathogenicity of poultry and wild bird strains in chickens

To investigate potential differences in pathogenicity among the H5N6 HPAIVs, chickens were intranasally inoculated with several doses of the Kagawa, Tokyo, and Hyogo strains and then observed for 14 days (Fig. 22). All of the chickens inoculated with 10^6 EID_{50} of Kagawa strain died within 3 days, and 4 of the 5 chickens inoculated with 10^5 EID_{50} of this isolate died within 4 days, whereas no chickens inoculated with 10^4 EID_{50} died during the observation period (Fig. 22a). All of the chickens inoculated with 10^5 or 10^6 EID_{50} of the Tokyo strain died within 5 and 3 days after inoculation, respectively, and 1 of the 5 chickens inoculated with 10^4 EID_{50} of the Tokyo strain died 3 days after inoculation (Fig. 22b). All of the chickens inoculated with 10^6 EID_{50} of the Hyogo strain died within 4 days, as did 1 of 5 and 2 of 5 chickens inoculated with 10^4 or 10^5 EID_{50} of Hyogo strain, respectively (Fig. 22c). For all strains, all chickens inoculated with 10^2 EID_{50} survived the observation period (data not shown). Therefore, the 50% chicken lethal doses of Kagawa, Tokyo, and Hyogo strains were calculated as $10^{4.63}$ EID_{50}, $10^{4.38}$ EID_{50}, and $10^{5.00}$ EID_{50}, respectively. None of the sera collected from surviving chickens on day 14 after inoculation contained detectable antibodies against IAV (data not shown).

The mean viral titer from tracheal swabs collected from dead chickens inoculated with 10^6 EID_{50} of the Kagawa strain (4.44 ± 0.53 $\log_{10}$ EID_{50}/mL) was

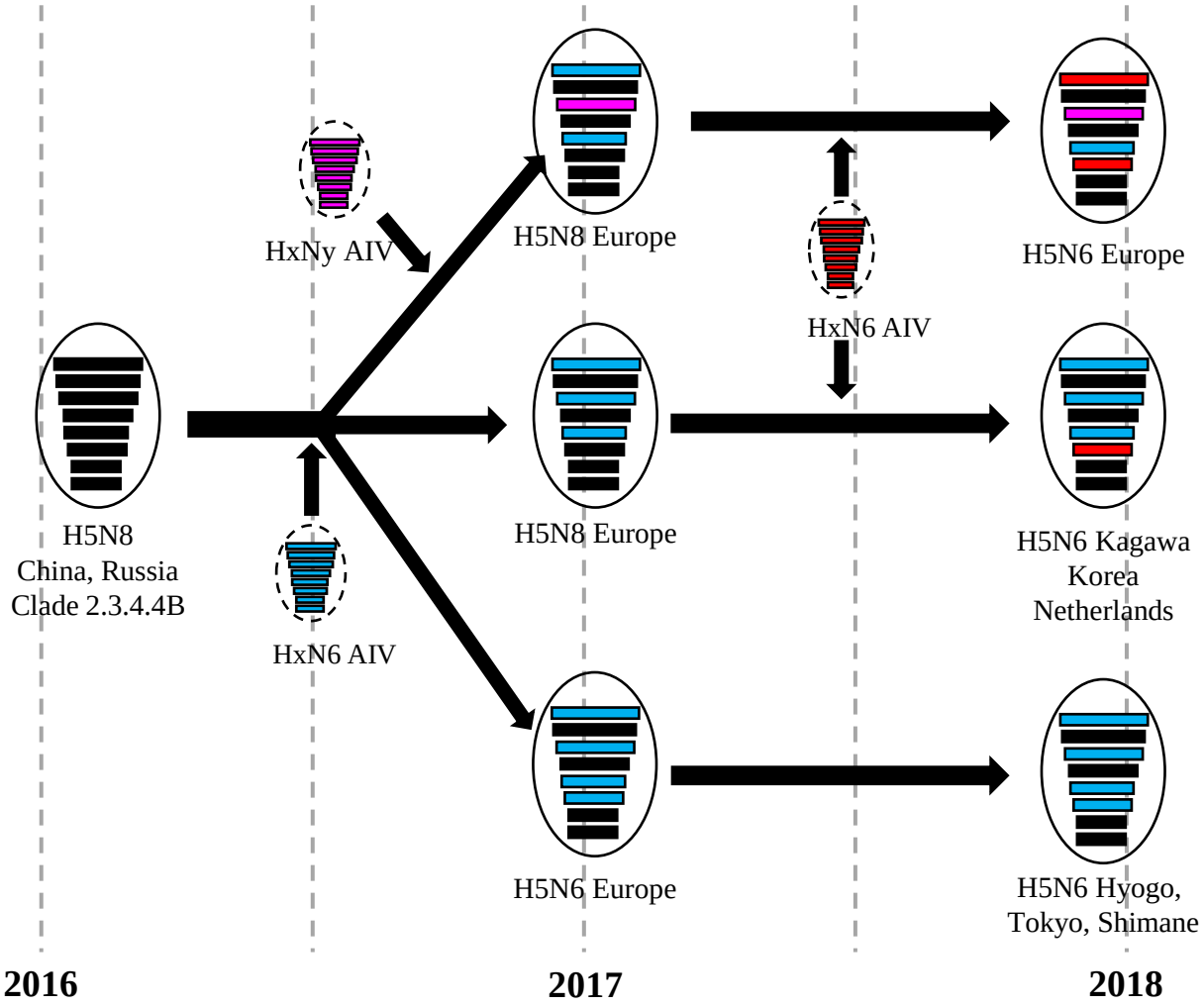

Fig. 21. Evolutionary timeline of generation of the Japanese H5N6 HPAIVs through reassortment between H5N8 HPAIVs and HxN6 AIVs. Black bars represent the lineage of the 2.3.4.4.B H5N8 HPAIVs in China and Russia in May 2016; the other colored bars represent lineage(s) of AIVs.

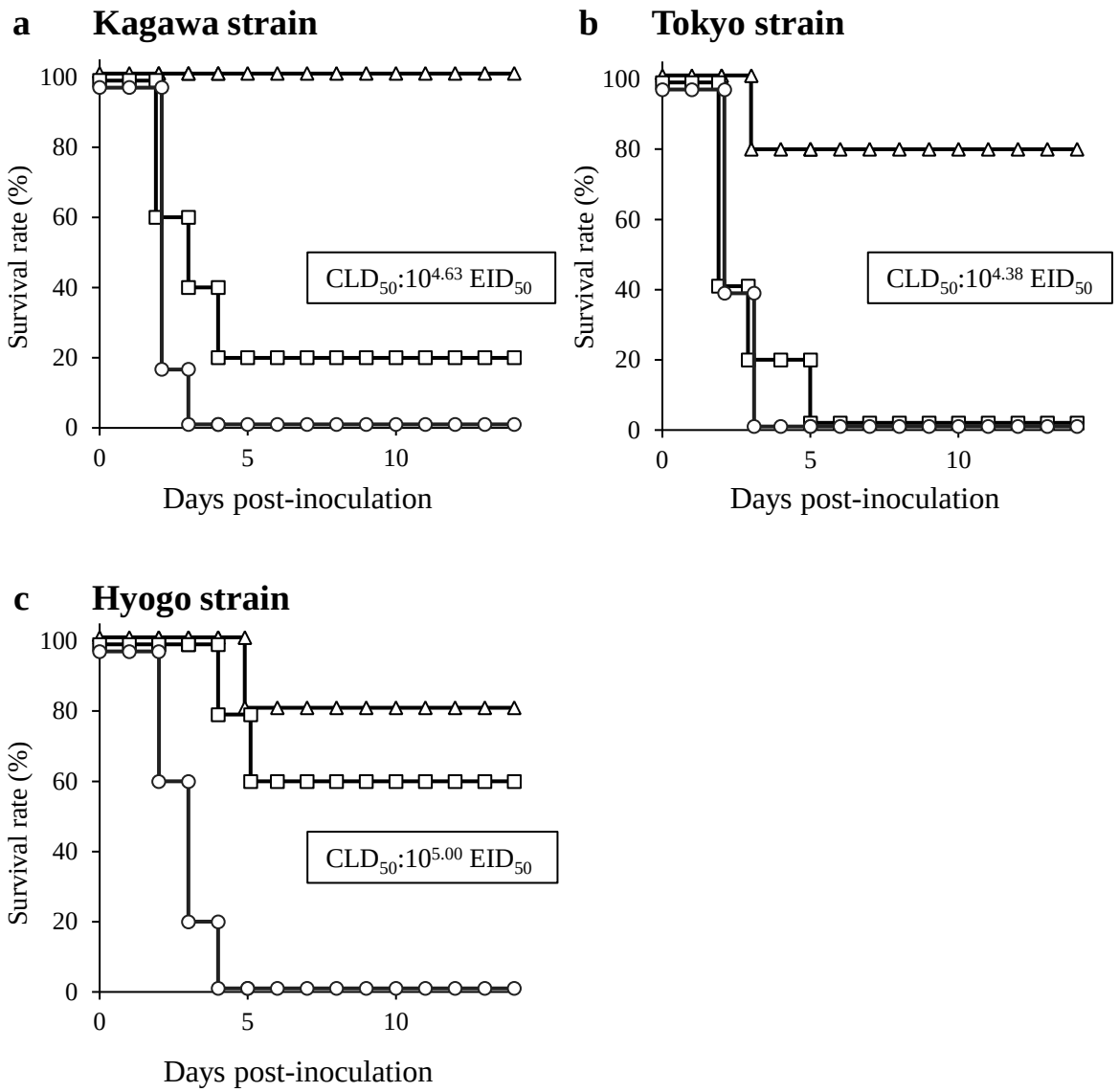

Fig. 22. Survival rates of chickens inoculated intranasally with 10^6, 10^5, or 10^4 EID_{50} of Kagawa strain (a), Tokyo strain (b), and Hyogo strain (c).
Circles, squares, and triangles indicate the survival rates of birds inoculated with 10^6, 10^5, or 10^4 EID_{50} of each virus, respectively.

significantly higher than that from their cloacal swabs (3.52 ± 0.80 $\log_{10}$ EID_{50}/mL) with *P* value < 0.01 (Fig. 23a and b). The same pattern emerged for chickens inoculated with 10^6 EID_{50} of Hyogo strain (4.62 ± 0.48 $\log_{10}$ EID_{50}/mL vs 3.52 ± 0.80 $\log_{10}$ EID_{50}/mL) with *P* value < 0.01 (Fig. 23e and f). The mean maximum viral titer of tracheal swabs from live chickens inoculated with the Kagawa strain did not differ from that of wild bird isolates at all inoculation doses (10^4, 10^5, and 10^6 EID_{50}). The same pattern was seen regarding the cloacal swabs from live chickens and the tracheal or cloacal swabs from dead birds, indicating the lack of a significant difference between the Kagawa strain and wild bird isolates regarding viral shedding. No viruses were obtained from the tracheal and cloacal swabs collected from surviving chickens inoculated with the Kagawa, Tokyo, or Hyogo strains on days 7, 10, or 14 after inoculation (data not shown).

Measurement of viral titers in tissues revealed that—unlike the Tokyo and Hyogo strains—the Kagawa strain propagated efficiently in several tissues (Table 13). At 2 days after inoculation of the Kagawa strain at 10^6 EID_{50}, the mean viral titers in kidney and cloacal swabs were significantly higher than those of the Tokyo strain; those in the brain and rectum were significantly higher than those of the Hyogo strain; and those in the muscle and trachea were significantly higher than those of both the Tokyo and Hyogo strains. Viral titers on day 1 after inoculation did not differ among any tissues or strains. No gross lesions were observed in tissues of all chickens at 1 and 2 day(s) after inoculation with each strain.

Transmission of Kagawa strain in chickens

In the transmission study, the 1 chicken inoculated with 10^6 EID_{50} of Kagawa strain died within 48 h after inoculation, whereas none of the 6 cohoused chickens died during the 14-day observation period (Fig. 24a). The viral titers of the tracheal and cloacal swabs collected from the dead chicken were 6.07 and 5.20 $\log_{10}$ EID_{50}/mL, respectively. No antibodies against IAV were detected in sera collected from the cohoused chickens that survived for 14 days after placement with the inoculated bird (data not shown), indicating a lack of viral transmission to the cohoused chickens.

Then 3 chickens were inoculated with 10^6 EID_{50} of Kagawa strain and housed them with 4 naïve chicken. The 3 inoculated chickens died within 66 h after inoculation, and the 4 cohoused chickens died 150 h after being penned with the inoculated birds (Fig. 24b). In addition, 2 of the cohoused chickens demonstrated viral shedding at 102 h after being placed with the inoculated chickens, and the 2 other chickens shed virus at 150 h. The viral titers (mean ± SEM) of the tracheal and cloacal swabs collected from the dead inoculated

chickens were 3.99 ± 0.26 and 3.80 ± 1.10 $\log_{10}$ EID_{50}/mL, respectively, and those of the dead cohoused chickens were 4.44 ± 0.55 and 2.81 ± 1.21 $\log_{10}$ EID_{50}/mL, respectively. There were no significant differences between mean viral titers collected from inoculated chicken(s) of two transmission studies. These results show that the 4 cohoused chickens were infected through viral transmission from the 3 inoculated chickens.

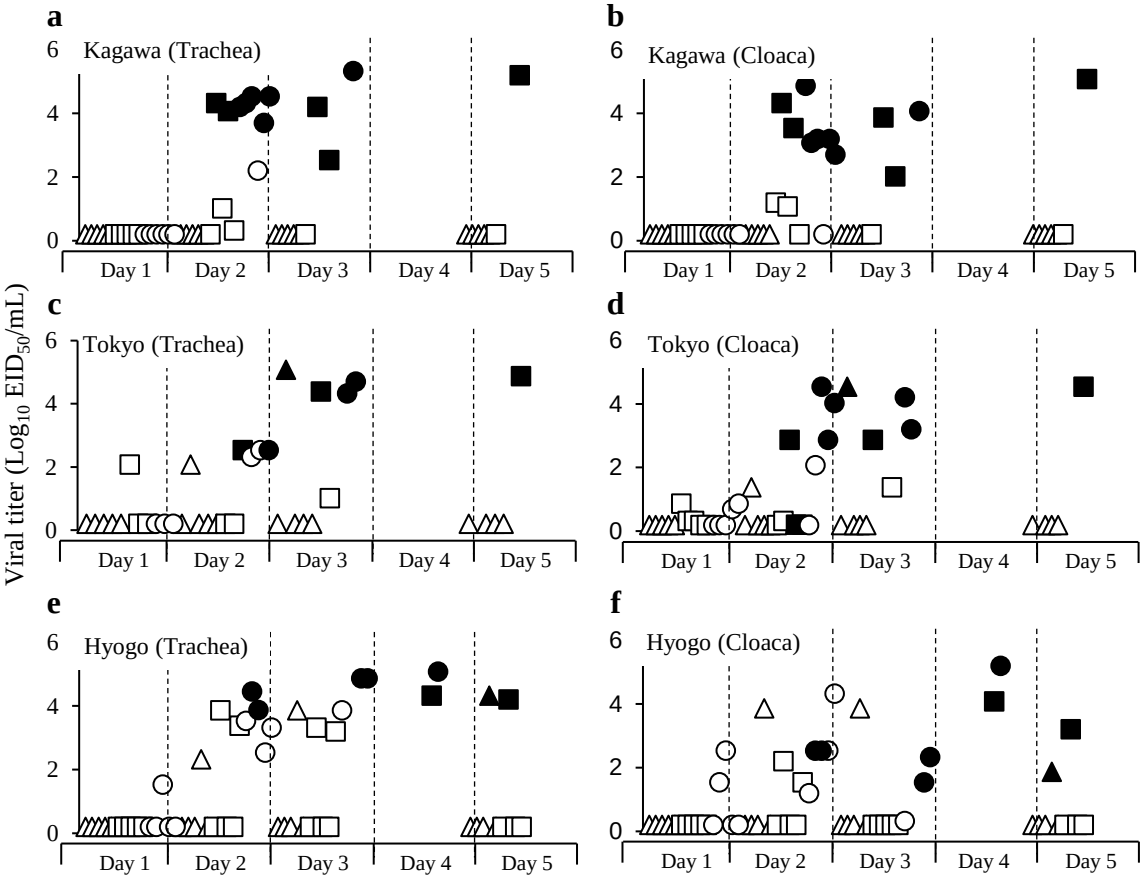

Fig. 23. Viral titers of tracheal and cloacal swabs collected from live and dead chickens that had been inoculated with 10^6, 10^5, or 10^4 EID_{50} of each virus.

Tracheal (a) and cloacal (b) swabs collected from chickens inoculated with Kagawa strain. Tracheal (c) and cloacal (d) swabs collected from chickens inoculated with Tokyo strain. Tracheal (e) and cloacal (f) swabs collected from chickens inoculated with Hyogo strain. White and black shapes indicate the results from live and dead chickens, respectively. Circles, squares, and triangles represent the viral titers of chickens inoculated with 10^6, 10^5, or 10^4 EID_{50} of each virus, respectively.

Table 13. Viral titers in organs, tissues, and swabs of chickens inoculated with 10^6 EID_{50} of H5N6 HPAIVs.

Sample	Log_{10} EID_{50}/mL at each							
	Kagawa		Tokyo		Hyogo		*P* value vs Kagawa on day 2	
	Day 1	Day 2	Day 1	Day 2	Day 1	Day 2	Tokyo	Hyogo
Pancreas	2.11 ± 1.29 (2/3)[†]	5.78 ± 1.27 (3/3)	3.42 ± 2.74 (3/3)	4.31 ± 2.41 (3/3)	4.03 ± 1.65 (2/3)	5.76 ± 0.62 (2/3)	0.4029	0.9848
Spleen	4.02 ± 1.50 (3/3)	6.39 ± 0.54 (3/3)	5.24 ± 2.06 (3/3)	6.75 ± 0.38 (3/3)	4.31 ± 3.46 (3/3)	3.89 ± 2.99 (3/3)	0.3954	0.2269
Muscle	1.76 ± 0.80 (2/3)	5.87 ± 0.58 (3/3)	3.42 ± 2.97 (2/3)	4.47 ± 0.54 (3/3)	2.87 ± 1.41 (2/3)	4.09 ± 0.32 (2/3)	0.0382*	0.0314*
Liver	2.75 ± 1.05 (3/3)	6.19 ± 0.28 (3/3)	5.63 ± 2.03 (2/3)	5.48 ± 0.54 (3/3)	5.51 ± 0.62 (2/3)	4.32 ± 1.24 (2/3)	0.1109	0.0724
Trachea	2.28 ± 0.82 (3/3)	6.75 ± 0.38 (3/3)	3.79 ± 2.86 (3/3)	5.68 ± 0.54 (3/3)	4.46 ± 0.11 (2/3)	5.35 ± 0.04 (2/3)	0.0480*	0.0165*
Lung	3.24 ± 1.79 (3/3)	7.43 ± 0.51 (3/3)	4.31 ± 3.01 (3/3)	6.09 ± 1.71 (3/3)	5.39 ± 0.67 (2/3)	4.20 ± 3.18 (3/3)	0.2629	0.1573
Kidney	2.53 ± 1.40 (3/3)	7.24 ± 0.14 (3/3)	3.56 ± 2.54 (3/3)	6.16 ± 0.40 (3/3)	3.37 ± 1.18 (2/3)	3.75 ± 2.80 (3/3)	0.0117*	0.0972
Heart	2.16 ± 1.15 (3/3)	6.05 ± 0.50 (3/3)	4.13 ± 1.50 (2/3)	6.58 ± 1.23 (3/3)	4.01 ± 0.44 (2/3)	7.11 ± 0.13 (2/3)	0.5214	0.0678
Brain	1.67 ± 0.49 (2/3)	5.74 ± 0.22 (3/3)	2.42 ± 2.42 (3/3)	5.25 ± 0.86 (3/3)	2.93 ± 0.86 (2/3)	4.26 ± 0.09 (2/3)	0.3954	0.0034*
Duodenum	1.93 ± 2.27 (2/3)	6.66 ± 0.66 (3/3)	4.37 ± 2.59 (2/3)	5.76 ± 0.65 (3/3)	3.80 ± 0.38 (2/3)	4.36 ± 1.90 (2/3)	0.1686	0.1306
Rectum	2.09 ± 1.53 (3/3)	7.14 ± 0.16 (3/3)	3.022.97 (3/3)	5.57 ± 1.08 (3/3)	3.87 ± 0.94 (2/3)	4.70 ± 0.88 (2/3)	0.0685	0.0148*
Blood	1.66 ± 0.56 (3/3)	-[§] (0/3)	4.70 ± 3.06 (2/3)	5.04 ± 0.95 (3/3)	2.62 ± 0.12 (2/3)	3.82 ± 0.88 (2/3)		
Trachea swab	<[‡] (0/3)	3.82 ± 1.11 (3/3)	2.07 (1/3)	< (0/3)	< (0/3)	2.53 ± 0.94 (2/3)		0.2767
Cloaca swab	0.32 (1/3)	2.45 ± 0.35 (2/3)	3.07 (1/3)	0.70 ± 0.48 (3/3)	< (0/3)	2.51 ± 1.15 (2/3)	0.0224*	0.9480
Conjunctiva swab	0.32 (1/3)	0.32 (1/3)	2.07 (1/3)	1.32 (1/3)	< (0/3)	1.24 ± 1.31 (2/3)		

†, Titers are shown as means ± standard error (range). Numbers in parentheses: number of chickens whose samples were positive/total number of chickens.
‡, <, no virus was detected from specimens collected during the observation period (detection limit <0.32 log_{10} EID_{50}/mL).
§, -, Blood samples were not collected because chickens died.
*, $P < 0.05$.

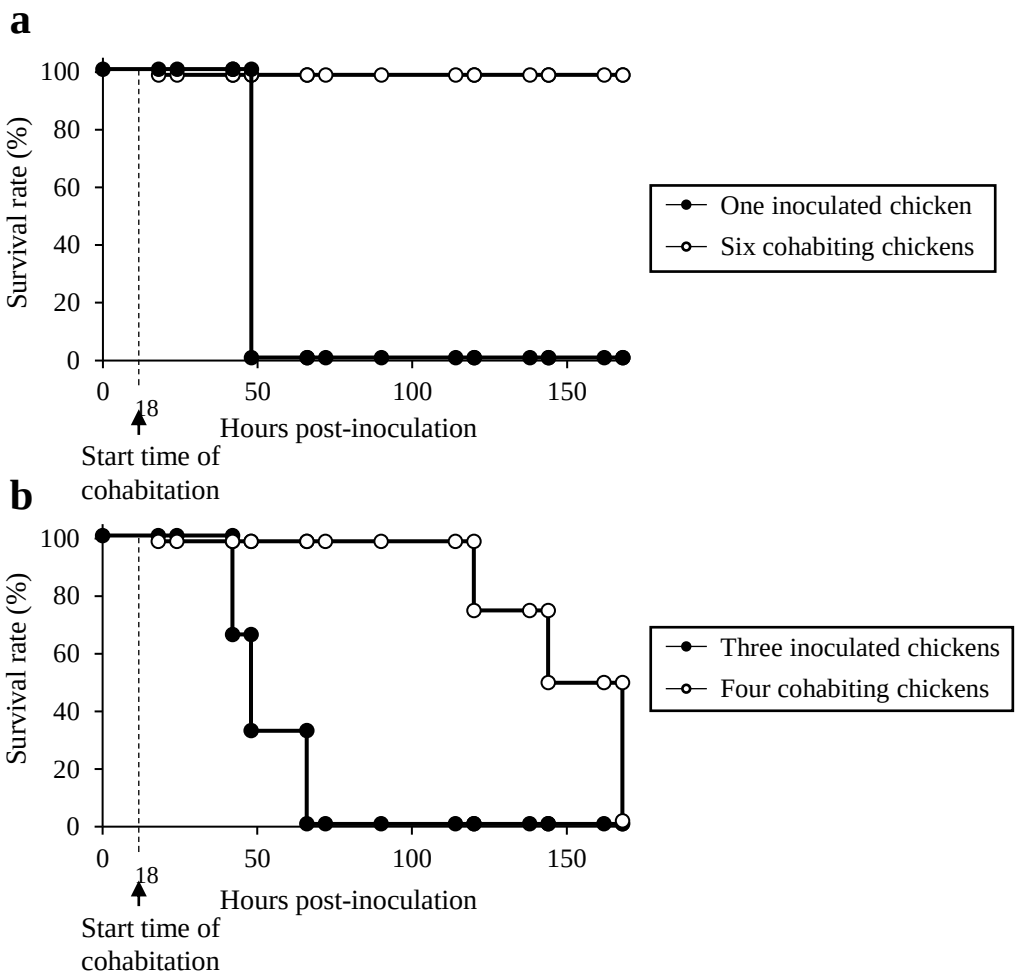

Fig. 24. Survival rates of chickens inoculated intranasally with 10^6 EID_{50} of Kagawa strain and of cohabiting chickens.

(a) One chicken was inoculated, and 6 chickens were cohoused. (b) Three chickens were inoculated and 4 chickens were cohoused. Survival rates of inoculated chicken(s) are indicated by black circles; survival rates for cohoused birds are shown as white circles.

Discussion

The H5N6 HPAIVs isolated in Japan during winter 2017–2018 were emerged through several reassortments between 2.3.4.4.B H5N8 HPAIVs that circulated in Europe during winter 2016–2017 and HxN6 AIVs in Europe, similar to the scenario regarding the H5N6 HPAIVs in Korea during the same season (52, 113). In addition, at least 3 distinct reassortments between H5N8 HPAIVs and HxN6 AIVs reportedly resulted in the appearance of the European H5N6 HPAIVs and 2 types of Korean H5N6 HPAIVs (114) as depicted in Fig. 21. However, note that the genetic flow of H5N8 and H5N6 HPAIVs depicted in Fig. 21 is simulated according to the time-measured phylogenetic tree for each gene. In Fig. 21, AIVs in which all 8 segments are red, blue, or purple have not actually been detected, indicating that even more complicated reassortment events might have occurred.

Phylogenetic analyses revealed that the relationship between Kagawa strain in January 2018 and Korean strains isolated from wild ducks as well as poultry in December 2017, suggesting that the H5N6 HPAIVs were introduced to Japan via migration of wild birds. Considering that the H5N6 HPAIVs were disseminated simultaneously to Europe and Asia by wild migratory birds, they might have originated at a breeding site, possibly in Siberia where migratory birds belonging to several flyways stretching across the Eurasian continent coexist during summer (117, 118); AIVs of various subtypes have been isolated in this area (119, 120). An AIV that carried the N6 NA gene related to the H5N6 HPAIVs during winter of 2017–2018 was isolated during September 2017 in the Novosibirsk region (A/teal/Ubinskoe_Lake/51/2017 H3N6; Fig. 18b), which is located in southeastern Siberia, supporting the hypothesis presented above. In addition, the internal genes of H5N6 HPAIVs in Europe and Asia during winter 2017–2018 originated from AIVs through reassortments that were estimated to have occurred during the summers of 2014–2017, highlighting the importance of Siberia as the accumulation place of various AIVs. However, few data were available regarding the relationship between the movements of migratory birds and the spread of H5N6 HPAIVs during winter of 2017–2018 across the Eurasian continent. Therefore, further analysis of genome sequences of AIVs and migration of wild birds in Siberia is needed to elucidate how AIVs/HPAIVs move cross-continentally.

The pathogenicity of clade 2.3.4.4 H5 reassortants to chickens is lower than that of ancestral H5N1 HPAIVs (121-123). In addition, previous experimental infections of several H5 HPAIVs revealed that the lethal infectious dose of the Kagawa, Tokyo, and Hyogo strains in chickens is relatively low because 50% chicken lethal doses of them ($10^{4.38}$ to $10^{5.00}$) were 10-fold more or

higher than those of H5N1 HPAIVs during winter 2010–2011 ($10^{3.00}$ to $10^{4.33}$)(48), some H5N8 HPAIVs of winter 2014–2015 ($10^{3.50}$) (50, 124), and the H5N6 HPAIVs of winter 2016–2017 ($10^{3.00}$) (54) under same experimental condition. 10^6 EID_{50} of Kagawa strain killed chickens relatively faster (5 chickens, 2 dpi; 1 chicken, 3 dpi) than Tokyo strain (3 chickens, 2 dpi; 2 chickens, 3 dpi) (Fig. 22), corresponding to higher viral titers in some tissues collected from chickens inoculated with 10^6 EID_{50} of Kagawa strain than Tokyo strain. However, Differences in viral titers in tissues did not explain the lower mortality in 10^4 EID_{50} and 10^2 EID_{50} with Kagawa strain than Tokyo strain, suggesting that capacity to propagate in tissues does not always corelate with the infectivity among the H5N6 HPAIVs. Current transmission study with a single inoculated chicken revealed that the Kagawa strain was less transmissible than the H5N1 HPAIVs of winter 2010–2011; in fact, regardless of whether the origins of the H5N1 HPAIVs during winter 2010–2011 were poultry or wild birds, a single chicken inoculated with 10^6 EID_{50} shed enough virus for transmission to cohoused four chickens in the same experimental setting (48). Furthermore the viral titers of the tracheal and cloacal swabs collected from Kagawa-inoculated chicken (6.1 and 5.2 $\log_{10}$ EID_{50}/mL, respectively) were equal to, or higher than, those of 3 H5N1 HPAIVs (3.3 to 6.5 and 2.5 to 5.0 $\log_{10}$ EID_{50}/mL, respectively) despite failure of transmission, suggesting that the differences in transmissibility were due to interstrain differences in the 50% chicken lethal doses. Similarly, low pathogenicity and transmissibility were observed for several 2.3.4.4 H5 HPAIVs isolated from wild birds (121, 125, 126), suggesting that those strains were not well evolved to disseminate among chickens. Therefore, these results may explain—at least in part—why the outbreaks in Japan during winter 2017–2018 were sporadic and constrained.

In conclusion, the results of the current study show that the H5N6 HPAIVs of poultry and wild birds in Japan during winter 2017–2018 were generated through several distinct reassortments between 2.3.4.4.B H5N8 HPAIVs and HxN6 AIVs that might have occurred during the summers of 2016 and 2017 in Siberia, where migratory birds wintering in Asia or Europe visit for breeding during summer. The finding that H5N6 HPAIVs with different gene cassettes intruded into Japan highlights the importance of understanding the behavior of AIVs at the breeding site in Siberia, where reassortments might occur, and of elucidating how HPAIVs are disseminated across Eurasian continents. Compared with the H5 HPAIVs that have caused past outbreaks in Japan, the Japanese H5N6 HPAIVs of winter 2017–2018 were lower in pathogenicity, and the Kagawa strain showed lower transmissibility in chickens, resulting in the limited outbreaks.

Summary

An H5N6 HPAIV outbreak occurred in poultry in Japan during January 2018, and H5N6 HPAIVs killed several wild birds in 3 prefectures during winter 2017–2018. Time-measured phylogenetic analyses demonstrated that the HA and internal genes of these isolates were genetically similar to clade 2.3.4.4.B H5N8 HPAIVs in Europe during winter 2016–2017, and NA genes of the poultry and wild bird isolates were gained through distinct reassortments with AIVs that were estimated to have circulated possibly in Siberia during summer 2017 and summer 2016, respectively. Lethal infectious dose to chickens was similar between the poultry and wild-bird isolates. H5N6 HPAIVs during winter 2017–2018 in Japan had higher 50% chicken lethal doses and lower transmission efficiency than the H5Nx HPAIVs that caused previous outbreaks in Japan, thus explaining in part why cases during the 2017–2018 outbreak were sporadic.

Chapter IV

Phylogeographic evidence for the inter- and intracontinental dissemination of avian influenza viruses via migration flyways.

Introduction

IAVs have been isolated from birds and from various mammals, including pigs and humans (127). Wild waterbirds (e.g., *Anseriformes* and *Charadriiformes*) form the natural reservoir of AIVs of H1–H16 HA and N1–N9 NA subtypes (3-7). AIVs often spread to geographically distinct regions or across major water bodies, or both, as wild birds migrate, because AIV infection usually does not cause clinical signs in these birds or disturb their long-distance migrations (128, 129). In fact, phylogenetic analyses of viral whole genomes revealed that AIVs carrying genes of the North American lineage were isolated in Europe, and AIVs carrying genes of the Eurasian lineage were isolated in the United States (130-135).

The isolation of HPAIVs from wild birds was rare (136, 137) until 1996, when the situation changed with the emergence of H5N1 HPAIVs that caused outbreaks among domestic geese in China (44). The first outbreak caused among wild birds by H5N1 HPAIVs was recognized in multiple bird species in Hong Kong in 2002 (138); this was followed by a die-off of *Anseriformes* and *Charadriiformes* in Qinghai Lake in April 2005 (139) and isolation of the viruses—so-called Qinghai strains—from wild birds in western Siberia in July 2005 (140). The strains spread to Europe and West Africa between October 2005 and February 2006 (141, 142). The movement of migratory birds, as well as the poultry trade, played an important role in the spread of these viruses (141, 143, 144). During the winter 2014–2015, H5 HPAIVs related to the viruses circulating in Asia spread to North America (145, 146). Some studies suggested that the movement of migratory birds from Asian wintering sites to breeding sites in Far East Siberia and the Alaskan Peninsula, and the subsequent southward movement along the Pacific coast of North America, could be related to this spread of HPAIVs (52, 147). In addition, a previous report demonstrated that H5 HPAIVs, which showed high pathogenicity in poultry under experimental infection, caused mild or no clinical signs in wild birds (148). These events highlight the involvement of wild birds in the spread of AIVs, including HPAIVs (149).

During the winter 2017–2018, both Asia and Europe experienced outbreaks of disease caused by H5N6 HPAIVs (111). Several reports demonstrated that H5N6 HPAIVs isolated at a duck farm in the Netherlands in December 2017 (112) were genetically related to H5N6 HPAIVs isolated from poultry in North Jeolla Province, Korea, in November 2017 (115). They were considered to have emerged through several reassortments between H5N8 HPAIVs causing outbreaks in 2016–2017 and HxN6 AIVs (113, 114).

In this study, phylogeographic analysis were performed for N6 NA

genes deposited in public databases and institutional repositories of National Institute of Animal Health in Japan, including the H5N6 HPAIVs isolated during the winter 2017–2018, to illustrate intra- and intercontinental dissemination of AIVs and to assess the relationship between virus dissemination and migration flyways of wild birds. Findings in the current study should contribute to the strategic monitoring of AIVs in wild birds as part of efforts to clarify the ecology of AIVs and forecast HPAI outbreaks.

Materials and Methods

Virus isolation and whole-genome sequencing

Nasal or cloacal swabs, or both, and feces were collected from poultry and wild birds in Japan, Vietnam, and Cambodia from 1977 to 2018 and preserved in media as described in Chapter III. At the National Institute of Animal Health in Japan, samples were inoculated into the allantoic cavities of 10- to 11-day-old embryonated chicken eggs and incubated for 24–48 h at 37 °C for virus isolation. The HA activity of allantoic fluid was tested by using 0.55% chicken red blood cells. A/duck/Japan/AnimalQuarantine-HE72/2015 (H5N6) and A/chicken/Japan/AnimalQuarantine-HE144/2016 (H5N6) originating in poultry meats that were illegally transported into Japan (150) were isolated by the Animal Quarantine Service, Ministry of Agriculture, Forestry and Fisheries of Japan.

The whole genomes of the isolated viruses were obtained by using next-generation sequencing as described in Chapter III. The N6 NA sequences of the viruses isolated in this study have been deposited in the GISAID database.

Phylogenetic and phylogeographic analysis

For phylogenetic analysis, sequences of the N6 NA genes were downloaded from the GISAID database in January 2019. Sequences of the AIVs that the National Institute of Animal Health, Japan possessed and of those isolated in Russia that the Federal Research Center of Fundamental and Translational Medicine, which collaborate with the National Institute of Animal Health, Japan, possessed were aligned with the sequences downloaded from GISAID by using BioEdit and MAFFT. After the alignment, a total of 3720 sequences were used in the phylogenetic analysis performed by using MEGA-CC with 1000 bootstrap replicates according to the ML method in a general time-reversible model.

The location-annotated MCC trees for selected clusters of the ML tree (see Results) were constructed according to Bayesian stochastic search variable selection by using the Bayesian Evolutionary Analysis by Sampling Tree package version 1.8.2 as described previously (54). Asymmetric substitution model with Bayesian stochastic search variable selection and a strict clock model were applied for calculating Bayes factors in the present analysis. Then the output tree was visualized by SPreaD3 version 0.9.7 (151). Lines with Bayes factors of 3.0 or more were indicated in each map.

Correlation analysis between traits and phylogeny

Identical sequences of strains isolated from the same species, on the same date, and in the same place were removed from the N6 NA sequence alignment,

and MCC trees without information about collection time were constructed. Calculations of constructed MCC trees were set as 1×10^7 steps long to generate 10,000 trees, and the last 1000 trees were then used for BaTS (152) to evaluate the correlation between traits such as host order and subtypes of isolated viruses and phylogeny. *P* values < 0.05 were used as evidence to support correlations between traits and tree topology.

Results

Clade definition of N6 NA genes

To elucidate the intra- and intercontinental dissemination of genetically related AIVs by using phylogeographic analysis, a phylogenetic tree was constructed on the basis of the N6 NA genes of AIVs isolated worldwide. Phylogenetic analysis revealed that the N6 NA genes could be categorized into an Eurasian (Fig. 25) and North American (Fig. 26) lineage, with a bootstrap value of 60 or more. By applying the criteria of the clade definition of H5 HA genes of Eurasian HPAIV (>1.5% average distances between other clades and <1.5% average distances within the clade)(153), eight and 25 clades that consisted of at least five strains were recognized in the Eurasian and North American lineages, respectively (Figs. 25 and 26). Among these, 17 clades (clades A to Q) were subjected to phylogeographic analysis because they consisted of strains originating from two or more countries (or states and provinces in the North American lineage) and were isolated in several years.

Dissemination of N6 NA genes across the Eurasian continent

N6 NA genes of the H5N6 HPAIVs isolated in Asia and Europe during the winter 2017–2018 were categorized into two clades, A and B (Fig. 27a), in the Eurasian lineage. The genes were significantly distinct from N6 NA genes of H5N6 HPAIVs that were enzootic in Asia before the 2017–2018 season, showing nucleotide identities with them of 83.8% and 84.1%, respectively. Clade A was composed of H5N6 HPAIVs isolated in East Asia, western Asia, and Europe; those isolated in East Asia formed a subcluster and those in western Asia and Europe formed another in the clade. Clade B was composed of those isolated in East Asia forming cluster B, along with isolates from poultry in Greece collected in February 2017. The identity between clades A and B was 97.3%. H3N6 AIVs isolated in the Netherlands in December 2014 and in Novosibirsk, Russia, in September 2017 were classified as an outgroup to clades A and B.

The spatial and temporal relationships of clades A and B were phylogeographically analyzed by calculating the Bayes factors between the locations where AIVs were isolated. The Bayes factor from the Netherlands to Korea was 4.77, and that from the Netherlands to the Republic of Georgia was 146.42, indicating the strong relationships among H5N6 HPAIVs in western and eastern Eurasia (Fig. 27b red type lines). Considering the simultaneous dissemination to Europe and Asia in the same season, it is reasonable to assume that H5N6 HPAIVs had emerged in neither Europe nor Asia before they reached those areas. On the other hand, in clade B, descendant viruses that shared a

Fig. 25. Entire N6 NA ML tree composed of genes of viruses analyzed in this study and downloaded from the GISAID databases.

AIVs classified as the Eurasian lineage are shown. Identified clades defined on the basis of the rule in this study are in green and red; red clades (A to M) were selected for phylogeographic analysis and correlation analyses of bird host species and subtypes with phylogeny.

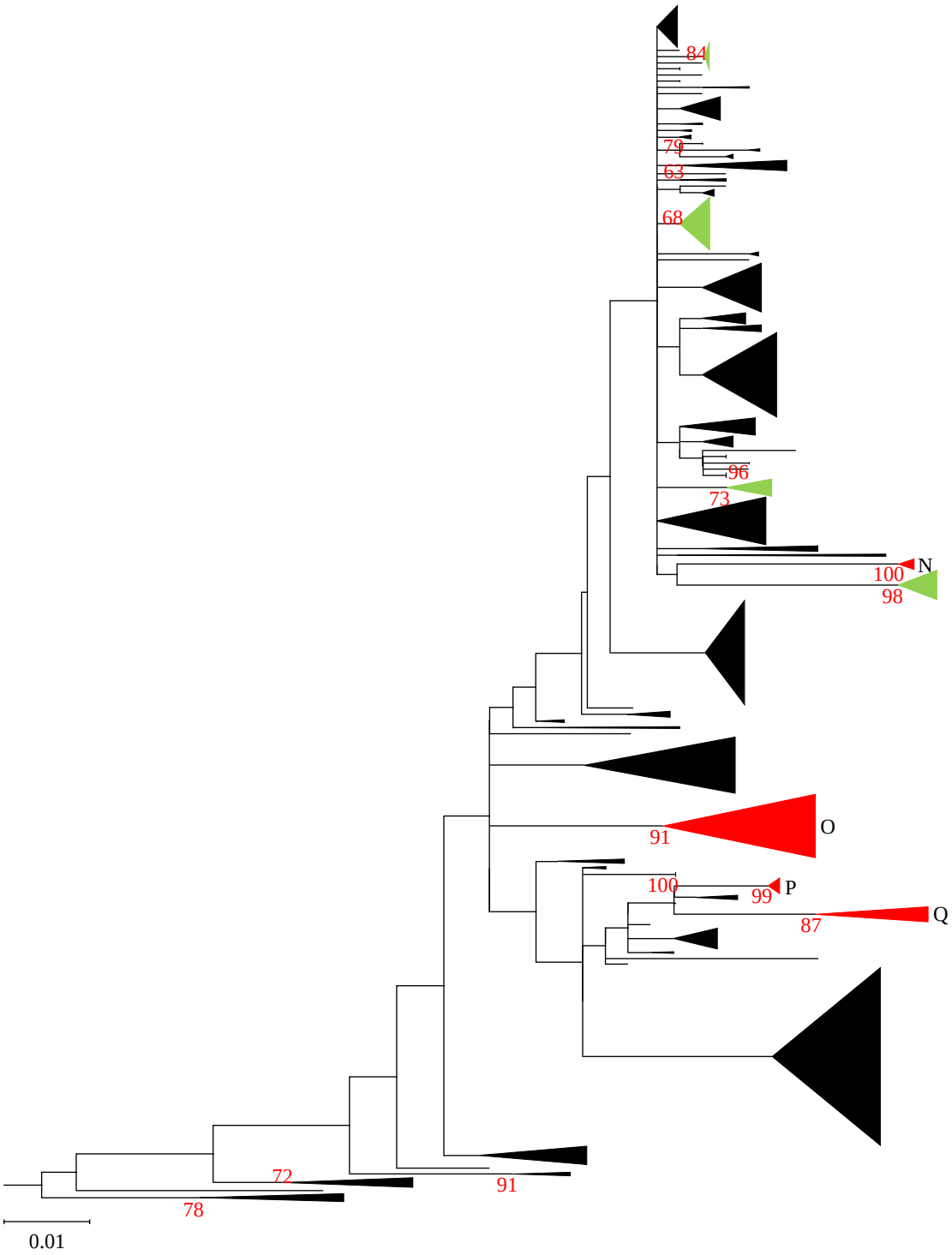

Fig. 26. Entire N6 NA ML tree composed of genes of viruses analyzed in this study and downloaded from the GISAID databases.

AIVs classified as the North American lineage are shown. Identified clades defined on the basis of the rule in this study are in green and red; red clades (N to Q) were selected for phylogeographic analysis and correlation analyses of bird host species and subtypes with phylogeny.

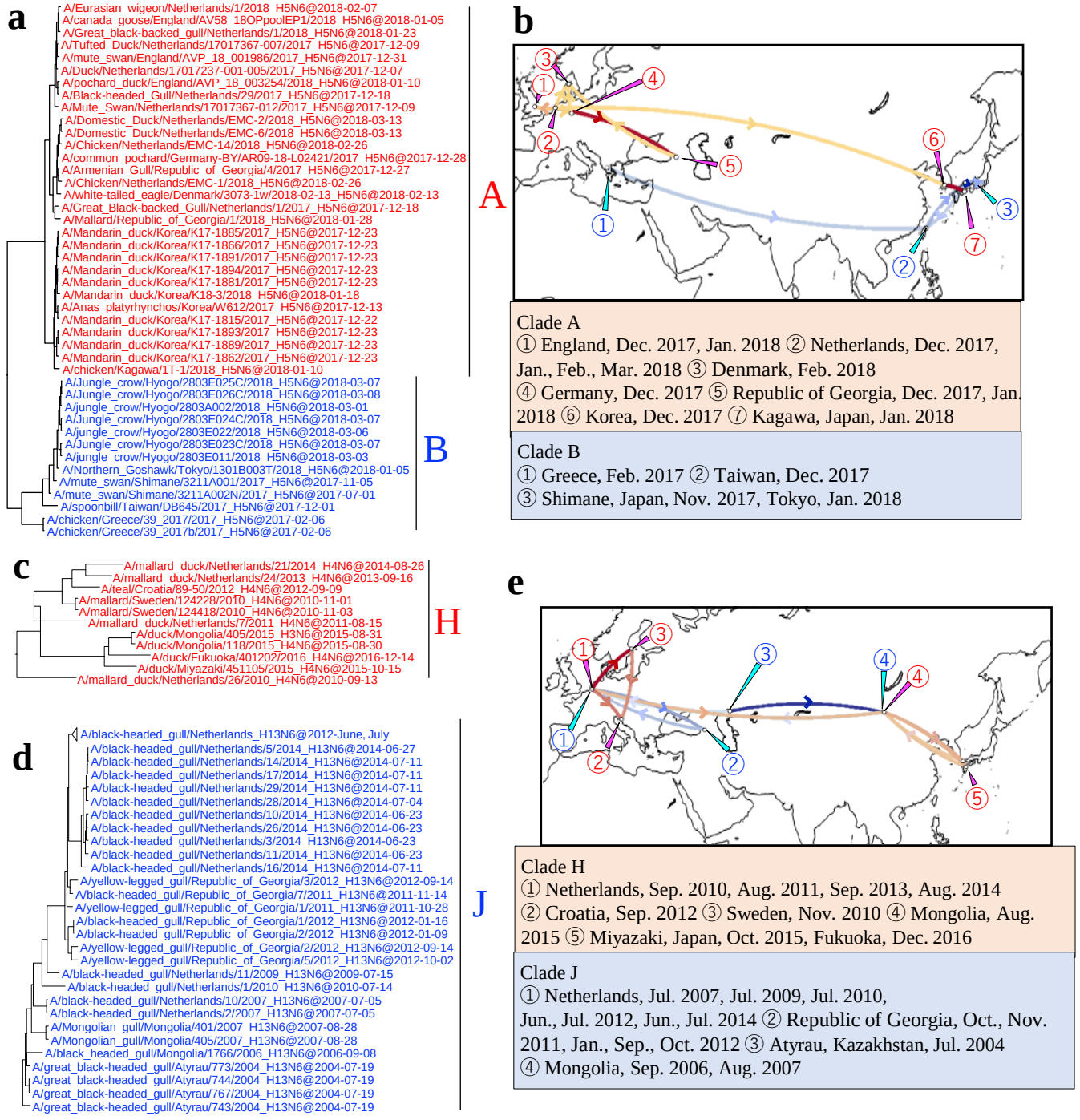

Fig. 27. Detail of MCC trees of N6 NA genes in clades A, B, H, and J and visualized location-annotated MCC trees for selected clades on the world map.
Clades A and B (described in Fig. 25) are red and blue, respectively, in tree (a), and colored type lines in (b) correspond to the clade colors. Clades H and J (described in Fig. 25) are red type and blue type, respectively, in each tree (c and d), and colored type lines in (e) correspond to those of clades. Lines with Bayes factors of 3.0 or more are shown in the map, and a deeper color means a higher Bayes factor.

common ancestor with Greek isolates were disseminated eastward and were detected in Japan and Taiwan in the winter 2017–2018 (Fig. 27b, blue type lines), although it is not plausible that Greek isolates were disseminated directly to Asia without any relay point after a year of absence.

Like clades A and B, clades H and J were composed of AIVs isolated in both Asia and Europe. In clade H, isolates collected in Sweden, the Netherlands, and Croatia from 2010 to 2014 were related to Mongolian isolates collected in August 2015 and to Japanese isolates in October 2015 and December 2016, with identity of 98.6% (Fig. 27c). Phylogeographic analysis suggested that H4N6 AIVs that had been isolated in Europe crossed the Eurasian continent and reached Japan (Fig. 27e, red type lines). This movement is similar to that observed in clade B, where H5N6 HPAIVs phylogenetically related to the isolates collected in Greece in February 2017 were isolated in Japan and Taiwan after the latter half of 2017, although the collection times of the Japanese and Dutch isolates in clade H differed by more than a year. Clade J was also composed of AIVs isolated in East Asia, central Asia, western Asia, and Europe, with an identity of 98.9% within the clade (Fig. 27d). In this clade, AIVs were disseminated between East Asia and Europe, as an isolate collected in Atyrau, Kazakhstan, in July 2004 was related to AIVs isolated in Mongolia in September 2006 and September 2007 and in the Netherlands from July 2007 onward (Fig. 27e, blue type lines).

Intracontinental dissemination of N6 NA genes within Asia, Europe, or North America

Clades C, D, E, and F were composed exclusively of AIVs isolated in Asia. AIVs isolated in Mongolia, the Asian part of Russia, Bangladesh, and Japan after 2011 formed clade C, showing identity of 98.5% within the clade (Fig. 28a). Isolates collected in Novosibirsk during summer in 2017 and 2018 were significantly related to the isolates collected in Mongolia in 2015, Bangladesh in 2015, and Tochigi Prefecture, Japan, in 2018, and the Mongolian isolates were significantly related to the isolates in Bangladesh and Okinawa Prefecture, Japan, in 2015 (Fig. 28c, red type lines). Clade D was composed of AIVs isolated in China, Mongolia, and India from August 2009 to March 2010, showing identity of 98.9% within the clade (Figs. 28b and 28c, blue type lines). It might be the case that a descendant of A/eurasian wigeon/Mongolia/340V/2009 (H4N6) was disseminated to India 4 months later. Clade E was composed of isolates gathered in Japan, China, and Mongolia from 2007 onward, with 98.6% identity within the clade (Fig. 28d). In this clade, descendants of the isolates collected in Shiga prefecture, Japan, in 2007 were found in China and Mongolia after 2010 and in Mie prefecture, Japan, in March 2017 (Fig. 28f, red type lines). Compared with

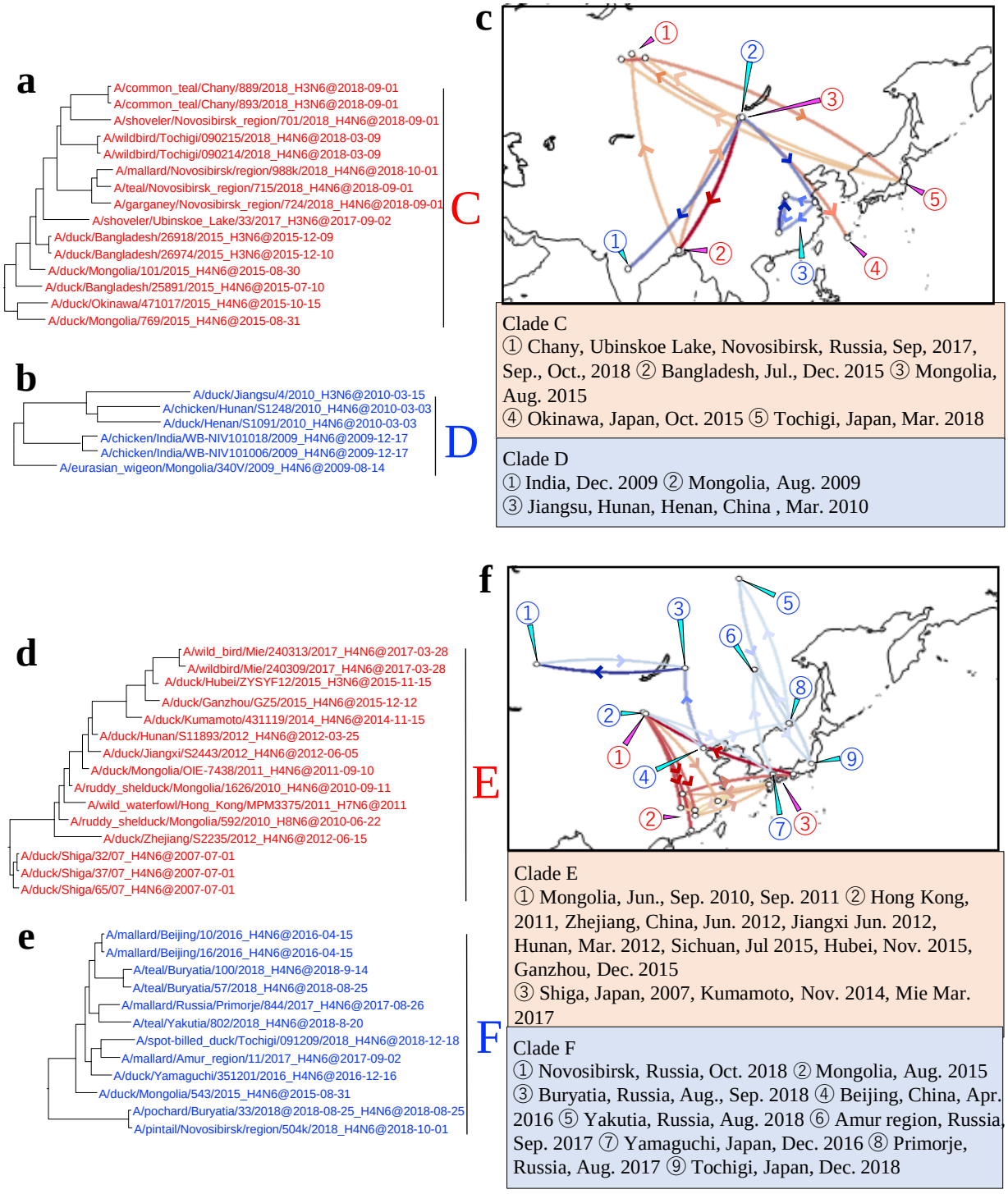

Fig. 28. Detail of MCC trees of N6 NA genes in clades C, D, E, and F and visualized location-annotated MCC trees for selected clades on the world map.

Clades C and D (described in Fig. 25) are red type and blue type, respectively in each tree (a and b), and colored type lines in (c) correspond to those of the clades. Clades E and F (described in Fig. 25) are red type and blue type, respectively, in each tree (d and e), and colored type lines in (f) correspond to those of the clades. Lines with Bayes factors of 3.0 or more are shown in the map, and a deeper color means a higher Bayes factor.

the Bayes factors between Japan and China (average: 5.76), those between Japan and Mongolia and between Mongolia and China (average: 13.16) were significantly higher. AIVs isolated from East Asia from August 2015 to 2017 formed a unique clade, designated as clade F (Fig. 28e). The identity of the clade was as high as 98.7%, and the gene sequences differed by 3% or more from those of the other clades. The viruses in clade F were from Far East Russia, Yamaguchi and Tochigi prefectures, Japan, Beijing, China, and Mongolia. On the basis of the phylogeographic analysis, it was postulated that descendants of the Japanese isolate collected in December 2016 appeared in Far East Russia (Amur region) in September 2017 and reappeared in Japan in December 2018 (Fig. 28f, blue type lines). Along with this dissemination, a relationship between AIVs farther north in Primorje and Yakutia was also found.

Intracontinental movements of AIVs in Europe (clade G) or North America (clades N, O, P, and Q) were recognized. In clade G, AIVs isolated in Croatia in November 2011 and in Moscow, Russia, in October 2011, and those isolated in Sweden in September 2013, shared a common ancestor, with an identity of 99.3% (Figs. 29a and 29b, red type lines). Clades N, O, P, and Q belonged to the North American lineage. More than 70 isolates collected from 1998 to 2009 across North America comprised Clade O, with an identity of 98.7% (Figs. 29d and 29e, blue type lines). As with the case of clade O, clade Q was composed of AIVs isolated on the west and east coasts of the North American continent, with an identity of 98.6% (Figs. 30a and 30c, red type lines). Clades N and P consisted of strains isolated from relatively small areas during brief periods. Isolates of clades N were collected from the neighboring states of Utah and Idaho in the United States in August 2016, with identity of 99.7% (Figs. 29c and 29e, red type lines). Those of clade P were collected from Canadian provinces along the Atlantic Ocean (i.e., Prince Edward Island, Nova Scotia, and New Brunswick) in August and September 2007, with identity of 99.9% (Figs. 30b and 30c, blue type lines).

Intercontinental dissemination of N6 NA genes between Europe and Africa and between Eurasia and North America

Intercontinental dissemination of N6 NA genes was observed in clades I, K, L, and M. Clade I consisted of AIVs isolated in Europe and Zambia, with identity of 98.7% within the clade (Fig. 31a). AIVs isolated in Sweden, the Netherlands, Norway, and Germany from October 2001 to September 2005 shared a common ancestor with isolates collected in Zambia in 2006 and 2008 (Fig. 31e, red type lines). One of the two Zambian strains was isolated from a pelican, a bird species that is rarely reported as carrying AIVs partially because

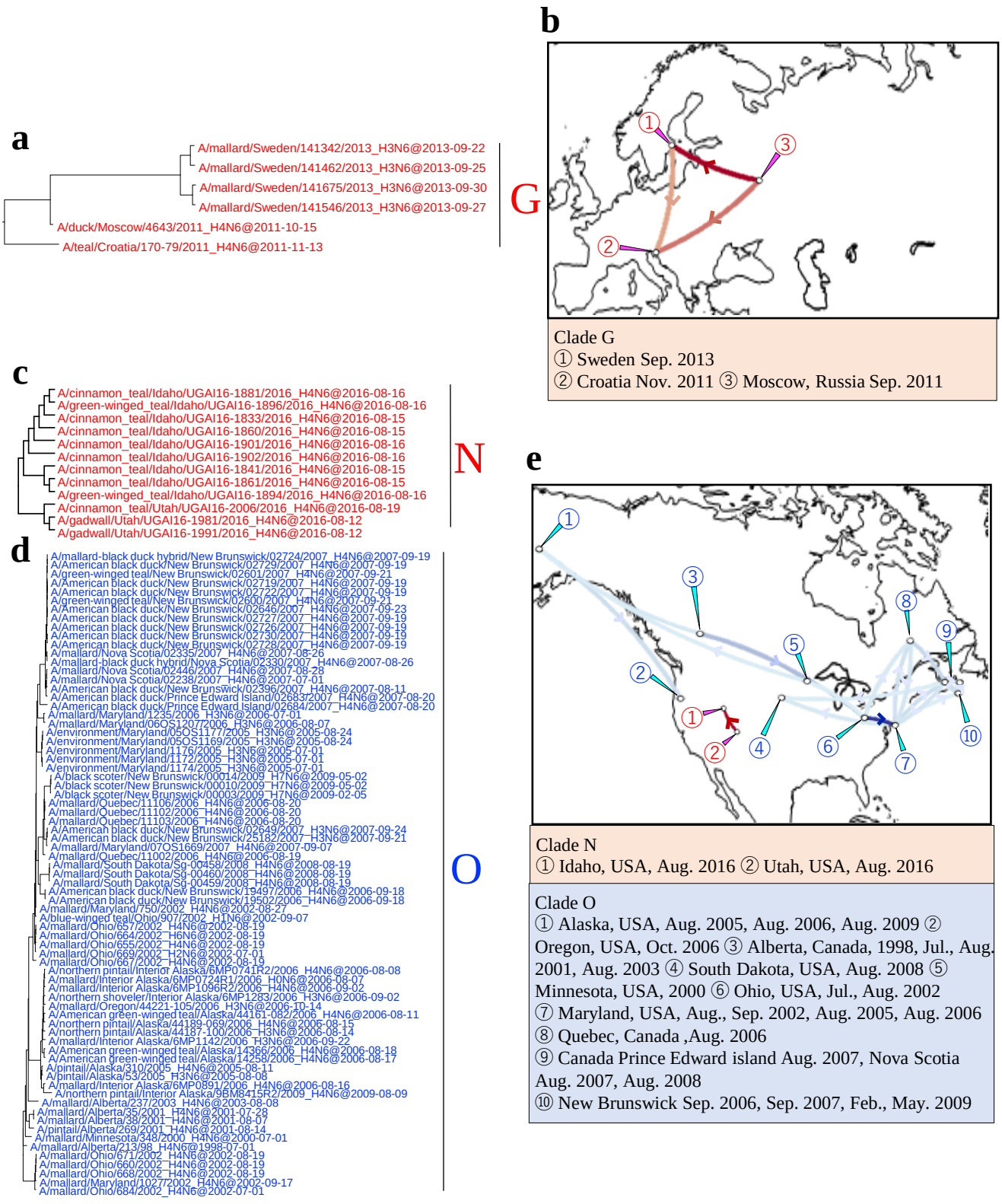

Fig. 29. Detail of MCC trees of N6 NA genes in clades G, N, and O and visualized location-annotated MCC trees for selected clades on the world map.

Clade G (described in Fig. 25) is red type in the tree (a), and colored type lines in (b) correspond to the clade. Clades N and O (described in Fig. 26) are red type and blue type, respectively, in each tree (c and d), and colored type lines in (e) correspond to those of the clade. Lines with Bayes factors of 3.0 or more are shown in the map, and a deeper color means a higher Bayes factor.

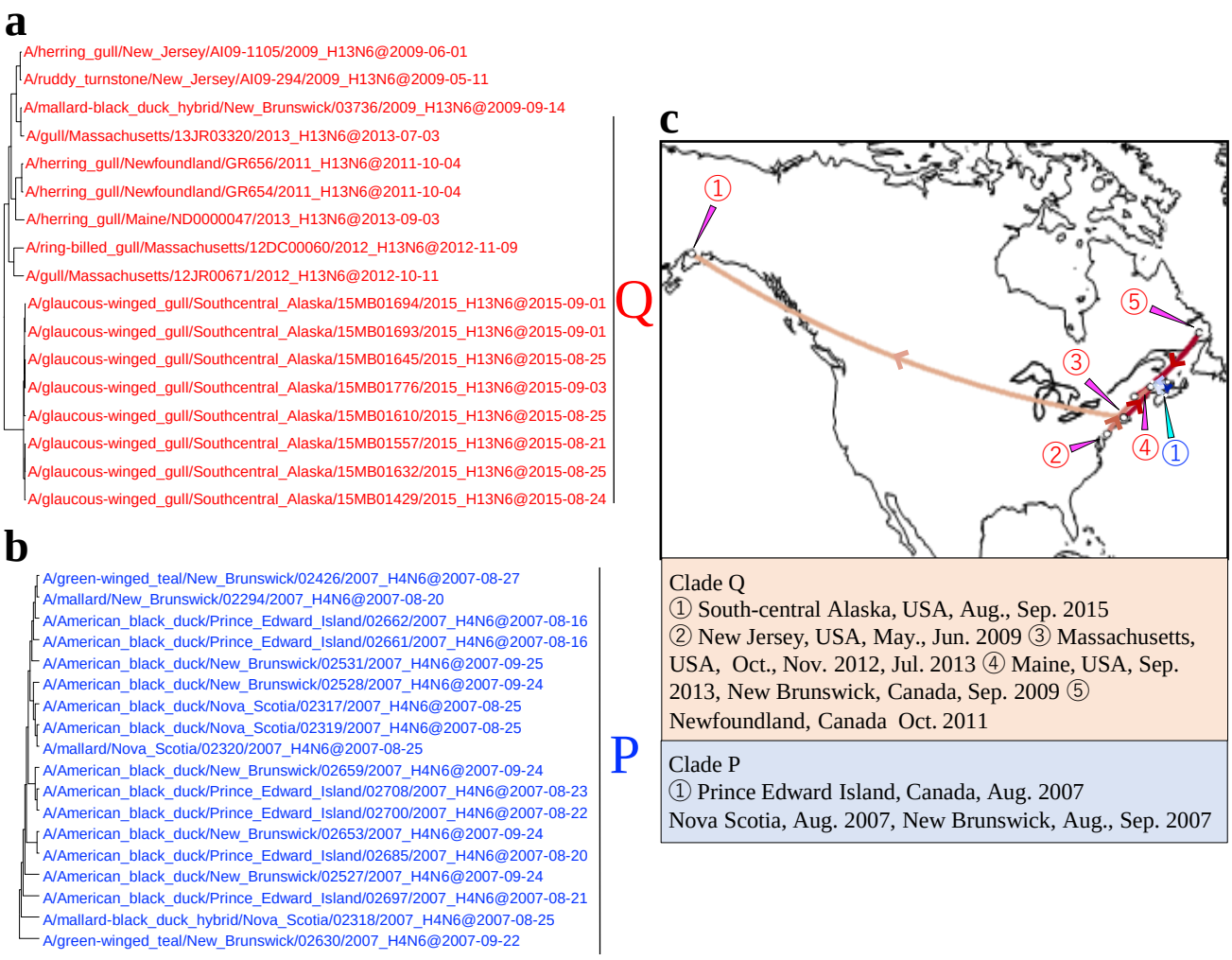

Fig. 30. Detail of MCC trees of N6 NA genes in clades Q and P and visualized location-annotated MCC trees for selected clades on the world map.
Clades Q and P (described in Fig. 26) are red type and blue type, respectively, in each tree (a and b), and colored type lines in (c) correspond to those of the clade. Lines with Bayes factors of 3.0 or more are shown in the map, and a deeper color means a higher Bayes factor.

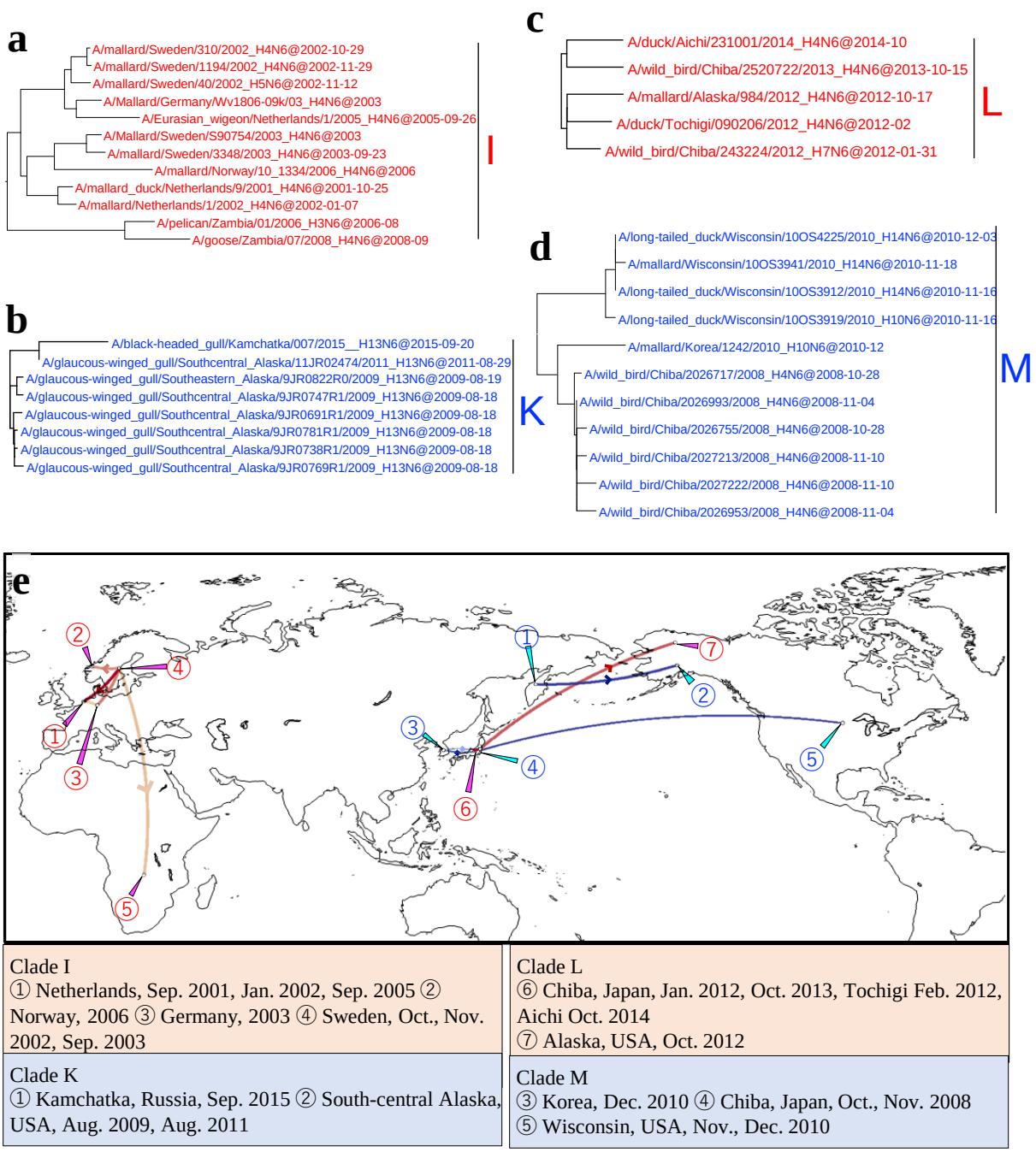

Fig. 31. Detail of MCC trees of N6 NA genes in clades I, K, L, and M and visualized location-annotated MCC trees for selected clades on the world map.

Clades I, K, L, and M (described in Fig. 25) are red type, blue type, red type, and blue type, respectively, in each tree (a, b, c, and d), and colored type lines in (e) correspond to those of the clades. Lines with Bayes factors of 3.0 or more are shown in the map, and a deeper color means a higher Bayes factor.

pelicans have less become the target of surveillance. Clades K, L, and M consisted of isolates from Far East Asia and the United States. N6 NA genes of isolates collected from south-central Alaska in 2009 and 2011 were closely related to those collected from the Kamchatka Peninsula in 2015, with identity of 99.5% in clade K (Figs. 31b and 31e, dark blue type line). Clade L was composed of Japanese and Alaskan strains (Fig. 31c). Japanese isolates from 2012 to 2014 formed clade L, with 99.4% identity, along with an Alaskan isolate collected in 2012 (Fig. 31e, red type lines). Isolates collected from Chiba prefecture, Japan, in 2008 formed clade M with those sampled from Korea in December 2010 and from Wisconsin in November and December 2010, with an identity of 99.5% (Figs. 31d and 31e, light blue type line).

Relationship between host, HA subtype, and clades

Classification of clades by phylogenetic analyses revealed that some, such as clades J and K, were composed of specific subtypes or had specific host species. To investigate the statistically significant correlations between topology and subtype or host specificity, N6 NA sequence alignment was calculated for BaTS analysis (Table 14). There was host specificity in approximately half of all species in *Anseriformes* (33 of 62 species) and *Charadriiformes* (10 of 20 species). All the *Charadriiformes* harboring clade J (black-headed gull, yellow-legged gull, Mongolian gull, and great black-headed gull) and clade K (black-headed gull and glaucous-winged gull) were calculated to significantly cluster together in the phylogenetic tree. In the case of other orders, there was no significant host specificity in the *Gruiformes*, *Pelecaniformes*, and *Galliformes* (except chicken and quail), although there was in two species of *Columbiformes* (pigeon and turtledove).

Of the 15 subtypes (H1–H14 and H16), 11 (H1N6, H3N6, H4N6, H5N6, H6N6, H7N6, H9N6, H10N6, H11N6, H13N6, and H14N6) were calculated to cluster together in a phylogenetic tree (data not shown). Such subtype specificity was depicted in H4N6 subtypes in clades F, N, and P and in H13N6 subtypes in clades K, J, and Q.

Table 14. Correlation of bird species with phylogeny.

Order	Number of species	Number of P<0.05 species	P<0.05 species
Accipitriformes	4	0	
Anseriformes	62	33	American black duck, Chilean teal, American, wigeon, Bewicks swan, duck, domestic duck, goose, mallard, muscovy, mute swan, northern pintail, northern shoveler, stellers, eider, black scoter, black swan, blue winged, teal, cinnamon teal, common shelduck, emperor goose, gadwall, gray teal, green, winged teal, migratory duck, migratory waterfowl, mule duck, pintail, pochard, redhead, ruddy shelduck, surf scoter, tundra swan, whooper swan, yellow billed pintail
Artiodactyla	1	1	swine
Carnivora	3	2	Caspian seal feline
Charadriiformes	20	10	black headed gull great black headed gull Mongolian gull glaucous winged gull gull herring gull ruddy turnstone sanderling shorebird yellow legged gull
Columbiformes	2	2	pigeon turtledove
Falconiformes	1	1	peregrine falcon
Galliformes	7	2	chicken quail
Gruiformes	4	0	
Passeriformes	3	2	jungle crow oriental magpie robin
Pelecaniformes	3	0	
Podicipediformes	1	0	
Primate	1	0	
Psittaciformes	1	0	
Pterocidiformes	1	0	
Rodentia	1	1	muskrat
Strigiformes	3	0	

Discussion

During the winter 2017–2018, genetically closely related H5N6 HPAIVs caused disease outbreaks in Asia and Europe (111). The current phylogeographic analysis of the N6 NA gene revealed that during that season the H5N6 HPAIVs in Asia and Europe diverged from a putative common ancestor and simultaneously reached both sides of the Eurasian continent. Considering that they were disseminated by wild birds, the H5N6 HPAIVs could have been disseminated from a breeding site, possibly in Siberia, where migratory birds following several flyways stretching across the Eurasian continent cohabitate during summer, although a direct ancestor could not be found (Fig. 32) (117, 118). Westward movement of HPAIVs from East Asia to Europe was recognized in the spread of the Qinghai strains from 2005 to 2006 (139-142), supporting this notion. The current study has demonstrated the similar flow of N6 NA genes of other HxN6 AIVs. Closely related N6 NA genes in clades H and J appeared to circulate among Japan, Mongolia, and Europe and among Mongolia, western Asia, and Europe, respectively.

Several migratory bird flyways have been considered to contribute to AIV dissemination across Eurasia, and the regions where flyways overlap play important roles as relay points in the spread of viruses (154, 155). The Central Asia Flyway, the East Africa – Western Asia Flyway, and the East Asia – Australia Flyway overlap in Mongolia and eastern Siberia (Fig. 32 tinted areas with purple) (118), and the genetic relationship among AIVs isolated along those flyways was evident in clades C, D, E, and F. AIVs that spread from Mongolia to southwestern Siberia, where the Black Sea – Mediterranean Flyway stretches to Europe and West Africa, were also observed in clades C and F. Therefore, AIVs in East Asia could spread to Europe via areas where the Black Sea – Mediterranean Flyway as well as the Central Asia and the East Africa – Western Asia Flyways overlap (Fig. 32 tinted areas with green), and vice versa. Previous reports highlighted the importance of southern Siberia for the dissemination of AIVs (52, 145, 156, 157). Lewis et al (156) revealed the dissemination of AIVs from Asian part of southern Siberia to Australia as well as to Europe and Asia by analyzing all segments and another study support that the European Russia facing Arctic ocean was estimated to be a relay point of the dissemination of H5N8 HPAIVs from Asia to Europe (145). On the other hand, few genetic data of AIVs are available from north of southern Siberia, where migratory birds flock for breeding via various flyways, in spite of the higher prevalence of wild birds in breeding areas than in non-breeding areas (119. 120, 154). Furthermore, the relationship between the migration of birds and the spread of viruses had not been clarified in this area.

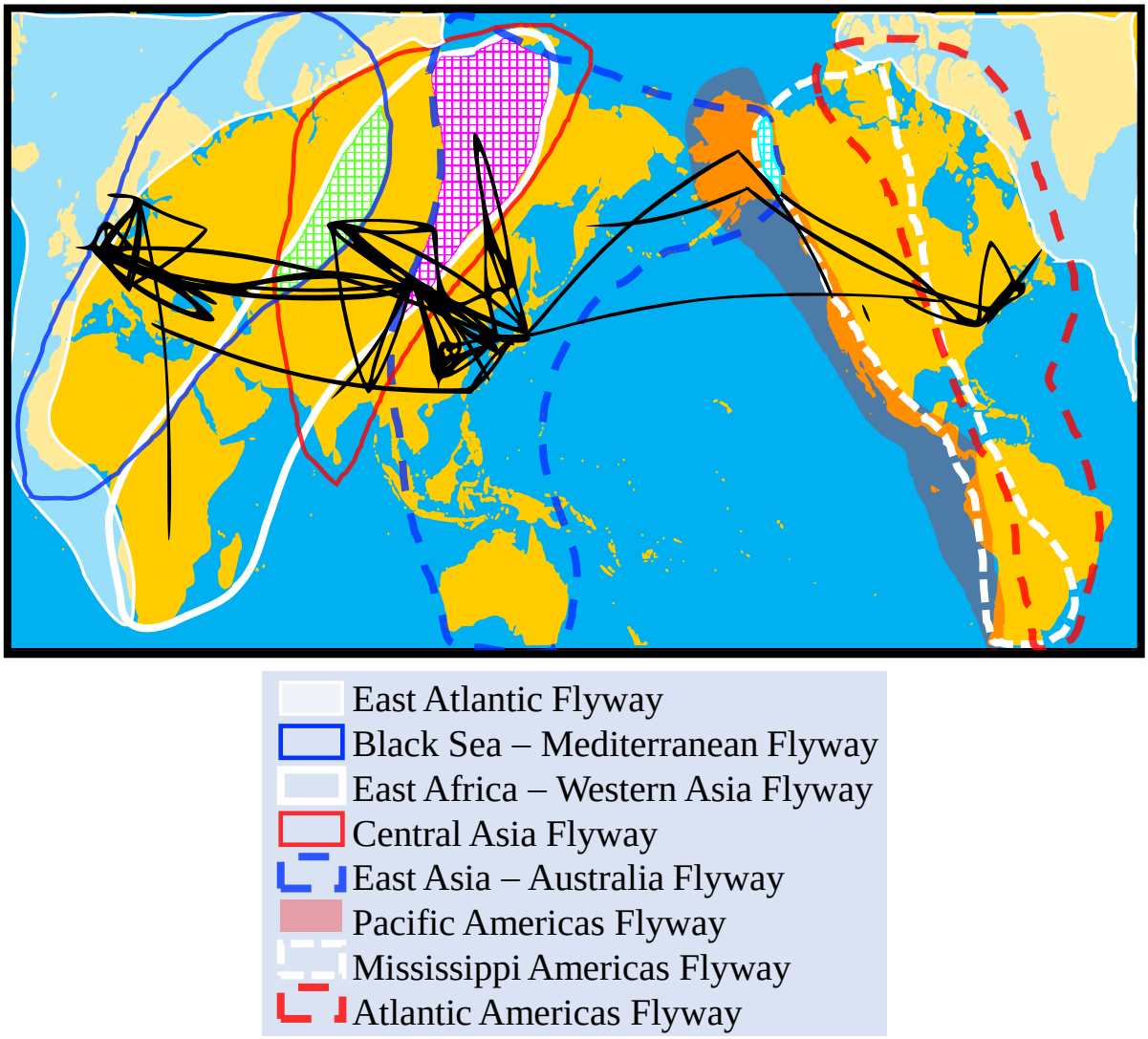

Fig. 32. Visualization of relationship between movement of shorebirds and spread of avian influenza viruses.
Location-annotated maximum clade credibility trees for all selected clades (A to Q described in Figs. 25 and 26) on a world map were merged with previously reported flyways of shorebirds (118). Regions where 3 flyways overlap are tinted with green, purple, and light blue.

Dissemination of AIVs between Yakutia and East Asia observed in the present study expand the understanding of the dynamics of AIVs along with previous studies. To further investigate the dynamics of viruses in areas where flyways overlap, it is essential to analyze AIVs as well as movements of birds in northern Siberia.

Overlapping of flyways also plays an important role in the intercontinental movement of AIVs between Eurasia and North America and between Eurasia and Africa. Previous studies revealed the importance of the Alaskan Peninsula, where the East Asia – Australia, the Pacific Americas, and the Mississippi Americas Flyways overlap, and a variety of AIVs were reported (Fig. 32 tinted areas with light blue) (116, 131, 158). Along the East Asia – Australia Flyway, some of the Japanese strains were genetically related to AIVs isolated in Alaska, consistent with the above-mentioned report. N6 NA genes from African and European strains comprised clade I and the African strain was isolated from a pelican (Fig. 31e). Great white pelicans habitually migrate from Europe to Africa through Israel (159), where the Black Sea – Mediterranean Flyway and the East Africa – Western Asia Flyway overlap. The close relationship between AIVs in Europe and Zambia suggests that European strains are relayed in those regions. Several reports regarding the dissemination of HPAIVs along each flyway have been published (160-163), but there are no such reports regarding overlap of these flyways. The migration flyways described in Fig. 32 are only those of shore birds, but there is also a possibility of the direct or indirect transmission of AIVs between Europe and Zambia through bird species such as white storks, which breed in Europe and overwinter in southern Africa, including Zambia (164).

There appear to be biases in traits such as host species and HA subtypes of AIVs constituting particular clades. *Charadriiformes* were clustered together as hosts of clade J. Previous BaTS analyses of several HA genes and all internal genes demonstrated that AIVs isolated from gulls cluster together more than those of ducks (165). The NS gene of H13 and H16 AIVs in clade J was conserved with 98.5% nucleotide identity, and some other internal genes in this clade showed high identity (PB1: 99.2%; NP: 99.0%; MP: 98.5%). The NS gene might be a factor that restricted the *Charadriiformes* to H13 and H16 AIVs in a particular lineage(s), as a previous report found H13- and H16-specific amino acid signatures mostly in the NS gene, and several were in the NP gene (166). However, another phylogenetic analysis indicated that the NS gene is not as important as the NP gene for host specificity in H13 AIVs (167). These results suggest that the gene constellations of H13/H16 AIVs examined in this study could be advantageous in *Charadriiformes*, resulting in a linkage between certain species and specific genes. It should be noted, however, that biases for targets

species, locations, and times in surveillance studies could influence the number of AIVs isolated from specific species, resulting in the possibility to influence the results of BaTs analyses. Additionally, annotation of host species was not well classified in some AIVs used in the current analyses; no species were noted in the case of ducks and gulls, and “wild bird” or “wild waterfowl” was used as the host annotation. Detailed identification and registration of host species would help researchers to scrutinize the relationships between viral genes and host specificity.

The map obtained by phylogeographic analysis does not always reflect the actual movements of viruses. Linkages between geographically distant places with blanks for several years, as in clade C (Fig. 28c, red type lines), clade E (Fig. 28f, red type lines), and clade M (Fig. 31e, blue type lines), probably imply that viruses were disseminated via other places where no isolates were reported. For example, in clade M, it is reasonable to consider that dissemination of AIVs between Japan and the north-central United States occurred via the Alaskan Peninsula rather than directly, when taking wild bird migration flyways into account. Another limitation in this study was that only N6 NA gene was phylogeographically analyzed, therefore, actual movement of viruses which involved reassortment events might be overlooked. For further study, phylogeographic analyses based on full genomes of AIVs could improve our understanding of how AIVs are spreading and appropriate setting of the areas for AIV surveillance on the basis of the ecology of wild birds would fill the gap. This in turn would help us to forecast HPAI outbreaks in specified regions.

Summary

Genetically related HPAIVs of H5N6 subtype caused outbreaks simultaneously in East Asia and Europe—geographically distinct regions—during winter 2017–2018. This situation prompted to consider whether the application of phylogeographic analysis to a particular gene segment of AIVs could provide clues for understanding how AIV had been disseminated across the continent. Here, the N6 NA genes of influenza viruses isolated across the world were subjected to phylogeographic analysis to illustrate the inter- and intracontinental dissemination of AIVs. Those isolated in East Asia during winter and in Mongolia/Siberia during summer were comingled within particular clades of the phylogeographic tree. For AIVs in one clade, their dissemination in eastern Eurasia extended from Yakutia, Russia, in the north to East Asia in the south. AIVs in western Asia, Europe, and Mongolia were also comingled within other clades, indicating that Mongolia/Siberia plays an important role in the dissemination of AIVs across the Eurasian continent. Mongolia/Siberia may therefore have played a role in the simultaneous outbreaks of H5N6 HPAIVs in Europe and East Asia during the winter 2017–2018. In addition to the long-distance intracontinental disseminations described above, intercontinental disseminations of AIVs between Eurasia and Africa and between Eurasia and North America were also observed. Integrating these results and known migration flyways suggested that the migration of wild birds and the overlap of flyways, such as that observed in Mongolia/Siberia and along the Alaskan Peninsula, contributed to the long-distance intra- and intercontinental dissemination of AIVs. These findings highlight the importance of understanding the movement of migratory birds and the dynamics of AIVs in breeding areas—especially where several migration flyways overlap—in forecasting outbreaks caused by HPAIVs.

Conclusion

Understanding of the dynamics of animal influenza viruses in Japan and in the world is critical not only to reduce the economic loss in the farms but also for the public health. IAVs-S are especially considered to be the thread to cause next-pandemic, although information regarding IAVs-S in Japan remains sparse and localized to limited areas. Characterization of HPAIVs in Japan is also important to prevent further damage and forecasting outbreaks caused by next HPAIVs.

In Chapter I, 424 IAVs-S isolated among surveillance in 21 prefectures during 2015–2019 were genetically characterized. Phylogenetic analyses of surface genes revealed that the 1A.1 classical swine H1 lineage has evolved uniquely since the late 1970s among pig populations in Japan. A(H1N1)pdm09 viruses have repeatedly been introduced into farms and reassorted with endemic H1N2 and H3N2 IAVs-S. H3N2 IAVs-S isolated during 2015–2019 formed a clade. At farms where IAVs-S were frequently isolated for at least 3 years, multiple introductions of IAVs-S with phylogenetically distinct HA genes occurred. In addition, at one farm, IAVs-S derived from a single introduction persisted for at least 3 years and carried no mutations at the deduced antigenic sites of the hemagglutinin protein except only one at the antigenic site (Sa). These results extend our understanding regarding the status of IAVs-S currently circulating in Japan and how they genetically evolve at the farm level.

In Chapter II, phylogenetically and antigenic analyses regarding 82 A(H1N1)pdm09 and 87 H3N2 IAVs-S in Thailand during 2011 through 2017 were performed to elucidate their evolution within each farm. Phylogenetic analyses demonstrated multiple intrusions of A(H1N1)pdm09 viruses that coincided with epidemic A(H1N1)pdm09 strains in humans in Thailand, and they reassorted with H3N2 IAVs-S as well as other A(H1N1)pdm09 viruses. Antigenic analyses revealed that the viruses acquired antigenic diversity either by accumulating substitutions in the hemagglutinin protein or through the intrusion of IAVs-S with different antigenicity. These results, obtained through continuous longitudinal surveillance, revealed that IAVs-S can be maintained in a pig farm over several years through the generation of antigenic diversity due to the accumulation of mutations, intrusion of viruses, and reassortment events.

In Chapter III, an H5N6 HPAIV that caused the outbreak in poultry during January 2018, and H5N6 HPAIVs that killed several wild birds in 3 prefectures during Winter 2017–2018 were characterized. Time-measured phylogenetic analyses demonstrated that the HA and internal genes of these isolates were genetically similar to clade 2.3.4.4.B H5N8 HPAIVs in Europe

during Winter 2016–2017, and NA genes of the poultry and wild bird isolates were gained through distinct reassortments with AIVs that were estimated to have circulated possibly in Siberia during Summer 2017 and Summer 2016, respectively. H5N6 HPAIVs during Winter 2017–2018 in Japan had higher 50% chicken lethal doses and lower transmission efficiency than the H5Nx HPAIVs that caused previous outbreaks in Japan, thus explaining in part why cases during the 2017–2018 outbreak were sporadic.

In Chapter IV, the N6 NA genes of influenza viruses isolated across the world were subjected to phylogeographic analysis to illustrate the inter- and intracontinental dissemination of AIVs. By the phylogeographic analyses, Mongolia/Siberia plays an important role in the dissemination of AIVs across the Eurasian continent and in the simultaneous outbreaks of H5N6 HPAIVs in Europe and East Asia during the winter of 2017–2018. Integrating the phylogeographic analyses and known migration flyways suggested that the migration of wild birds and the overlap of flyways, such as that observed in Mongolia/Siberia and along the Alaskan Peninsula, contributed to the long-distance intra- and intercontinental dissemination of AIVs. These findings highlight the importance of understanding the movement of migratory birds and the dynamics of AIVs in breeding areas—especially where several migration flyways overlap—in forecasting outbreaks caused by HPAIVs.

Approaches based on genetic and time information revealed the characters and dynamics of the IAVs-S in Japan and Thailand. Other phylogenetic approaches considering genetic, time, and location information suggested mechanism of the dissemination of AIVs in the world. Continuing to update the status of AIVs and IAVs-S in Japan and the world with evolving genetic analyses are important for the countermeasures against them such as selection of vaccine strain that could fit to the recent strains and forecasting of newly-introduced HPAIVs in Japan.

Acknowledgements

The author would like to acknowledge Prof. Y. Sakoda, Laboratory of Microbiology, Department of Disease Control, Faculty of Veterinary Medicine, Hokkaido University (Sapporo, Japan), for his guidance, encouragement, and detailed review of the manuscript.

The author express great appreciation to Prof. K. Ohashi, Laboratory of Infectious Diseases, Department of Disease Control, Faculty of Veterinary Medicine, Hokkaido University; Prof. H. Kariwa, Laboratory of Public Health, Department of Preventive Veterinary Medicine, Faculty of Veterinary Medicine, Hokkaido University; Dr. T. Hiono, Laboratory of Microbiology, Department of Disease Control, Faculty of Veterinary Medicine, Hokkaido University for their critical review of the manuscript.

The author thanks the National Institute of Animal Health (Thailand) for arranging and supporting the collection of pig swab samples in Thailand, Federal Research Center of Fundamental and Translational Medicine (Russia) for sharing information and data, and the National Institute of Infectious Diseases (Japan) for kindly providing sera and inactivated antigens for antigenic analyses.

The author also thanks Miwa Takahashi and Sayuri Nakamura for their skilled techniques at the NIAH; Takehiko Saito, Yuko Uchida, Nobuhiro Takemae, Taichiro Tanikawa, Ryota Tsunekuni, Momoko Nakayama, and Saki Sakuma for their valuable support, advice, and discussion.

The author owes his deepest gratitude to his family for their encouragement, love, and devoted support to his education.

References

1 Lamb, R.A., Choppin, P.W., 1983. The gene structure and replication of influenza virus. Annu Rev Biochem 52, 467-506.

2 Hause, B.M., Ducatez, M., Collin, E.A., Ran, Z., Liu, R., Sheng, Z., Armien, A., Kaplan, B., Chakravarty, S., Hoppe, A.D., Webby, R.J., Simonson, R.R., Li, F., 2013. Isolation of a novel swine influenza virus from Oklahoma in 2011 which is distantly related to human influenza C viruses. PLoS Pathog 9, e1003176.

3 World health organization, 1980. A revision of the system of nomenclature for influenza viruses: a WHO memorandum. Bull. World Health Organ 58, 585-591.

4 Hinshaw, V.S., Air, G.M., Gibbs, A.J., Graves, L., Prescott, B., Karunakaran, D., 1982. Antigenic and genetic characterization of a novel hemagglutinin subtype of influenza A viruses from gulls. J Virol 42, 865-872.

5 Kawaoka, Y., Yamnikova, S., Chambers, T.M., Lvov, D.K., Webster, R.G., 1990. Molecular characterization of a new hemagglutinin, subtype H14, of influenza A virus. Virology 179, 759-767.

6 Rohm, C., Zhou, N., Suss, J., Mackenzie, J., Webster, R.G., 1996. Characterization of a novel influenza hemagglutinin, H15: criteria for determination of influenza A subtypes. Virology 217, 508-516.

7 Fouchier, R.A., Munster, V., Wallensten, A., Bestebroer, T.M., Herfst, S., Smith, D., Rimmelzwaan, G.F., Olsen, B., Osterhaus, A.D., 2005. Characterization of a novel influenza A virus hemagglutinin subtype (H16) obtained from black-headed gulls. J Virol 79, 2814-2822.

8 Ma, W., Lager, K.M., Vincent, A.L., Janke, B.H., Gramer, M.R., Richt, J.A., 2009. The role of swine in the generation of novel influenza viruses. Zoonoses Public Health 56, 326-337.

9 Kitikoon, P., Vincent, A.L., Jones, K.R., Nilubol, D., Yu, S., Janke, B.H., Thacker, B.J., Thacker, E.L., 2009. Vaccine efficacy and immune response to swine influenza virus challenge in pigs infected with porcine reproductive and respiratory syndrome virus at the time of SIV vaccination. Vet Microbiol 139, 235-244.

10 Vincent, A., Awada, L., Brown, I., Chen, H., Claes, F., Dauphin, G., Donis, R., Culhane, M., Hamilton, K., Lewis, N., Mumford, E., Nguyen, T., Parchariyanon, S., Pasick, J., Pavade, G., Pereda, A., Peiris, M., Saito, T., Swenson, S., Van Reeth, K., Webby, R., Wong, F., Ciacci-Zanella, J., 2014. Review of influenza A virus in swine worldwide: a call for increased surveillance and research. Zoonoses Public Health 61, 4-17.

11 Bennett, R., Ijpelaar, J., 2005. Updated estimates of the costs associated with thirty four endemic livestock diseases in Great Britain: A note. J Agr Econ 56, 135-144.

12 World organization for animal health, 2009. The human influenza due to a novel subtype H1N1. http://www.fao.org/3/a-ak061e.pdf Accessed 26 January 2016.

13 Ito, T., Couceiro, J.N., Kelm, S., Baum, L.G., Krauss, S., Castrucci, M.R., Donatelli, I., Kida, H., Paulson, J.C., Webster, R.G., Kawaoka, Y., 1998. Molecular basis for the generation in pigs of influenza A viruses with pandemic potential. J Virol 72, 7367-7373.

14 Brown, I.H., 2000. The epidemiology and evolution of influenza viruses in pigs. Vet Microbiol 74, 29-46.

15 Zell, R., Scholtissek, C., Ludwig, S., 2013. Genetics, evolution, and the zoonotic capacity of European swine influenza viruses. Curr Top Microbiol Immunol 370, 29-55.

16 Zhu, H., Webby, R., Lam, T.T., Smith, D.K., Peiris, J.S., Guan, Y., 2013. History of swine influenza viruses in Asia. Curr Top Microbiol Immunol 370, 57-68.

17 Guan, Y., Shortridge, K.F., Krauss, S., Li, P.H., Kawaoka, Y., Webster, R.G., 1996. Emergence of avian H1N1 influenza viruses in pigs in China. J Virol 70, 8041-8046.

18 Takemae, N., Parchariyanon, S., Damrongwatanapokin, S., Uchida, Y., Ruttanapumma, R., Watanabe, C., Yamaguchi, S., Saito, T., 2008. Genetic diversity of swine influenza viruses isolated from pigs during 2000 to 2005 in Thailand. Influenza Other Respir Viruses 2, 181-189.

19 Poonsuk, S., Sangthong, P., Petcharat, N., Lekcharoensuk, P., 2013. Genesis and genetic constellations of swine influenza viruses in Thailand. Vet Microbiol 167, 314-326.

20 Nonthabenjawan, N., Chanvatik, S., Chaiyawong, S., Jairak, W., Boonyapisusopha, S., Tuanudom, R., Thontiravong, A., Bunpapong, N., Amonsin, A., 2015. Genetic diversity of swine influenza viruses in Thai swine farms, 2011-2014. Virus Genes 50, 221-230.

21 Abe, H., Mine, J., Parchariyanon, S., Takemae, N., Boonpornprasert, P., Ubonyaem, N., Patcharasinghawut, P., Nuansrichay, B., Tanikawa, T., Tsunekuni, R., Saito, T., 2015. Co-infection of influenza A viruses of swine contributes to effective shuffling of gene segments in a naturally reared pig. Virology 484, 203-212.

22 Lee, J.H., Pascua, P.N., Decano, A.G., Kim, S.M., Park, S.J., Kwon, H.I., Kim, E.H., Kim, Y.I., Kim, H., Kim, S.Y., Song, M.S., Jang, H.K., Park, B.K., Choi, Y.K., 2015. Evaluation of the zoonotic potential of a novel reassortant H1N2

swine influenza virus with gene constellation derived from multiple viral sources. Infect Genet Evol 34, 378-393.

23 Takemae, N., Nguyen, P.T., Le, V.T., Nguyen, T.N., To, T.L., Nguyen, T.D., Pham, V.P., Vo, H.V., Le, Q.V.T., Do, H.T., Nguyen, D.T., Uchida, Y., Saito, T., 2018. Appearance of reassortant European avian-origin H1 influenza A viruses of swine in Vietnam. Transbound Emerg Dis 65, 1110-1116.

24 Kundin, W.D., 1970. Hong Kong A-2 influenza virus infection among swine during a human epidemic in Taiwan. Nature 228, 857.

25 Tumova, B., Mensik, J., Stumpa, A., Fedova, D., Pospisil, Z., 1976. Serological evidence and isolation of a virus closely related to the human A/Hong Kong/68 (H3N2) strain in swine populations in Czechoslovakia in 1969-1972. Zentralbl Veterinarmed B 23, 590-563.

26 Shortridge, K.F., Webster, R.G., 1979. Geographical distribution of swine (Hsw1N1) and Hong Kong (H3N2) influenza virus variants in pigs in Southeast Asia. Intervirology 11, 9-15.

27 Nerome, K., Ishida, M., Nakayama, M., Oya, A., Kanai, C., Suwicha, K., 1981. Antigenic and genetic analysis of A/Hong Kong (H3N2) influenza viruses isolated from swine and man. J Gen Virol 56, 441-445.

28 Ottis, K., Sidoli, L., Bachmann, P.A., Webster, R.G., Kaplan, M.M., 1982. Human influenza A viruses in pigs: isolation of a H3N2 strain antigenically related to A/England/42/72 and evidence for continuous circulation of human viruses in the pig population. Arch Virol 73, 103-108.

29 Zhou, N.N., Senne, D.A., Landgraf, J.S., Swenson, S.L., Erickson, G., Rossow, K., Liu, L., Yoon, K., Krauss, S., Webster, R.G., 1999. Genetic reassortment of avian, swine, and human influenza A viruses in American pigs. J Virol 73, 8851-8856.

30 Garten, R.J., Davis, C.T., Russell, C.A., Shu, B., Lindstrom, S., Balish, A., Sessions, W.M., Xu, X., Skepner, E., Deyde, V., Okomo-Adhiambo, M., Gubareva, L., Barnes, J., Smith, C.B., Emery, S.L., Hillman, M.J., Rivailler, P., Smagala, J., de Graaf, M., Burke, D.F., Fouchier, R.A., Pappas, C., Alpuche-Aranda, C.M., Lopez-Gatell, H., Olivera, H., Lopez, I., Myers, C.A., Faix, D., Blair, P.J., Yu, C., Keene, K.M., Dotson, P.D., Jr., Boxrud, D., Sambol, A.R., Abid, S.H., St George, K., Bannerman, T., Moore, A.L., Stringer, D.J., Blevins, P., Demmler-Harrison, G.J., Ginsberg, M., Kriner, P., Waterman, S., Smole, S., Guevara, H.F., Belongia, E.A., Clark, P.A., Beatrice, S.T., Donis, R., Katz, J., Finelli, L., Bridges, C.B., Shaw, M., Jernigan, D.B., Uyeki, T.M., Smith, D.J., Klimov, A.I., Cox, N.J., 2009. Antigenic and genetic characteristics of swine-origin 2009 A(H1N1) influenza viruses circulating in humans. Science 325, 197-201.

31 Smith, G.J., Vijaykrishna, D., Bahl, J., Lycett, S.J., Worobey, M., Pybus, O.G., Ma, S.K., Cheung, C.L., Raghwani, J., Bhatt, S., Peiris, J.S., Guan, Y., Rambaut, A., 2009. Origins and evolutionary genomics of the 2009 swine-origin H1N1 influenza A epidemic. Nature 459, 1122-1125.

32 Sreta, D., Tantawet, S., Na Ayudhya, S.N., Thontiravong, A., Wongphatcharachai, M., Lapkuntod, J., Bunpapong, N., Tuanudom, R., Suradhat, S., Vimolket, L., Poovorawan, Y., Thanawongnuwech, R., Amonsin, A., Kitikoon, P., 2010. Pandemic (H1N1) 2009 virus on commercial swine farm, Thailand. Emerg Infect Dis 16, 1587-1590.

33 Vijaykrishna, D., Poon, L.L., Zhu, H.C., Ma, S.K., Li, O.T., Cheung, C.L., Smith, G.J., Peiris, J.S., Guan, Y., 2010. Reassortment of pandemic H1N1/2009 influenza A virus in swine. Science 328, 1529.

34 Ducatez, M.F., Hause, B., Stigger-Rosser, E., Darnell, D., Corzo, C., Juleen, K., Simonson, R., Brockwell-Staats, C., Rubrum, A., Wang, D., Webb, A., Crumpton, J.C., Lowe, J., Gramer, M., Webby, R.J., 2011. Multiple reassortment between pandemic (H1N1) 2009 and endemic influenza viruses in pigs, United States. Emerg Infect Dis 17, 1624-1629.

35 Howard, W.A., Essen, S.C., Strugnell, B.W., Russell, C., Barass, L., Reid, S.M., Brown, I.H., 2011. Reassortant pandemic (H1N1) 2009 virus in pigs, United Kingdom. Emerg Infect Dis 17, 1049-1052.

36 Kitikoon, P., Sreta, D., Na Ayudhya, S.N., Wongphatcharachai, M., Lapkuntod, J., Prakairungnamthip, D., Bunpapong, N., Suradhat, S., Thanawongnuwech, R., Amonsin, A., 2011. Brief report: molecular characterization of a novel reassorted pandemic H1N1 2009 in Thai pigs. Virus Genes 43, 1-5.

37 Lam, T.T., Zhu, H., Wang, J., Smith, D.K., Holmes, E.C., Webster, R.G., Webby, R., Peiris, J.M., Guan, Y., 2011. Reassortment events among swine influenza A viruses in China: implications for the origin of the 2009 influenza pandemic. J Virol 85, 10279-10285.

38 Moreno, A., Di Trani, L., Faccini, S., Vaccari, G., Nigrelli, D., Boniotti, M.B., Falcone, E., Boni, A., Chiapponi, C., Sozzi, E., Cordioli, P., 2011. Novel H1N2 swine influenza reassortant strain in pigs derived from the pandemic H1N1/2009 virus. Vet Microbiol 149, 472-477.

39 Hiromoto, Y., Parchariyanon, S., Ketusing, N., Netrabukkana, P., Hayashi, T., Kobayashi, T., Takemae, N., Saito, T., 2012. Isolation of the pandemic (H1N1) 2009 virus and its reassortant with an H3N2 swine influenza virus from healthy weaning pigs in Thailand in 2011. Virus Res 169, 175-181.

40 Kirisawa, R., Ogasawara, Y., Yoshitake, H., Koda, A., Furuya, T., 2014. Genomic reassortants of pandemic A (H1N1) 2009 virus and endemic porcine H1 and H3 viruses in swine in Japan. J Vet Med Sci 76, 1457-1470.

41 Kanehira, K., Takemae, N., Uchida, Y., Hikono, H., Saito, T., 2014. Reassortant swine influenza viruses isolated in Japan contain genes from pandemic A(H1N1) 2009. Microbiol Immunol 58, 327-341.

42 Diaz, A., Marthaler, D., Culhane, M., Sreevatsan, S., Alkhamis, M., Torremorell, M., 2017. Complete genome sequencing of influenza A viruses within swine farrow-to-wean farms reveals the emergence, persistence, and subsidence of diverse viral genotypes. J Virol 91, e00745-17

43 Gao S, Anderson TK, Walia RR, Dorman KS, Janas-Martindale A, Vincent AL. 2017. The genomic evolution of H1 influenza A viruses from swine detected in the United States between 2009 and 2016. J Gen Virol 98, 2001-2010.

44 Xu, X., Subbarao, Cox, N.J., Guo, Y., 1999. Genetic characterization of the pathogenic influenza A/Goose/Guangdong/1/96 (H5N1) virus: similarity of its hemagglutinin gene to those of H5N1 viruses from the 1997 outbreaks in Hong Kong. Virology 261, 15-19.

45 Mase, M., Tsukamoto, K., Imada, T., Imai, K., Tanimura, N., Nakamura, K., Yamamoto, Y., Hitomi, T., Kira, T., Nakai, T., Kiso, M., Horimoto, T., Kawaoka, Y., Yamaguchi, S., 2005. Characterization of H5N1 influenza A viruses isolated during the 2003-2004 influenza outbreaks in Japan. Virology 332, 167-176.

46 Shivakoti, S., Ito, H., Otsuki, K., Ito, T., 2010. Characterization of H5N1 highly pathogenic avian influenza virus isolated from a mountain hawk eagle in Japan. J Vet Med Sci 72, 459-463.

47 Sakoda, Y., Ito, H., Uchida, Y., Okamatsu, M., Yamamoto, N., Soda, K., Nomura, N., Kuribayashi, S., Shichinohe, S., Sunden, Y., Umemura, T., Usui, T., Ozaki, H., Yamaguchi, T., Murase, T., Ito, T., Saito, T., Takada, A., Kida, H., 2012. Reintroduction of H5N1 highly pathogenic avian influenza virus by migratory water birds, causing poultry outbreaks in the 2010-2011 winter season in Japan. J Gen Virol 93, 541-550.

48 Uchida, Y., Suzuki, Y., Shirakura, M., Kawaguchi, A., Nobusawa, E., Tanikawa, T., Hikono, H., Takemae, N., Mase, M., Kanehira, K., Hayashi, T., Tagawa, Y., Tashiro, M., Saito, T., 2012. Genetics and infectivity of H5N1 highly pathogenic avian influenza viruses isolated from chickens and wild birds in Japan during 2010-11. Virus Res 170, 109-117.

49 Saito, T., Tanikawa, T., Uchida, Y., Takemae, N., Kanehira, K., Tsunekuni, R., 2015. Intracontinental and intercontinental dissemination of Asian H5 highly pathogenic avian influenza virus (clade 2.3.4.4) in the winter of 2014-2015. Rev Med Virol 25, 388-405.

50 Tanikawa, T., Kanehira, K., Tsunekuni, R., Uchida, Y., Takemae, N., Saito, T., 2016. Pathogenicity of H5N8 highly pathogenic avian influenza viruses isolated

from a wild bird fecal specimen and a chicken in Japan in 2014. Microbiol Immunol 60, 243-252.

51 Lee, Y.J., Kang, H.M., Lee, E.K., Song, B.M., Jeong, J., Kwon, Y.K., Kim, H.R., Lee, K.J., Hong, M.S., Jang, I., Choi, K.S., Kim, J.Y., Lee, H.J., Kang, M.S., Jeong, O.M., Baek, J.H., Joo, Y.S., Park, Y.H., Lee, H.S., 2014. Novel reassortant influenza A(H5N8) viruses, South Korea, 2014. Emerg Infect Dis 20, 1087-1089.

52 Lee, D.H., Torchetti, M.K., Winker, K., Ip, H.S., Song, C.S., Swayne, D.E., 2015. Intercontinental spread of Asian-origin H5N8 to North America through Beringia by migratory birds. J Virol 89, 6521-6524.

53 Si, Y.J., Lee, I.W., Kim, E.H., Kim, Y.I., Kwon, H.I., Park, S.J., Nguyen, H.D., Kim, S.M., Kwon, J.J., Choi, W.S., Beak, Y.H., Song, M.S., Kim, C.J., Webby, R.J., Choi, Y.K., 2017. Genetic characterisation of novel, highly pathogenic avian influenza (HPAI) H5N6 viruses isolated in birds, South Korea, November 2016. Euro Surveill 22, 30434

54 Takemae, N., Tsunekuni, R., Sharshov, K., Tanikawa, T., Uchida, Y., Ito, H., Soda, K., Usui, T., Sobolev, I., Shestopalov, A., Yamaguchi, T., Mine, J., Ito, T., Saito, T., 2017. Five distinct reassortants of H5N6 highly pathogenic avian influenza A viruses affected Japan during the winter of 2016-2017. Virology 512, 8-20.

55 Tsunekuni, R., Yaguchi, Y., Kashima, Y., Yamashita, K., Takemae, N., Mine, J., Tanikawa, T., Uchida, Y., Saito, T., 2018. Spatial transmission of H5N6 highly pathogenic avian influenza viruses among wild birds in Ibaraki Prefecture, Japan, 2016-2017. Arch Virol 163, 1195-1207.

56 Ozawa, M., Matsuu, A., Khalil, A.M., Nishi, N., Tokorozaki, K., Masatani, T., Horie, M., Okuya, K., Ueno, K., Kuwahara, M., Toda, S., 2018. Phylogenetic variations of highly pathogenic H5N6 avian influenza viruses isolated from wild birds in the Izumi plain, Japan, during the 2016-17 winter season. Transbound Emerg Dis 66, 797-806

57 Food and agriculture organization, 2015. FAOSTAT data, Available from http://faostat.fao.org/. Accessed 4 October 2018 for Chapter II and 1 March 2020 for Chapter I.

58 Yamane, N., Arikawa, J., Odagiri, T., Ishida, N., 1979. Annual examination of influenza virus infection among pigs in Miyagi prefecture, Japan: the appearance of Hsw1N1 virus. Acta Virol 23, 240-248.

59 Sugimura, T., Yonemochi, H., Ogawa, T., Tanaka, Y., Kumagai, T., 1980. Isolation of a recombinant influenza virus (Hsw 1 N2) from swine in Japan. Arch Virol 66, 271-274.

60 Ozawa, M., Matsuu, A., Yonezawa, K., Igarashi, M., Okuya, K., Kawabata, T., Ito, K., Tsukiyama-Kohara, K., Taneno, A., Deguchi, E., 2015. Efficient isolation of swine influenza viruses by age-targeted specimen collection. J Clin Microbiol 53, 1331-1338.

61 Okuya, K., Matsuu, A., Kawabata, T., Koike, F., Ito, M., Furuya, T., Taneno, A., Akimoto, S., Deguchi, E., Ozawa, M., 2018. Distribution of gene segments of the pandemic A(H1N1) 2009 virus lineage in pig populations. Transbound Emerg Dis 65, 1502-1513.

62 Ito, T., Kawaoka, Y., Vines, A., Ishikawa, H., Asai, T., Kida, H., 1998. Continued circulation of reassortant H1N2 influenza viruses in pigs in Japan. Arch Virol 143, 1773-1782.

63 Saito, T., Suzuki, H., Maeda, K., Inai, K., Takemae, N., Uchida, Y., Tsunemitsu, H., 2008. Molecular characterization of an H1N2 swine influenza virus isolated in Miyazaki, Japan, in 2006. J Vet Med Sci 70, 423-427.

64 Yoneyama, S., Hayashi, T., Kojima, H., Usami, Y., Kubo, M., Takemae, N., Uchida, Y., Saito, T., 2010. Occurrence of a pig respiratory disease associated with swine influenza A (H1N2) virus in Tochigi Prefecture, Japan. J Vet Med Sci 72, 481-488.

65 Takemae, N., Parchariyanon, S., Ruttanapumma, R., Hiromoto, Y., Hayashi, T., Uchida, Y., Saito, T., 2011. Swine influenza virus infection in different age groups of pigs in farrow-to-finish farms in Thailand. Virol J 8, 537.

66 Huddleston, J.A., Brownlee, G.G., 1982. The sequence of the nucleoprotein gene of human influenza A virus, strain A/NT/60/68. Nucleic Acids Res 10, 1029-1038.

67 Ngo, L.T., Hiromoto, Y., Pham, V.P., Le, H.T., Nguyen, H.T., Le, V.T., Takemae, N., Saito, T., 2012. Isolation of novel triple-reassortant swine H3N2 influenza viruses possessing the hemagglutinin and neuraminidase genes of a seasonal influenza virus in Vietnam in 2010. Influenza Other Respir Viruses 6, 6-10.

68 Heine, H.G., Trinidad, L., Selleck, P., Lowther, S., 2007. Rapid detection of highly pathogenic avian influenza H5N1 virus by TaqMan reverse transcriptase-polymerase chain reaction. Avian diseases 51, 370-372.

69 Heine, H.G., Foord, A.J., Wang, J., Valdeter, S., Walker, S., Morrissy, C., Wong, F.Y., Meehan, B., 2015. Detection of highly pathogenic zoonotic influenza virus H5N6 by reverse-transcriptase quantitative polymerase chain reaction. Virol J 12, 18.

70 Takemae, N., Nguyen, T., Ngo, L.T., Hiromoto, Y., Uchida, Y., Pham, V.P., Kageyama, T., Kasuo, S., Shimada, S., Yamashita, Y., Goto, K., Kubo, H., Le, V.T., Van Vo, H., Do, H.T., Nguyen, D.H., Hayashi, T., Matsuu, A., Saito, T.,

2013. Antigenic variation of H1N1, H1N2 and H3N2 swine influenza viruses in Japan and Vietnam. Arch Virol 158, 859-876.

71 Takemae, N., Shobugawa, Y., Nguyen, P.T., Nguyen, T., Nguyen, T.N., To, T.L., Thai, P.D., Nguyen, T.D., Nguyen, D.T., Nguyen, D.K., Do, H.T., Le, T.Q., Hua, P.T., Van Vo, H., Nguyen, D.T., Nguyen, D.H., Uchida, Y., Saito, R., Saito, T., 2016. Effect of herd size on subclinical infection of swine in Vietnam with influenza A viruses. BMC Vet Res 12, 227.

72 World health organization, 2002. The human influenza due to a novel subtype H1N1. Available from http://www.who.int/csr/resources/publications/influenza/whocdscsrncs20025rev.pdf Accessed 10 March 2016.

73 Hall, T.A., 1999. BioEdit: a user-friendly biological sequence alignment editor and analysis program for Windows 95/98/NT. Nucl. Acids Symp. Ser.41:95–98

74 Katoh, K., Standley, D.M., 2016. A simple method to control over-alignment in the MAFFT multiple sequence alignment program. Bioinformatics 32, 1933-1942.

75 Price, M.N., Dehal, P.S., Arkin, A.P., 2010. FastTree 2--approximately maximum-likelihood trees for large alignments. PLoS One 5, e9490.

76 Drummond, A.J., Suchard, M.A., Xie, D., Rambaut, A., 2012. Bayesian phylogenetics with BEAUti and the BEAST 1.7. Mol Biol Evol 29, 1969-1973.

77 Fu, L., Niu, B., Zhu, Z., Wu, S., Li, W., 2012. CD-HIT: accelerated for clustering the next-generation sequencing data. Bioinformatics 28, 3150-3152.

78 Matsuu, A., Uchida, Y., Takemae, N., Mawatari, T., Yoneyama, S.K., Kasai, T., Nakamura, R., Eto, M., Saito, T., 2012. Genetic characterization of swine influenza viruses isolated in Japan between 2009 and 2012. Microbiol Immunol 56, 792-803.

79 Ma, J., Shen, H., McDowell, C., Liu, Q., Duff, M., Lee, J., Lang, Y., Hesse, D., Richt, J.A., Ma, W., 2019. Virus survival and fitness when multiple genotypes and subtypes of influenza A viruses exist and circulate in swine. Virology 532, 30-38.

80 Mancera Gracia, J.C., Van den Hoecke, S., Richt, J.A., Ma, W., Saelens, X., Van Reeth, K., 2017. A reassortant H9N2 influenza virus containing 2009 pandemic H1N1 internal-protein genes acquired enhanced pig-to-pig transmission after serial passages in swine. Sci Rep 7, 1323.

81 Ryt-Hansen, P., Pedersen, A.G., Larsen, I., Krog, J.S., Kristensen, C.S., Larsen, L.E., 2019. Acute Influenza A virus outbreak in an enzootic infected sow herd: impact on viral dynamics, genetic and antigenic variability and effect of maternally derived antibodies and vaccination. PLoS One 14, e0224854.

82 Sun, H., Cunningham, F.L., Harris, J., Xu, Y., Long, L.P., Hanson-Dorr, K., Baroch, J.A., Fioranelli, P., Lutman, M.W., Li, T., Pedersen, K., Schmit, B.S., Cooley, J., Lin, X., Jarman, R.G., DeLiberto, T.J., Wan, X.F., 2015. Dynamics of virus shedding and antibody responses in influenza A virus-infected feral swine. J Gen Virol 96, 2569-2578.

83 Both, G.W., Shi, C.H., Kilbourne, E.D., 1983. Hemagglutinin of swine influenza virus: a single amino acid change pleiotropically affects viral antigenicity and replication. Proc Natl Acad Sci U S A 80, 6996-7000.

84 Pulit-Penaloza, J.A., Jones, J., Sun, X., Jang, Y., Thor, S., Belser, J.A., Zanders, N., Creager, H.M., Ridenour, C., Wang, L., Stark, T.J., Garten, R., Chen, L.M., Barnes, J., Tumpey, T.M., Wentworth, D.E., Maines, T.R., Davis, C.T., 2018. Antigenically diverse swine origin H1N1 variant influenza viruses exhibit differential ferret pathogenesis and transmission phenotypes. J Virol 92, e00095-18

85 Rajao, D.S., Anderson, T.K., Kitikoon, P., Stratton, J., Lewis, N.S., Vincent, A.L., 2018. Antigenic and genetic evolution of contemporary swine H1 influenza viruses in the United States. Virology 518, 45-54.

86 Koel, B.F., Burke, D.F., Bestebroer, T.M., van der Vliet, S., Zondag, G.C., Vervaet, G., Skepner, E., Lewis, N.S., Spronken, M.I., Russell, C.A., Eropkin, M.Y., Hurt, A.C., Barr, I.G., de Jong, J.C., Rimmelzwaan, G.F., Osterhaus, A.D., Fouchier, R.A., Smith, D.J., 2013. Substitutions near the receptor binding site determine major antigenic change during influenza virus evolution. Science 342, 976-979.

87 Santos, J.J.S., Abente, E.J., Obadan, A.O., Thompson, A.J., Ferreri, L., Geiger, G., Gonzalez-Reiche, A.S., Lewis, N.S., Burke, D.F., Rajao, D.S., Paulson, J.C., Vincent, A.L., Perez, D.R., 2019. Plasticity of Amino Acid Residue 145 Near the receptor binding site of H3 swine influenza A viruses and its impact on receptor binding and antibody recognition. J Virol 93, e01413-18

88 Nerome, K., Ishida, M., Oya, A., Kanai, C., Suwicha, K., 1982. Isolation of an influenza H1N1 virus from a pig. Virology 117, 485-489.

89 Chutinimitkul, S., Thippamom, N., Damrongwatanapokin, S., Payungporn, S., Thanawongnuwech, R., Amonsin, A., Boonsuk, P., Sreta, D., Bunpong, N., Tantilertcharoen, R., Chamnanpood, P., Parchariyanon, S., Theamboonlers, A., Poovorawan, Y., 2008. Genetic characterization of H1N1, H1N2 and H3N2 swine influenza virus in Thailand. Arch Virol 153, 1049-1056.

90 Charoenvisal, N., Keawcharoen, J., Sreta, D., Chaiyawong, S., Nonthabenjawan, N., Tantawet, S., Jittimanee, S., Arunorat, J., Amonsin, A., Thanawongnuwech, R., 2013. Genetic characterization of Thai swine influenza viruses after the introduction of pandemic H1N1 2009. Virus Genes 47, 75-85.

91 Arunorat, J., Charoenvisal, N., Woonwong, Y., Kedkovid, R., Thanawongnuwech, R., 2016. Determination of current reference viruses for serological study of swine influenza viruses after the introduction of pandemic 2009 H1N1 (pdmH1N1) in Thailand. J Virol Methods 236, 5-9.

92 Simon-Grife, M., Martin-Valls, G.E., Vilar, M.J., Busquets, N., Mora-Salvatierra, M., Bestebroer, T.M., Fouchier, R.A., Martin, M., Mateu, E., Casal, J., 2012. Swine influenza virus infection dynamics in two pig farms; results of a longitudinal assessment. Vet Res 43, 24.

93 Rose, N., Herve, S., Eveno, E., Barbier, N., Eono, F., Dorenlor, V., Andraud, M., Camsusou, C., Madec, F., Simon, G., 2013. Dynamics of influenza A virus infections in permanently infected pig farms: evidence of recurrent infections, circulation of several swine influenza viruses and reassortment events. Vet Res 44, 72.

94 Thrusfield, M., 1995. Veterinary Epidemiology. Oxford: Blackwell Science Ltd, 2, 117-198

95 Kumar, S., Stecher, G., Peterson, D., Tamura, K., 2012. MEGA-CC: computing core of molecular evolutionary genetics analysis program for automated and iterative data analysis. Bioinformatics 28, 2685-2686.

96 Bouckaert, R., Heled, J., Kuhnert, D., Vaughan, T., Wu, C.H., Xie, D., Suchard, M.A., Rambaut, A., Drummond, A.J., 2014. BEAST 2: a software platform for Bayesian evolutionary analysis. PLoS Comput Biol 10, e1003537.

97 Anderson, T.K., Macken, C.A., Lewis, N.S., Scheuermann, R.H., Van Reeth, K., Brown, I.H., Swenson, S.L., Simon, G., Saito, T., Berhane, Y., Ciacci-Zanella, J., Pereda, A., Davis, C.T., Donis, R.O., Webby, R.J., Vincent, A.L., 2016. A Phylogeny-based global nomenclature system and automated annotation tool for H1 hemagglutinin genes from swine influenza A viruses. mSphere 1, e00275-16

98 Caton, A.J., Brownlee, G.G., Yewdell, J.W., Gerhard, W., 1982. The antigenic structure of the influenza virus A/PR/8/34 hemagglutinin (H1 subtype). Cell 31, 417-427.

99 Igarashi, M., Ito, K., Yoshida, R., Tomabechi, D., Kida, H., Takada, A., 2010. Predicting the antigenic structure of the pandemic (H1N1) 2009 influenza virus hemagglutinin. PLoS One 5, e8553.

100 Matsuzaki, Y., Sugawara, K., Nakauchi, M., Takahashi, Y., Onodera, T., Tsunetsugu-Yokota, Y., Matsumura, T., Ato, M., Kobayashi, K., Shimotai, Y., Mizuta, K., Hongo, S., Tashiro, M., Nobusawa, E., 2014. Epitope mapping of the hemagglutinin molecule of A/(H1N1)pdm09 influenza virus by using monoclonal antibody escape mutants. J Virol 88, 12364-12373.

101 Wiley, D.C., Wilson, I.A., Skehel, J.J., 1981. Structural identification of the antibody-binding sites of Hong Kong influenza haemagglutinin and their involvement in antigenic variation. Nature 289, 373-378.

102 Kryazhimskiy, S., Plotkin, J.B., 2008. The population genetics of dN/dS. PLoS Genet 4, e1000304.

103 Murcia, P.R., Hughes, J., Battista, P., Lloyd, L., Baillie, G.J., Ramirez-Gonzalez, R.H., Ormond, D., Oliver, K., Elton, D., Mumford, J.A., Caccamo, M., Kellam, P., Grenfell, B.T., Holmes, E.C., Wood, J.L., 2012. Evolution of an Eurasian avian-like influenza virus in naive and vaccinated pigs. PLoS Pathog 8, e1002730.

104 Diaz, A., Allerson, M., Culhane, M., Sreevatsan, S., Torremorell, M., 2013. Antigenic drift of H1N1 influenza A virus in pigs with and without passive immunity. Influenza Other Respir Viruses 7 Suppl 4, 52-60.

105 Fitch, W.M., Leiter, J.M., Li, X.Q., Palese, P., 1991. Positive Darwinian evolution in human influenza A viruses. Proc Natl Acad Sci U S A 88, 4270-4274.

106 Rambaut, A., Pybus, O.G., Nelson, M.I., Viboud, C., Taubenberger, J.K., Holmes, E.C., 2008. The genomic and epidemiological dynamics of human influenza A virus. Nature 453, 615-619.

107 Nelson, M.I., Stratton, J., Killian, M.L., Janas-Martindale, A., Vincent, A.L., 2015. Continual reintroduction of human pandemic H1N1 influenza A viruses into swine in the United States, 2009 to 2014. J Virol 89, 6218-6226.

108 Tinoco, Y.O., Montgomery, J.M., Kasper, M.R., Nelson, M.I., Razuri, H., Guezala, M.C., Azziz-Baumgartner, E., Widdowson, M.A., Barnes, J., Gilman, R.H., Bausch, D.G., Gonzalez, A.E., 2016. Transmission dynamics of pandemic influenza A(H1N1)pdm09 virus in humans and swine in backyard farms in Tumbes, Peru. Influenza Other Respir Viruses 10, 47-56.

109 Prachayangprecha, S., Makkoch, J., Vuthitanachot, C., Vuthitanachot, V., Payungporn, S., Chieochansin, T., Theamboonlers, A., Poovorawan, Y., 2011. Epidemiological and serological surveillance of human pandemic influenza A virus infections during 2009-2010 in Thailand. Jpn J Infect Dis 64, 377-381.

110 Prachayangprecha, S., Vichaiwattana, P., Korkong, S., Felber, J.A., Poovorawan, Y., 2015. Influenza activity in Thailand and occurrence in different climates. Springerplus 4, 356.

111 World organization for animal health: Update on avian influenza in animals (types H5 and H7). http://www.oie.int/en/animal-health-in-the-world/update-on-avian-influenza Accessed 5 December 2018.

112 Beerens, N., Koch, G., Heutink, R., Harders, F., Vries, D.P.E., Ho, C., Bossers, A., Elbers, A., 2018. Novel Highly Pathogenic Avian Influenza A(H5N6) Virus in the Netherlands, December 2017. Emerg Infect Dis 24, 770-773

113 Lee, E.K., Lee, Y.N., Kye, S.J., Lewis, N.S., Brown, I.H., Sagong, M., Heo, G.B., Kang, Y.M., Cho, H.K., Kang, H.M., Cheon, S.H., Lee, M., Park, B.K., Kim, Y.J., Lee, Y.J., 2018. Characterization of a novel reassortant H5N6 highly pathogenic avian influenza virus clade 2.3.4.4 in Korea, 2017. Emerg Microbes Infect 7, 103.

114 Lee, Y.N., Cheon, S.H., Kye, S.J., Lee, E.K., Sagong, M., Heo, G.B., Kang, Y.M., Cho, H.K., Kim, Y.J., Kang, H.M., Lee, M.H., Lee, Y.J., 2018. Novel reassortants of clade 2.3.4.4 H5N6 highly pathogenic avian influenza viruses possessing genetic heterogeneity in South Korea in late 2017. J Vet Sci 19, 850-854.

115 Kim, Y.I., Si, Y.J., Kwon, H.I., Kim, E.H., Park, S.J., Robles, N.J., Nguyen, H.D., Yu, M.A., Yu, K.M., Lee, Y.J., Lee, M.H., Choi, Y.K., 2018. Pathogenicity and genetic characterisation of a novel reassortant, highly pathogenic avian influenza (HPAI) H5N6 virus isolated in Korea, 2017. Euro Surveill 23, 18-00045

116 Huson, D.H., Scornavacca, C., 2012. Dendroscope 3: an interactive tool for rooted phylogenetic trees and networks. Syst Biol 61, 1061-1067.

117 Alerstam, T., Backman, J., Gudmundsson, G.A., Hedenstrom, A., Henningsson, S.S., Karlsson, H., Rosen, M., Strandberg, R., 2007. A polar system of intercontinental bird migration. Proc Biol Sci 274, 2523-2530.

118 Boere, G.C., Stroud, D.A., 2006. The flyway concept: what it is and what it isn't. Waterbirds around the World 40-47.

119 Sivay, M.V., Sayfutdinova, S.G., Sharshov, K.A., Alekseev, A.Y., Yurlov, A.K., Runstadler, J., Shestopalov, A.M., 2012. Surveillance of influenza A virus in wild birds in the Asian portion of Russia in 2008. Avian Dis 56, 456-463.

120 Sharshov, K., Sivay, M., Liu, D., Pantin-Jackwood, M., Marchenko, V., Durymanov, A., Alekseev, A., Damdindorj, T., Gao, G.F., Swayne, D.E., Shestopalov, A., 2014. Molecular characterization and phylogenetics of a reassortant H13N8 influenza virus isolated from gulls in Mongolia. Virus Genes 49, 237-249.

121 Lee, D.H., Kwon, J.H., Noh, J.Y., Park, J.K., Yuk, S.S., Erdene-Ochir, T.O., Lee, J.B., Park, S.Y., Choi, I.S., Lee, S.W., Song, C.S., 2016. Pathogenicity of the Korean H5N8 highly pathogenic avian influenza virus in commercial domestic poultry species. Avian Pathol 45, 208-211.

122 Lee, D.H., Bertran, K., Kwon, J.H., Swayne, D.E., 2017. Evolution, global spread, and pathogenicity of highly pathogenic avian influenza H5Nx clade 2.3.4.4. J Vet Sci 18, 269-280.

123 Sun, H., Pu, J., Hu, J., Liu, L., Xu, G., Gao, G.F., Liu, X., Liu, J., 2016. Characterization of clade 2.3.4.4 highly pathogenic H5 avian influenza viruses in ducks and chickens. Vet Microbiol 182, 116-122.

124 Kanehira, K., Uchida, Y., Takemae, N., Hikono, H., Tsunekuni, R., Saito, T., 2015. Characterization of an H5N8 influenza A virus isolated from chickens during an outbreak of severe avian influenza in Japan in April 2014. Arch Virol 160, 1629-1643.

125 Bertran, K., Swayne, D.E., Pantin-Jackwood, M.J., Kapczynski, D.R., Spackman, E., Suarez, D.L., 2016. Lack of chicken adaptation of newly emergent Eurasian H5N8 and reassortant H5N2 high pathogenicity avian influenza viruses in the U.S. is consistent with restricted poultry outbreaks in the Pacific flyway during 2014-2015. Virology 494, 190-197.

126 DeJesus, E., Costa-Hurtado, M., Smith, D., Lee, D.H., Spackman, E., Kapczynski, D.R., Torchetti, M.K., Killian, M.L., Suarez, D.L., Swayne, D.E., Pantin-Jackwood, M.J., 2016. Changes in adaptation of H5N2 highly pathogenic avian influenza H5 clade 2.3.4.4 viruses in chickens and mallards. Virology 499, 52-64.

127 Webster, R.G., Bean, W.J., Gorman, O.T., Chambers, T.M., Kawaoka, Y., 1992. Evolution and ecology of influenza A viruses. Microbiol Rev 56, 152-179.

128 van Gils, J.A., Munster, V.J., Radersma, R., Liefhebber, D., Fouchier, R.A., Klaassen, M., 2007. Hampered foraging and migratory performance in swans infected with low-pathogenic avian influenza A virus. PLoS One 2, e184.

129 Latorre-Margalef, N., Gunnarsson, G., Munster, V.J., Fouchier, R.A., Osterhaus, A.D., Elmberg, J., Olsen, B., Wallensten, A., Haemig, P.D., Fransson, T., Brudin, L., Waldenstrom, J., 2009. Effects of influenza A virus infection on migrating mallard ducks. Proc Biol Sci 276, 1029-1036.

130 Dugan, V.G., Chen, R., Spiro, D.J., Sengamalay, N., Zaborsky, J., Ghedin, E., Nolting, J., Swayne, D.E., Runstadler, J.A., Happ, G.M., Senne, D.A., Wang, R., Slemons, R.D., Holmes, E.C., Taubenberger, J.K., 2008. The evolutionary genetics and emergence of avian influenza viruses in wild birds. PLoS Pathog 4, e1000076.

131 Koehler, A.V., Pearce, J.M., Flint, P.L., Franson, J.C., Ip, H.S., 2008. Genetic evidence of intercontinental movement of avian influenza in a migratory bird: the northern pintail (Anas acuta). Mol Ecol 17, 4754-4762.

132 Wille, M., Robertson, G.J., Whitney, H., Bishop, M.A., Runstadler, J.A., Lang, A.S., 2011. Extensive geographic mosaicism in avian influenza viruses from gulls in the northern hemisphere. PLoS One 6, e20664.

133 Wille, M., Robertson, G.J., Whitney, H., Ojkic, D., Lang, A.S., 2011. Reassortment of American and Eurasian genes in an influenza A virus isolated from a great black-backed gull (Larus marinus), a species demonstrated to move between these regions. Arch Virol 156, 107-115.

134 Hall, J.S., Teslaa, J.L., Nashold, S.W., Halpin, R.A., Stockwell, T., Wentworth, D.E., Dugan, V., Ip, H.S., 2013. Evolution of a reassortant North American gull influenza virus lineage: drift, shift and stability. Virol J 10, 179.

135 Dusek, R.J., Hallgrimsson, G.T., Ip, H.S., Jonsson, J.E., Sreevatsan, S., Nashold, S.W., TeSlaa, J.L., Enomoto, S., Halpin, R.A., Lin, X., Fedorova, N., Stockwell, T.B., Dugan, V.G., Wentworth, D.E., Hall, J.S., 2014. North Atlantic migratory bird flyways provide routes for intercontinental movement of avian influenza viruses. PLoS One 9, e92075.

136 Becker, W.B., 1966. The isolation and classification of Tern virus: influenza A-Tern South Africa--1961. J Hyg 64, 309-320.

137 Morgan, I.R., Kelly, A.P., 1990. Epidemiology of an avian influenza outbreak in Victoria in 1985. Aust Vet J 67, 125-128.

138 Ellis, T.M., Bousfield, R.B., Bissett, L.A., Dyrting, K.C., Luk, G.S., Tsim, S.T., Sturm-Ramirez, K., Webster, R.G., Guan, Y., Malik Peiris, J.S., 2004. Investigation of outbreaks of highly pathogenic H5N1 avian influenza in waterfowl and wild birds in Hong Kong in late 2002. Avian Pathol 33, 492-505.

139 Chen, H., Smith, G.J., Zhang, S.Y., Qin, K., Wang, J., Li, K.S., Webster, R.G., Peiris, J.S., Guan, Y., 2005. Avian flu: H5N1 virus outbreak in migratory waterfowl. Nature 436, 191-192.

140 Lipatov, A.S., Evseenko, V.A., Yen, H.L., Zaykovskaya, A.V., Durimanov, A.G., Zolotykh, S.I., Netesov, S.V., Drozdov, I.G., Onishchenko, G.G., Webster, R.G., Shestopalov, A.M., 2007. Influenza (H5N1) viruses in poultry, Russian Federation, 2005-2006. Emerg Infect Dis 13, 539-546.

141 Kilpatrick, A.M., Chmura, A.A., Gibbons, D.W., Fleischer, R.C., Marra, P.P., Daszak, P., 2006. Predicting the global spread of H5N1 avian influenza. Proc Natl Acad Sci U S A 103, 19368-19373.

142 Ducatez, M.F., Olinger, C.M., Owoade, A.A., Tarnagda, Z., Tahita, M.C., Sow, A., De Landtsheer, S., Ammerlaan, W., Ouedraogo, J.B., Osterhaus, A.D., Fouchier, R.A., Muller, C.P., 2007. Molecular and antigenic evolution and geographical spread of H5N1 highly pathogenic avian influenza viruses in western Africa. J Gen Virol 88, 2297-2306.

143 Zhou, S., Tian, H., Wu, X., Xu, B., Yang, J., Chan, K.K., Huang, S., Dong, L., Brownstein, J., Xu, B., 2016. Genetic evidence for avian influenza H5N1 viral transmission along the Black Sea-Mediterranean Flyway. J Gen Virol 97, 2129-2134.

144 Li, S., Meng, W., Liu, D., Yang, Q., Chen, L., Dai, Q., Ma, T., Gao, R., Ru, W., Li, Y., Yu, P., Lu, J., Zhang, G., Tian, H., Chai, H., Li, Y., 2018. Migratory whooper swans Cygnus cygnus transmit H5N1 virus between China and Mongolia: combination evidence from satellite tracking and phylogenetics analysis. Sci Rep 8, 7049.

145 Global Consortium for, H.N., Related Influenza, V., 2016. Role for migratory wild birds in the global spread of avian influenza H5N8. Science 354, 213-217.

146 Pasick, J., Berhane, Y., Joseph, T., Bowes, V., Hisanaga, T., Handel, K., Alexandersen, S., 2015. Reassortant highly pathogenic influenza A H5N2 virus containing gene segments related to Eurasian H5N8 in British Columbia, Canada, 2014. Sci Rep 5, 9484.

147 Bevins, S.N., Dusek, R.J., White, C.L., Gidlewski, T., Bodenstein, B., Mansfield, K.G., DeBruyn, P., Kraege, D., Rowan, E., Gillin, C., Thomas, B., Chandler, S., Baroch, J., Schmit, B., Grady, M.J., Miller, R.S., Drew, M.L., Stopak, S., Zscheile, B., Bennett, J., Sengl, J., Brady, C., Ip, H.S., Spackman, E., Killian, M.L., Torchetti, M.K., Sleeman, J.M., Deliberto, T.J., 2016. Widespread detection of highly pathogenic H5 influenza viruses in wild birds from the Pacific flyway of the United States. Sci Rep 6, 28980.

148 Perkins, L.E., Swayne, D.E., 2003. Comparative susceptibility of selected avian and mammalian species to a Hong Kong-origin H5N1 high-pathogenicity avian influenza virus. Avian diseases 47, 956-967.

149 Bodewes, R., Kuiken, T., 2018. Changing role of wild birds in the epidemiology of avian influenza A viruses. Adv Virus Res 100, 279-307.

150 Shibata, A., Hiono, T., Fukuhara, H., Sumiyoshi, R., Ohkawara, A., Matsuno, K., Okamatsu, M., Osaka, H., Sakoda, Y., 2018. Isolation and characterization of avian influenza viruses from raw poultry products illegally imported to Japan by international flight passengers. Transbound Emerg Dis 65, 465-475.

151 Bielejec, F., Baele, G., Vrancken, B., Suchard, M.A., Rambaut, A., Lemey, P., 2016. SpreaD3: interactive visualization of spatiotemporal history and trait evolutionary processes. Mol Biol Evol 33, 2167-2169.

152 Parker, J., Rambaut, A., Pybus, O.G., 2008. Correlating viral phenotypes with phylogeny: accounting for phylogenetic uncertainty. Infect Genet Evol 8, 239-246.

153 World health organization/World organization for animal health/Food and agriculture organization H5N1 Evolution Working Group, 2008. Toward a

unified nomenclature system for highly pathogenic avian influenza virus (H5N1). Emerg Infect Dis 14, e1.

154 Olsen, B., Munster, V.J., Wallensten, A., Waldenstrom, J., Osterhaus, A.D., Fouchier, R.A., 2006. Global patterns of influenza a virus in wild birds. Science 312, 384-388.

155 Verhagen, J.H., van der Jeugd, H.P., Nolet, B.A., Slaterus, R., Kharitonov, S.P., de Vries, P.P., Vuong, O., Majoor, F., Kuiken, T., Fouchier, R.A., 2015. Wild bird surveillance around outbreaks of highly pathogenic avian influenza A(H5N8) virus in the Netherlands, 2014, within the context of global flyways. Euro Surveill 20, 21069

156 Lewis, N.S., Verhagen, J.H., Javakhishvili, Z., Russell, C.A., Lexmond, P., Westgeest, K.B., Bestebroer, T.M., Halpin, R.A., Lin, X., Ransier, A., Fedorova, N.B., Stockwell, T.B., Latorre-Margalef, N., Olsen, B., Smith, G., Bahl, J., Wentworth, D.E., Waldenstrom, J., Fouchier, R.A., de Graaf, M., 2015. Influenza A virus evolution and spatio-temporal dynamics in Eurasian wild birds: a phylogenetic and phylogeographical study of whole-genome sequence data. J Gen Virol 96, 2050-2060.

157 Yang, L., Zhu, W., Li, X., Bo, H., Zhang, Y., Zou, S., Gao, R., Dong, J., Zhao, X., Chen, W., Dong, L., Zou, X., Xing, Y., Wang, D., Shu, Y., 2017. Genesis and dissemination of highly pathogenic H5N6 avian influenza viruses. J Virol 91: e02199-16

158 Ip, H.S., Flint, P.L., Franson, J.C., Dusek, R.J., Derksen, D.V., Gill, R.E., Jr., Ely, C.R., Pearce, J.M., Lanctot, R.B., Matsuoka, S.M., Irons, D.B., Fischer, J.B., Oates, R.M., Petersen, M.R., Fondell, T.F., Rocque, D.A., Pedersen, J.C., Rothe, T.C., 2008. Prevalence of influenza A viruses in wild migratory birds in Alaska: patterns of variation in detection at a crossroads of intercontinental flyways. Virol J 5, 71.

159 Shmueli, M., Izhaki, I., Zinder, O., Arad, Z., 2000. The physiological state of captive and migrating Great White Pelicans (Pelecanus onocrotalus) revealed by their blood chemistry. Comp Biochem Physiol A Mol Integr Physiol 125, 25-32.

160 Shittu, I., Meseko, C.A., Gado, D.A., Olawuyi, A.K., Chinyere, C.N., Anefu, E., Solomon, P., Okewole, P.A., Shamaki, D., Joannis, T.M., 2017. Highly pathogenic avian influenza (H5N1) in Nigeria in 2015: evidence of widespread circulation of WA2 clade 2.3.2.1c. Arch Virol 162, 841-847.

161 Selim, A.A., Erfan, A.M., Hagag, N., Zanaty, A., Samir, A.H., Samy, M., Abdelhalim, A., Arafa, A.A., Soliman, M.A., Shaheen, M., Ibraheem, E.M., Mahrous, I., Hassan, M.K., Naguib, M.M., 2017. Highly pathogenic avian influenza virus (H5N8) clade 2.3.4.4 infection in migratory birds, Egypt. Emerg Infect Dis 23, 1048-1051.

162 Twabela, A.T., Tshilenge, G.M., Sakoda, Y., Okamatsu, M., Bushu, E., Kone, P., Wiersma, L., Zamperin, G., Drago, A., Zecchin, B., Monne, I., 2018. Highly pathogenic avian influenza A(H5N8) virus, Democratic Republic of the Congo, 2017. Emerg Infect Dis 24, 1371-1374.

163 Wade, A., Jumbo, S.D., Zecchin, B., Fusaro, A., Taiga, T., Bianco, A., Rodrigue, P.N., Salomoni, A., Kameni, J.M.F., Zamperin, G., Nenkam, R., Foupouapouognigni, Y., Abdoulkadiri, S., Aboubakar, Y., Wiersma, L., Cattoli, G., Monne, I., 2018. Highly pathogenic avian influenza A(H5N8) virus, Cameroon, 2017. Emerg Infect Dis 24, 1367-1370.

164 Mediterranean/ Black Sea Flyway - BirdLife Data Zone (http://datazone.birdlife.org/userfiles/file/sowb/flyways/5_Mediterranean_Black_Sea_Factsheet.pdf) Accessed 5 December 2018.

165 Venkatesh, D., Poen, M.J., Bestebroer, T.M., Scheuer, R.D., Vuong, O., Chkhaidze, M., Machablishvili, A., Mamuchadze, J., Ninua, L., Fedorova, N.B., Halpin, R.A., Lin, X., Ransier, A., Stockwell, T.B., Wentworth, D.E., Kriti, D., Dutta, J., van Bakel, H., Puranik, A., Slomka, M.J., Essen, S., Brown, I.H., Fouchier, R.A.M., Lewis, N.S., 2018. Avian influenza viruses in wild birds: virus evolution in a multihost ecosystem. J Virol 92, e00433-18

166 Tonnessen, R., Hauge, A.G., Hansen, E.F., Rimstad, E., Jonassen, C.M., 2013. Host restrictions of avian influenza viruses: in silico analysis of H13 and H16 specific signatures in the internal proteins. PLoS One 8, e63270.

167 Kawaoka, Y., Gorman, O.T., Ito, T., Wells, K., Donis, R.O., Castrucci, M.R., Donatelli, I., Webster, R.G., 1998. Influence of host species on the evolution of the nonstructural (NS) gene of influenza A viruses. Virus Res 55, 143-156.

Summary in Japanese（和文要旨）

インフルエンザはオルソミクソウイルス科インフルエンザウイルスを原因とする感染症である。インフルエンザウイルスはその遺伝子、抗原性の違いにより A から D 型に分かれるが、ヒト、ブタ、鳥含む様々な動物に感染し、人獣共通感染症として問題を引き起こすのは A 型インフルエンザウイルス（IAV）である。IAV は 8 分節の遺伝子を有するマイナス鎖の一本鎖 RNA ウイルスであり、一つの細胞に複数のウイルスが感染した際に遺伝子の交換を行うことがある（遺伝子再集合）。IAV は表面蛋白であるヘマグルチニン（HA）およびノイラミニダーゼ（NA）の亜型により、H1 から H18、N1 から N11 に分類され、自然宿主であるカモなどの水禽類はこれらのウイルス（H17、H18、N10、N11 亜型のウイルスを除く）を有している。多様な亜型のウイルスが存在する中で、自然界でニワトリに対して高い病原性を示す鳥インフルエンザウイルス（AIV）は H5 亜型と H7 亜型の AIV に限定されている。亜型や遺伝的特徴は宿主により異なるものの、遺伝子再集合により新たな宿主で増殖可能なウイルスが選抜されることがある。豚インフルエンザウイルス（IAV-S）は単独あるいは他の病原体との共感染により養豚場に経済的損失を与える。さらに、2009 年のパンデミックを引き起こしたウイルスのように、他のウイルスとの遺伝子再集合によりパンデミックを起こす能力を獲得する可能性があることから、ウイルスを監視することの重要性が増している。本研究は、国内あるいは世界で分離された IAV-S および AIV について遺伝子情報に加え時期情報、位置情報を加味した系統解析を行うことで、ウイルスの特徴や拡散の背景を詳細に明らかにすることを目的とした。近年の IAV-S の浸潤状況が追究されていなかった日本およびタイの養豚場において分離された IAV-S について時期情報を加味した遺伝子解析を行い、両国で循環している IAV-S の特徴と養豚場内での動態の解析を試みた。さらに、2017-2018 年冬季に日本で分離された H5N6 亜型高病原性 AIV（HPAIV）の病態を明らかにし、時期情報と位置情報を加えた系統解析により日本でウイルスが拡散する経路の解明を試みた。

日本においては、1970 年以降散発的に IAV-S が分離された報告があるものの、養豚場における IAV-S の循環状況を示すデータは少なく、地域も限られている。そこで第 I 章では、2015 年から 2019 年の間に国内の 21 道県のブタから分離された 424 株の IAV-S について遺伝子の系統学的な解析を試みた。その結果、356 株の IAV-S は 1A.1 classical swine 系統に属する H1 遺伝子を有しており、この遺伝子は他国の IAV-S のものとは遺伝的に大きく異なる独立したクレードを形成した。一方、2015 年から 2019 年に分離された 15 株の H3N2 亜型 IAV-S は全て近縁であったことから、国内の豚群に定着していることが示唆された。さらに、2009 年にパンデミックを起こした H1N1 ウイルスの HA 遺伝子を有する IAV-S が 53 株分離された。本研究で分離された IAV-S は 1 株を除き全ての IAV-

S が 2009 年にパンデミックを起こした H1N1 ウイルス由来の遺伝子を有していたことから、1970 年以降国内で循環していた日本の IAV-S と遺伝子再集合を起こしていることが示唆された。以上の結果は、近年の国内流行株の遺伝的特徴を示しており、有効なワクチンの開発につながる基礎的知見である。

第Ⅱ章では、2011 年から 2017 年にかけてタイの 2 県 4 養豚場において継続的に IAV-S をモニタリングし、合計で 169 株の IAV-S を分離した。このうち 82 株は 2009 年にパンデミックを起こした H1N1 亜型ウイルス由来であった。また、87 株の H3N2 亜型 IAV-S の内部遺伝子は全て 2009 年のパンデミックウイルス由来の遺伝子に置き換わっていたことから、遺伝子再集合が起こったことが示唆された。呼吸器症状を示すブタが頻繁に報告されていた 2 つの養豚場において、H1N1 亜型および H3N2 亜型 IAV-S の抗原性が変化したことが継続的な IAV-S のモニタリングにより明らかになった。系統解析の結果、この農場では抗原性の異なる 2 種類のウイルスが侵入することで、あるいは 1 種類のウイルスが HA 遺伝子への変異の蓄積により抗原性が変化していることがわかった。以上の結果は、IAV-S が実際に野外でどのように多様性を獲得し進化していくかを明らかにするものである。

1996 年に Goose/Guangdong 系統の H5 亜型 HPAIV が中国で発生を起こして以降、このウイルスは世界中に拡散し 20 年以上にわたり循環し続けている。国内での最初の発生は 2004 年に報告され、以降近年まで家禽および野鳥に脅威を与えている。2017-2018 年冬季には、アジアならびにヨーロッパで同時期に H5N6 亜型 HPAIV による発生が記録された。アジアでは 2017 年 11 月に韓国で最初の発生が報告された後、2017-2018 年冬季に家禽の高病原性鳥インフルエンザが香川県で発生し、また島根県、東京都、兵庫県において、死亡野鳥から同じ亜型のウイルスが検出された。第Ⅲ章では、2017-2018 年冬季に家禽ならびに野鳥から分離された H5N6 亜型 HPAIV の遺伝的由来と、ニワトリに対する病原性ならびに伝播能を明らかにした。時期系統解析を行った結果、2017-2018 年冬季に日本で発生を起こした H5N6 亜型 HPAIV（香川株及び日本野鳥株）は、ヨーロッパの H5N8 亜型 HPAIV と野鳥の N6 亜型 AIV が、日本野鳥株については 2016 年夏季に、日本家禽株については 2017 年夏季に遺伝子再集合を起こし出現したと推定された。香川株についてニワトリにおける 50%致死量（EID50）を調べたところ、過去に日本で発生を起こした H5 亜型 HPAIV に比べて 10 倍以上多かった。また、過去の H5 亜型 HPAIV においては、感染した 1 羽のニワトリから同居した 6 羽全てのニワトリへの伝播が成立していたものの、香川株では成立しなかった。以上の結果から、香川株のニワトリに対する病原性は過去に日本で発生を起こした H5 亜型 HPAIV に比べて低く、また伝播能も低いことが示された。2017-2018 年冬季に日本で流行した HPAIV のニワトリに対する病原性が低いことと伝播能の低さは、当該シーズンの流行が大きく広がらなかったことの要因の一つと考えられる。

第 IV 章では、2017-2018 年冬季の H5N6 亜型 HPAIV の N6 遺伝子を含む世界中の AIV の N6 遺伝子を地理的・系統的に解析することで、AIV の拡散動態ならびに渡り鳥の移動との関連性を明らかにした。2018 年 1 月の高病原性鳥インフルエンザ発生原因となった H5N6 亜型 HPAIV の N6 遺伝子を含む 163 株の AIV の NA 遺伝子、2019 年 1 月時点でデータベース（GISAID）に登録されていた 3720 株全ての N6 遺伝子データを収集し地理系統解析を行った。その結果、モンゴルあるいはシベリアの HxN6 亜型 AIV がヨーロッパの AIV と近縁である事例、アジアの AIV と近縁である事例、そしてその両方とも近縁である事例が確認された。このことは、この地域がユーラシア大陸の長距離拡散に重要であることを示唆している。また、近縁な N6 遺伝子を有する AIV が、ユーラシア大陸内だけでなくユーラシア大陸―北アメリカ大陸間、ユーラシア大陸―アフリカ大陸間の長距離を拡散している例が確認された。これらの事例を渡り鳥の飛行経路と照らし合わせると、AIV の広範囲拡散は渡り鳥の飛行経路が関与しており、複数の飛行経路が重なる地点はウイルス拡散の中継点として重要であることが示唆された。

本研究は、IAV-S の養豚場での動態や日本の流行状況、AIV の国間、大陸間の拡散機構の一端を遺伝子情報だけでなく、時期情報、位置情報を加味した系統解析により明らかにしたものである。今後、日本および世界の IAV-S や AIV 循環状況を最新の遺伝子解析手法で把握し続けることが、近年流行株に見合ったワクチンの選定や国内に侵入しうる HPAIV の予見といった、現場へ還元できる対策へつながると期待される。